THE DEVELOPMENT OF PHOSPHATE STRESS AND ITS FUNCTIONAL CONSEQUENCES IN THE MODEL LEGUME PLANT *MEDICAGO TRUNCATULA*

by

LIDA-MARI GROENEWALD

Thesis presented in partial fulfilment of the requirements for the degree of Master of Science in the Faculty of Natural Sciences at Stellenbosch University.

Supervisor: Prof A.J. Valentine

Co-supervisor: Dr A. Kleinert

December 2016

The financial assistance of the National Research Foundation (NRF) towards this research is hereby acknowledged. Opinions expressed and conclusions arrived at, are those of the author and are not necessarily to be attributed to the NRF.

DECLARATION

By submitting this thesis/dissertation electronically, I declare that the entirety of the work contained therein is my own, original work, that I am the sole author thereof (save to the extent explicitly otherwise stated), that reproduction and publication thereof by Stellenbosch University will not infringe any third party rights and that I have not previously in its entirety or in part submitted it for obtaining any qualification.

December 2016

Signed Date

SUMMARY

Phosphate is an abundant nutrient in the soil; however it is mostly bound to other elements that make phosphate unavailable for plant uptake. This bound state makes phosphate the second most limiting nutrient for plant growth. Phosphate is also a non-renewable mined resource that forms a major constituent of fertiliser given to crops grown in nutrient poor soils. The second most important crop family in agriculture is Leguminosae. In an attempt to to reduse possible nitrogen stress, legumes can form a symbiosis with nitrogen-fixing soil bacteria. This symbiosis, found in the nodules, exchanges fixed nitrogen with host photosynthate and phosphate. The nodules are thus a phosphate sink that place stress on the rest of the plant. Legumes have adapted different ways to optimise the limited available phosphate to continue their own growth while maintaining the adenosine-triphosphate expensive nitrogen-fixing reaction.

In this study, we looked at how the genetic model legume, *Medicago truncatula* Gaertner, has adapted to phosphate stressed conditions as it relied solely on biological nitrogen fixation as a source of nitrogen.

In the first treatment, *Medicago truncatula* seedlings were infected with *Sinorhizobium meliloti* and received a low concentration of phosphate throughout the growth period. This was done to simulate *Medicago truncatula* growing in already phosphate deprived soils. The comparisons of biomass and growth, internal free phosphate concentrations, and organic acid and acid phosphatases enzyme activities were done on the above versus below ground tissues. Photosynthesis parameters were also recorded. Above ground tissues responded to phosphate stress with increased activity of bypass enzymes at the steps that required adenosine-triphosphate. While the below ground tissues focused on using acid phosphatases to recycle phosphate. Although the rate of photosynthesis had decreased in the phosphate stressed plants, the efficiency of photosynthesis with the phosphate that was available in the leaves had increased.

The second treatment involved the growth of nodulated *Medicago truncatula* with an optimal phosphate concentration, followed by an induced phosphate stress period. In this manner, soil that had been depleted of phosphate during plant growth was simulated. With

the addition of determining differences in activities of nitrogen assimilating enzymes, the above-mentioned comparisons were made on the nodules and roots of the sample plants. Under the induced stress condition, available phosphate was concentrated to the nodules. A possible cause for this was the increase in activity of the organic acid synthesising enzymes present in the nodule. The nitrogen assimilating enzyme activities indicated that stressed nodules may export glutamine rather than asparagine to the roots. Root nitrogen assimilating enzyme activities remained relatively constant during phosphate stress. Reduced nitrogen and carbon content of stressed plants indicated that phosphate had a direct impact on nitrogen fixation.

From this study, we deduced that above ground tissues adapted metabolically for improved photosynthesis phosphate use efficiency; while below ground tissues recycle the available phosphate to be used for nitrogen-fixation. After the induction of phosphate stress it was found that the nodules relied on saving available phosphate for nitrogen-fixation, while the roots recyled assimilated glutamine to maintain function.

OPSOMMING

Fosfaat is volop in die grond, maar dit is gebind aan ander elemente soos metale wat die plante hinder om dit op te neem. Hierdie voedingstof is die tweede mees beperkende voedingstof vir die groei van plante. Fosfaat is ‘n gemynde nie-hernubare hulpbron wat ‘n groot deel beslaan van kunsmis. Hiedie hulpbron word veral gebruik in kunsmis wat toegedien word aan grond met lae konsentrasies van voedingstowwe. Peulplante is die tweede mees belangrikste landbou gewas ter wêreld. Om moontlike sitkstofstres te bekamp, vorm peulplante ‘n simbiose met grond bakterieë om wortelknoppies te vorm. Binne die wortelknoppies ruil die bakterieë stikstof, wat hul fikseer vanaf die atmosfeer, vir fosfaat en produkte van fotosintese vanaf die gasheer plant. Die aanwensel van wortelknoppies het ‘n groot aanvaag na fosfaat wat stres plaas op die res van die gasheer plant. Peulplante het in verskeie maniere aangepas tot beperkte fosfaat kondisies om sodoende te kan oorleef en die onkoste van stikstoffiskering te kan handhaaf.

Vir hierdie studie het ons gekyk hoe die genetiese model peulplant, *Medicago truncatula* Gaertner, aangepas is vir fosfaatstres wanneer dit uitsluitlik op biologiese stikstoffiksering moet staatmaak as stikstofbron.

Tydens die eerste behandeling was *Medicago truncatula* saailinge geïnokuleer met *Sinorhizobium meliloti* en het regdeur hul groeiperiode slegs ‘n lae konsentrasie fosfaat ontvang. In hierdie manier was *Medicago truncatula* wat in fosfaat arme grond groei gesimuleer. Vergelykings tuseen biomassa en groei; interne fosfaat, koolstof en stikstof konsentrasies; organiese suur produserende en suurfosfatases ensiemaktiwiteit was bepaal op bo- en ondergrondse weefsel. Fotosintese lesings was ook vergelyk tussen plante wat onder fosfaatstres gegroei is teenoor die wat met optimale omstandighede volwassenheid bereik het. Hieruit het ons gevind dat die bogrondse weefsels reageer op fosfaatstres deur aktiwiteit van ensieme, wat reakies wat adenosine trifosfaat vereis vebysteek, te verhoog. Terwyl die ondergrondese weefsels fokus op die herwinning van fosfaat deur die gebruik van suur fofatases. Alhoewel die tempo van fotosintese tydens die fosfaatstres afgeneem het, het die doeltreffendheid van fotosintese tenopsigte van die beskikbare fosfaat aansienlik toegeneem.

Tydens the tweede behandeling was geïnokuleerde *Medicago truncatula* tot volwassenheid gegroei met optimale kondisies en daarna van fosfaat onttrek. Op hierdie wyse is grond wat ‘n verlaging van fosfaat vlakke tydens groei gesimuleer. Die bogenoemde vergelykings was gemaak met die wortelkonoopies en wortels van hierdie plante. Die analiese van die verskille in aktiwiteit van stikstofverwerkendsensieme was bygevoeg tot die analieses van die eerste behandelingseksperiment. Tydens die geïnduseerde stres toestand, word vrye fosfaat gekonsentreer vanaf die wortels na die wortelknoppies. Verhoogde aktiwiteit van ensieme wat die energie benodigende stappe verbysteek in die wortelknoppies help met die besparing van fosfaat vir die optimale werking van die stikstoffikserings- en verwerkingsensieme. Die verskuiwing in aktiwiteit van die stikstofverwerkende ensieme dui daarop dat die wortelknoppies tydens fosfaatstres eerder glutamien as asparagien uitvoer na die wortels. Die wortel stikstofverwerkingsensieme het relatief constant gebly tydens die fosfaatstresperiode en mag daarna toe lei dat die wortels glutamine herwin. Die verminderde koolstof en stikstof inhoud van die plante tydens stress het dus ‘n direkte invloed op stikstoffiksering.

Vanuit hierdie studie kon ons aflei dat die metabolisme van plant weefsel wat bo die grond gevind word aangepas word om fosfaat te bewaar vir verhoogde fosfaat gebruik tydens fotosintese; terwyl ondergrondse weefsel die fosfaat herwin vir stikstof-fiksering. Wanneer daar gekyk was na die ondergrondse weefsels na ‘n geïnduseerde fosfaat stres periode, was daar gevind dat die wortelknoppies fosfaat bewaar; terwyl die wortels die geassimileerde glutamien herwin om sodoende hul funksie te kan onderhou.

ACKNOWLEDGEMENTS

I have always believed that no scientific endeavour is an island and would hereby truly and greatly thank every individual contribution to this study.

However a special mention of acknowledgement is made to my supervisors Prof AJ Valentine and Dr A Kleinert for the endless support, guidance and advice given and for enduring my constant questioning in all matters science.

In the same breath, no project can run smoothly without the assistance of our experienced technical staff.

The experience, help, support and coffee from my fellow students throughout the years will always bring a smile to my face.

The Stellenbosch University and the Department of Botany and Zoology are thanked for the use of facilities and financial support.

The National Research Foundation is thanked for personal financial support.

Lastly, no amount of words will suffice for the gratitude that I have towards my family and friends. Thank you for your endless patience and love and for nodding while I convey my excitement towards my work to you.

CONTENTS

LIST OF FIGURES

LIST OF TABLES

LIST OF ABBREVIATIONS

α	alpha
β	beta
δ	isotope
∂	new biomass produced during the time the plant had grown
$\frac{df}{dt}$	derivate function
‰	per mille
%	percentage
% (v/v)	millilitre substance per 100 millilitre solution
% (w/v)	gramme substance per 100 millilitre solution
%NDFA	percentage nitrogen derived from the atmosphere
℃	degrees Celsius
~	approximately
ΔW_C	change in root content
(g)	gaseous phase
(w/v)	weight per volume
$^{-1}$	per
$^{-2}$	per squared
^{2}	squared
µl	microlitre
µM	micromolar
µmol	micromole
AG	above ground
AM	Arbuscular Mycorrhizal
ANOVA	analysis of variance

B	B-value
Benth.	Bentham
BG	below ground
BNF	biological nitrogen fixation
Br	organ biomass
Bt	total plant biomass
C	concentration of carbon in the sample
CAM	Crassulacean acid metabolism
C_i	stomatal carbon dioxide concentration
cm	centimetre
C_t	carbon needed to construct new tissue
C-terminal	carbon terminal
C_W	construction cost
DW	dry weight
EC number	enzyme commission number
Eqn	equation
et al.	et alia
Fig.	figure
FW	fresh weight
g	gramme
GA	growth allocation rate
HP	high phosphate
Hz	Hertz
IRGA	infrared gas analyser
k	nitrogen substrate reduction state
kDA	kilodalton
kJ/mol	kilojoule per mole
K_m	Michaelis constant

L.	Linnaeus
LCP	light compensation point
LP	low phosphate
LRC	light response curve
m	metre
M	molar
M. truncatula	*Medicago truncatula*
Mb	megabase
mg	milligramme
min	minute
ml	millilitre
mm	millimetre
mM	millimolar
mmol	millimole
mol	mole
mya	million years ago
N	organic content of nitrogen in the sample
nm	nanometre
p.	page / pagina
P / *P*-value	probability value
PAR	photosynthetic active radiance
pH	power of hydrogen
Pmax	saturated photosynthetic rate
ppm	parts per million
PPP	possible photosynthetic productivity
PPUE	photosynthetic phosphate use efficiency
PR	photosynthetic respiration rate
PVPP	insoluble polyvinylpyrrolidone

QY	quantum yield
R	molar ratio between heavy and light isotopes of sample and standard
RGR	relative growth rate
$R_g(t)$	growth respiration rate
s	second
S. meliloti	*Sinorhizobium meliloti*
SNAR	specific nitrogen absorption rate
SNF	symbiotic nitrogen fixation
SNUR	specific nitrogen utilisation rate
TCA cycle	tricarboxylic acid cycle
U	Unit(s)
USA	United States of America

Molecules

Abbreviation and or formula	Name
$(NH_4)_2SO_4$	ammonium sulphate
2,4-D	2,4-dichlorophenoxyacetate
ADP ($C_{10}H_{16}N_5O_{13}P_2$)	adenosine 5’-diphosphate
Al^{3+}	aluminium
aspartate ($C_4H_7NO_4^{1-}$)	aspartic acid
ATP ($C_{10}H_{16}N_5O_{13}P_3$)	adenosine 5’-triphosphate
$C_{23}H_{38}N_7O_{17}P_3S$	acetyl-CoA
C_2H_2	acetylene
C_2H_4	ethylene
$C_2O_4^{2-}$	oxalate
$C_3H_4O_3$	pyruvate
$C_3H_7NO_2$	alanine

$C_4H_4O_5$	oxaloacetate
$C_4H_6O_5^{2-}$	malate
$C_4H_8N_2O_3$	asparagine
$C_4H_9NO_3$	threonine
$C_5H_{10}N_2O_3$	glutamine
$C_5H_{10}O_7P$	γ-glutamyl phosphate
$C_5H_{11}NO_2$	valine
$C_5H_{11}NO_2S$	methionine
$C_5H_8NO_4$	glutamate
$C_6H_{12}O_6$	glucose
$C_6H_{13}NO_2$	isoleucine, leucine
$C_6H_{13}O_9P$	glucose 6-phosphate
$C_6H_{14}N_2O$	lysine
$C_6H_6MgO_7$	magnesium citrate
$C_6H_8O_7$	citrate
$C_{12}H_{22}O_{11}$	sucrose
$Ca_{10}(PO_4)_6(OHFCl)_2$	apatite
Ca^{2+}	calcium ion
$CaCl_2.2H_2O$	calcium chloride dihydrate
CO_2	carbon dioxide
Co^{2+}	cobalt ion
$CuSO_4.5H_2O$	copper(II) sulfate pentahydrate
DNA	deoxyribonucleic acid
e^-	electrons
EDTA	ethylenediaminetetraacetic acid
FAD ($C_{27}H_{33}P_2N_9O_{15}$)	flavin adenine dinucleotide
Fe	iron
Fe^{3+}	ferric iron

H^+	protons
H_2	hydrogen
H_2O	water
H_2O_2	hydrogen peroxide
$H_2PO_4^-$	dihydrogen phosphate
H_2SO_4	sulphuric acid
H_3BO_3	boric acid
H_3PO_4	phosphoric acid
HCO_3^-	bicarbonate
HNO_3	nitric acid
HPO_4^{2-}	monohydrogen phosphate
K^+	potassium ion
K_2SO_4	potassium sulphate
KCl	potassium chloride
KH_2PO_4	potassium phosphate
KNO_3	potassium nitrate
MES	2-(N-morpholino)ethane sulfonic acid
$MgCl_2$	magnesium chloride
$MgSO_4.7H_2O$	magnesium sulphate heptahydrate
Mn^{2+}	manganese ion
$MnSO_4.4H_2O$	manganese sulphate tetrahydrate
Mo	molybdenum
Mo-MPT	molybdenum-molybdopterin
N_2	dinitrogen or atmospheric nitrogen
N_2H_2	diimine
N_2H_4	hydrazine
$Na_2MoO_4.2H_2O$	sodium molybdate dehydrate
$NADP^-$ & NADPH ($C_{21}H_{29}N_7O_{17}P_3$)	nicotinamide adenine dinucleotide phosphate

$NaH_2PO_4 \cdot 2H_2O$	sodium dihydrate phosphate
$NaHCO_3$	sodium bicarbonate
NH_3 / NH_3^+	ammonia / ammonia ion
NH_4 / NH_4^+	ammonium / ammonium ion
NO	nitrogen oxide
NO_2^-	nitrite
NO_3^-	nitrate
O_2	oxygen
$O_2^-\bullet$	superoxide radicals
O_3	ozone
OH•	hydroxyl radicals
PEG	polyethylene glycol
PEP ($C_3H_5O_6P$)	phospho*enol*pyuvate
P_i (H_3PO_4)	inorganic phosphate or orthophosphate
PLP ($C_8H_{10}NO_6P$)	pyridoxal 5'-phosphate, active form of vitamin B_6
pNP ($C_6H_5NO_3$)	para-nitrophenol
pNPP ($C_6H_6NO_6P$)	para-nitrophenyl phosphate
RNA	ribonucleic acid
S	sulfur
Tris-HCl	Tris(hydroxymethyl)aminomethane hydrochloride
W	tungsten
Zn^{2+}	zinc ion
$ZnSO_4.7H_2O$	zinc sulphate heptahydrate
α-ketoglutarate ($C_5H_6O_5$)	2-oxoglutarate

Enzymes

Abbreviation (EC number)	Name
APase (3.1.3.2)	Acid phosphatase
ATPase (3.6.3.52)	Adenylpyrophosphatase
AS (6.3.5.4)	Asparagine synthetase
AAT (2.6.1.1)	Aspartate aminotransferase
GOGAT (1.4.1.14)	Glutamate synthase / Glutamine:2-oxoglutarate aminotransferase
GS (6.3.1.2)	Glutamine synthetase
LDH (1.1.1.27)	Lactate dehydrogenase
MDH (1.1.1.37)	Malate dehydrogenase
ME (1.1.1.40)	Malic enzyme
GDH (1.4.1.2)	NAD(H)-glutamate dehydrogenase
NR (1.6.6.1)	Nitrate reductase
NIP	Nitrate reductase inhibitor protein
NiR (1.7.7.1)	Nitrite reductase
PEPc (4.1.1.31)	Phosphoenolpyruvate carboxylase
PAP	Purple acid phosphatase
PK (2.7.1.40)	Pyruvate kinase
RuBisCo (4.1.1.39)	Ribulose-1,5-bisphosphate carboxylase/oxygenase

CHAPTER 1
LITERATURE REVIEW

1.1 Introduction

Plant physiology studies the fundamental processes of plant life. Plants are made up of different sections or organs. Some organs look similar between plants, while some look specialised for a plant species. These differences are attributed to the adaptations that different plant species have accumulated in order to grow and reproduce in the most efficient manner in response to the conditions they are found in. These adaptations are based on the fundamental processes of photosynthesis, transpiration, respiration and nutrition.

It is only by understanding the mechanisms of these fundamental processes and the constant alterations thereof that humankind can plan to utilise the resources that plant domain offers in an efficient sustainable manner.

One plant family, in particular, has been used by mankind for more than 8 000 years in various applications (Aykroyd and Doughty, 1982). Leguminosae members are well known and the species therein are found in most regions of the world (Doyle and Luckow, 2003). In order to do this, Leguminosae members have a high degree of diversity with special adaptations to the fundamental processes of plants. In this chapter, a brief overview was given on this plant family, its adaptations to enable growth and reproduction during nitrogen stress and possible phosphate stress as a consequence thereof.

1.2 Leguminosae

The plant family of Leguminosae is also known as Fabaceae or more commonly as Legumes. Leguminosae is joined with Quillajaceae, Polygalaceae and Surianaceae in the

order of Fabales (Fig. 1.1). This family is classified as Angiosperm Eudicots (Judd and Olmstead, 2004).

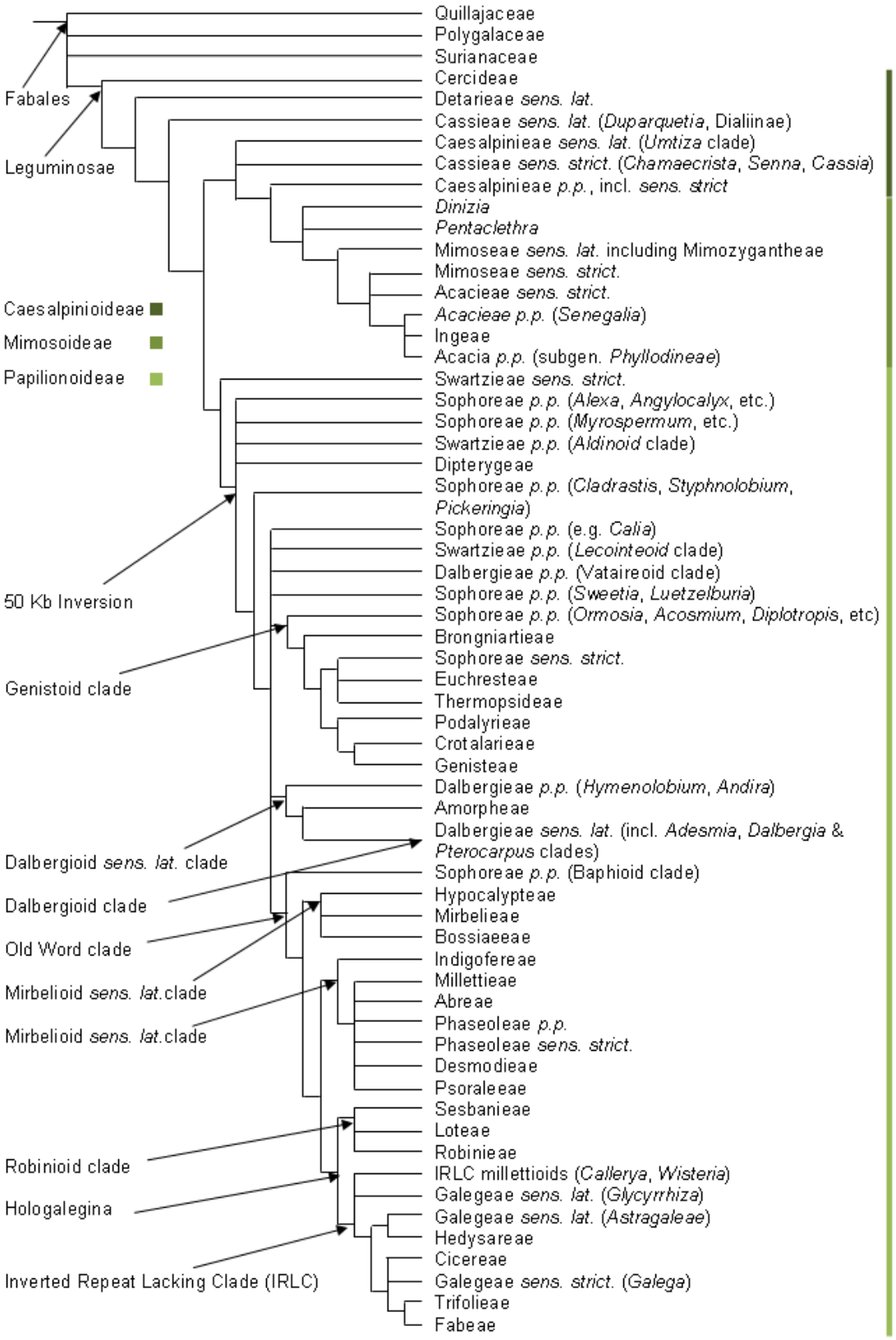

Fig. 1.1 Phylogenetic tree of Leguminosae to tribe level. Leguminosae shares the order of Fabales with Quillajaceae, Polygalaceae and Surianaceae. Legumes are split into three sub-families that are made up of ten clades. Adapted from Lewis (2005).

1.2.1 The sub-families

Leguminosae itself is divided into three sub-families, namely Papilionoideae, Caesalpinioideae and Mimosoideae. Members of Leguminosae are placed in these three sub-families based on flower morphology (Fig. 1.2).

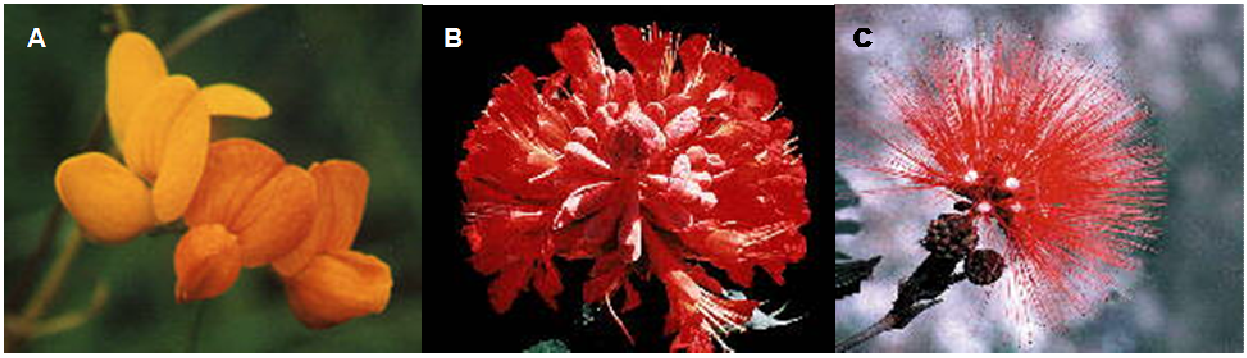

Fig. 1.2 Distinctive flower morphology of the three sub-families of Leguminosae. (A) Papilionoideae, (B) Caesalpinioideae and (C) Mimosoideae (Information about the Family Leguminosae, 2006).

Papilionoideae, the largest sub-family, contains ~480 genera with about 14 000 species (Doyle and Luckow, 2003). Although there are some shrubs and trees in this sub-family, the majority of the species are herbaceous. Papilionoideae flowers are recognised as seemingly butterfly-like. These reproductive organs are zygomorphic and the five petals form a banner, two wings and two partially fused petals to produce a keel that encloses the stamens (Information about the Family Leguminosae, 2006).

Caesalpinioideae harbours ~160 genera containing approximately 3 000 species (Doyle and Luckow, 2003). These tropical or sub-tropical shrubs and trees also have zygomorphic flowers with five petals, however, the petals are not differentiated into specific wings or keel, but the stamens are externally visible (Information about the Family Leguminosae, 2006).

Mimosoideae is made up of ~80 genera for 3 000 species (Doyle and Luckow, 2003). Mimosoideae also share the tropics and sub-tropical regions and display their small, actinomorphic flowers by crowding them together to resemble a pom-pom structure. The five petals have become inconspicuous to further expose the stamens (Information about the Family Leguminosae, 2006).

1.2.2 Applications

Legume species that yield seeds containing high concentrations of protein are called the Pulses. Many Pulses including *Phaseolus* and *Vicia* (beans), *Glycine max* (Linnaeus) Merrill (soybean), *Lens culinaris* Medikus (lentil), *Pisum sativum* L. (pea), *Cajanus cajan* (L.) Millspaugh (pigeon pea), *Vigna unguiculata* (L.) Walpers (cowpea) and *Cicer arietinum* L. (chickpea) have been domesticated and contribute to at least a third of the dietary nitrogen and protein needs of humans. Pulses are used as a substitute for meat for vegetarians and in communities where it is difficult to keep livestock (or preserve meat) or it is not financially viable to purchase meat. *Glycine max* and *Arachis hypogaea* L. (peanut) are not only eaten but are also used to produce vegetable oil. *Glycyrrhiza glabra* L. (liquorice) root and other legumes are used as a flavouring of food and sweets (Lewis, 2005).

Legumes such as *Lupinus*, *Trifolium* (clover), *Melilotus* (sweet clover), *Medicago sativa* L. (lucerne) and *Lotus corniculatus* L. (trefoil) are used as pasture to increase the nitrogen content of dairy products. Many of the plants are also used as cover crops, green manure, intercrops and rotational crops. Legumes are sometimes used to restore pasture systems, for example, *Stylosanthes* in the tropical regions (Lewis, 2005).

1.3 Nitrogen

Dinitrogen or atmospheric nitrogen (N_2) is an abundant molecule as there are 25 parts per million (ppm) found in the earth's crust and it makes up 75.5% of the earth's atmosphere by weight (78.1% by volume). Thus N_2 is mainly found in colourless gas phase as it liquefies at -196ºC. However, the triple bond requires 945 kJ/mol energy in order to dissociate. Thus it is not highly reactive with other atoms or molecules, but it is not as non-reactive as the noble gases (Banfield, 2006, Horton et al., 2006).

1.3.1 Nitrogen in nature

Although N_2 is not highly reactive it can be split and oxidised to nitrogen oxide (NO) or reduced to ammonia (NH_3). These forms of nitrogen are then used or further oxidised or

reduced for biochemical use in organisms. The biologically active nitrogen-containing molecules, or nitrogen in organic form, can also be denitrified back to N_2. Thus the nitrogen cycle is complete (Fig. 1.3).

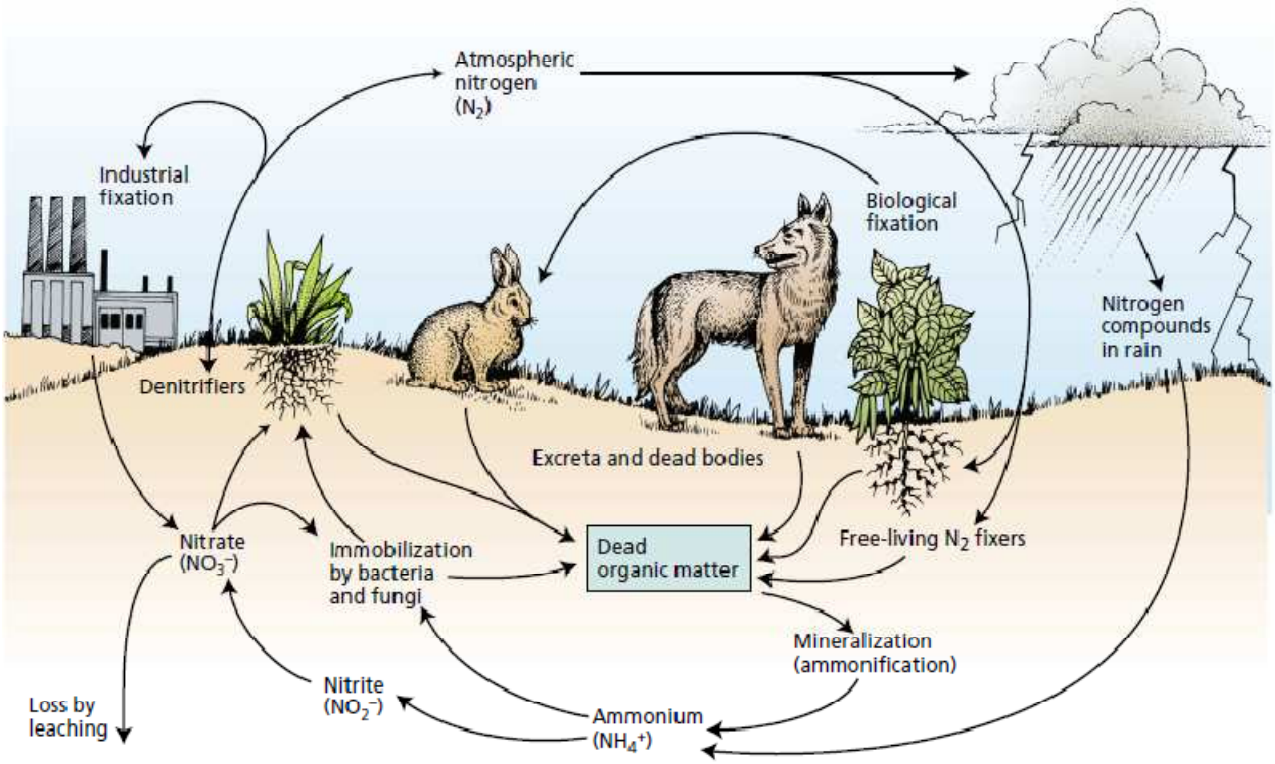

Fig. 1.3 The terrestrial nitrogen cycle. Elemental nitrogen is fixed from the atmosphere to be metabolised by microorganisms into organic nitrogen. Plants utilise the nitrogen in the soil. As herbivores eat the plants, nitrogen is taken up into the food web. The decomposition of these organisms replaces nitrogen in the soil. Denitrifying bacteria metabolises organic nitrogen to elemental nitrogen to close the cycle (Bloom, 2006).

Naturally, 190×10^{12} g of nitrogen is fixed per year via three main routes. Firstly, photochemical reactions between ozone (O_3) molecules and gaseous NO produces nitric acid (HNO_3) in the atmosphere. This amounts to 2% of annually fixed nitrogen. A more rapid route involves lightning (Bloom, 2006). When lightning strikes, the high-voltage discharge causes oxygen and water vapour to convert into hydroxyl free radicals, and free oxygen and hydrogen atoms that are highly reactive (Horton et al., 2006). These atoms react with N_2 and become HNO_3 that falls to the earth's surface with the rain. In this manner, 8% of organic nitrogen is fixed. The third route for N_2 to enter the nitrogen cycle is through biological nitrogen fixation (BNF). This route of nitrogen fixing accounts for the remaining 90% of naturally fixed nitrogen. Diazotroph bacteria as well as cyanobacteria (*Trichodesmium*) have the ability to reduce N_2 into NH_4^+ (Bloom, 2006). This can be done by the free-living bacteria (such as *Azotobacter*, *Clostridium*, *Klebsiella* and *Agrobacteria* genera) or in a symbiotic association (such as Rhizobia and *Frankia*) (Horton et al., 2006).

1.3.2 Biological nitrogen fixation

As stated above, the majority of nitrogen that is fixed from the atmosphere is done biologically by diazotrophic soil bacteria. For these bacteria to break the triple bond of N_2 and reduce it to NH_3 in a single cell requires a complex and regulated environment. As done in the Haber-Bosch process, the reaction catalysed. However, this is not accomplished by using high temperatures or with high pressure. The biological fixation of nitrogen is catalysed by an enzyme, nitrogenase.

Nitrogenase (EC 1.18.6.1) (Fig. 1.4) itself is a complex protein. It is comprised of two metalloproteins, yet the polypeptides are not the same. The smaller polypeptide consists of two identical subunits of 30-72 kDa each (depending on the species). It is called the iron protein (Fe protein) as it contains two iron-sulfur [4 Fe-4 S] clusters per subunit. The other polypeptide is composed of four subunits that collectively make a molecule of 180-235 kDa (depending on the species) (Bloom, 2006). Each of the subunits contains two molybdenum-iron-sulfur [Mo-7 Fe-9 S] clusters and a phosphate cluster. This metalloprotein is called the molybdenum-iron protein (MoFe protein). The molybdenum cofactor can be substituted with iron or vanadium (Rees and Howard, 2000).

The combined subunits create an enzyme that catalyses the reactions of (i) N_2 into NH_3; (ii) nitrous oxide (N_2O) into N_2 and water (H_2O); (iii) azide (N_3) into N_2 and NH_3; (iv) acetylene (C_2H_2) into ethylene (C_2H_4); (v) protons (H^+) into H_2; and (vi) ATP into ADP and orthophosphate (P_i). However the exact enzyme configuration and the detailed reaction mechanism have yet to have been fully understood, even after more than 40 years of research (Rees and Howard, 2000).

The general scientific consensus revealed that a complex of the Fe-protein, two ATP molecules and the MoFe-protein must be formed (Rees and Howard, 2000). Reduced ferredoxin or reduced flavodoxin acts as a strong reducing agent to donate e^- to the Fe-protein. The ATP molecules are hydrolysed as the e^- are transferred to the MoFe-protein through the phosphate cluster and MoFe-protein becomes reduced (Horton et al., 2006). The Fe-protein then dissociates as it becomes re-reduced from the ADP molecules exchange. This process is repeated until enough protons and e^- are accumulated to reduce the available substrates (Bloom, 2006).

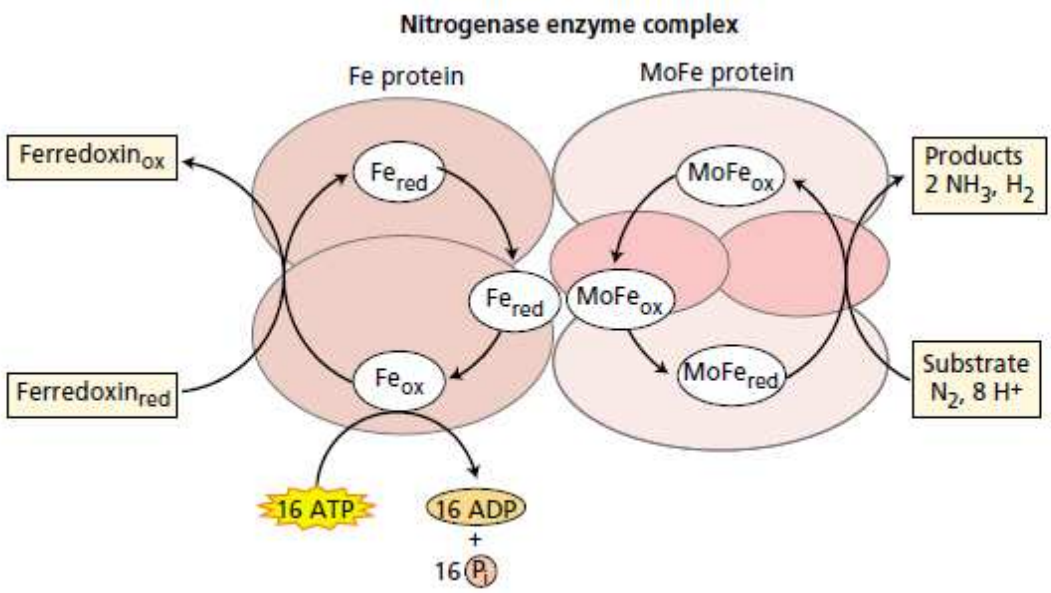

Fig. 1.4 Simplified nitrogenase action. Reduced ferredoxin molecules donate electrons to the Fe-protein. ATP molecules become hydrolysed as electrons are transferred to the MoFe-protein. The MoFe-protein becomes reduced. When the MoFe-protein has accumulated the required amount of protons and electrons, one dinitrogen molecule is reduced to two ammonia molecules (Bloom, 2006).

When the MoFe-protein has accumulated the required amount of H^+ and e^- it is thought that N_2 is reduced to diimine (N_2H_2) to hydrazine (N_2H_4) and then to NH_3 in the molybdenum-iron-sulfur cluster. These steps are shown in the following formulas (Horton et al., 2006):

N_2 to diimine: $\mathrm{N \equiv N + 2H^+ + 2}e^- \rightarrow \mathrm{H - N = N - H}$

Diimine to hydrazine: $\mathrm{H - N = N - H + 2H^+ + 2}e^- \rightarrow \mathrm{H_2N - NH_2}$

Hydrazine to NH_3: $\mathrm{H_2N\text{-}NH_2 + 2H^+ + 2}e^- \rightarrow \mathrm{H_3N + NH_3}$

The essential coupled production of H_2 from the reduction of two H^+ is made possible by an additional two e^- from the ferredoxin or flavodoxin donor. Thus the full reaction of nitrogenase nitrogen fixation is as follows (Bloom, 2006, Hotron et al., 2006, Willey, 2008):

$$\mathrm{N_2 + 8H^+ + 8}e^- + \mathrm{16ATP \rightarrow 2NH_3 + H_2 + 16ADP + 16P_i}$$

The use of 16 ATP molecules to reduce one molecule of N_2 indicates a very energy expensive reaction as with the Haber-Bosch process. As some of the energy is used for the other reactions that nitrogenase can catalyse such as the production of H_2, some

species of Rhizobia use hydrogenase to oxidise H_2 and redirect the e^- to nitrogen fixation (Bloom, 2006).

As oxygen receives e^- very easily, it is important that nitrogenase interacts with as little oxygen as possible. Enzymes such as nitrogenase that are involved with electron transport are inactivated in the presence of oxygen. Reduced oxygen, such as superoxide radicals (O_2^-•), hydrogen peroxide (H_2O_2) or hydroxyl radicals (OH•), has the ability to oxidise and in a short space of time, one of the molecules can destroy cellular constituents. These nitrogen-fixing microorganisms must either be anaerobic, have specialised cells in the colony that produce the microanaerobic conditions (such as the heterocyst cells in cyanobacteria colonies), or find other ways to protect nitrogenase (Willey et al., 2008).

A number of free-living nitrogen-fixing bacteria have the ability to form associations with other organisms. In this manner, more controlled conditions are produced to optimize nitrogenase function. The exchange of nitrogen for other nutrients, for example, causes strain on the other symbiont, thus the association is usually only induced when the other symbiont is in need of the very important nutrient of nitrogen.

1.3.3 Symbiotic nitrogen fixation

A legume response to nitrogen stress is to secrete certain betaines and flavonoids into the rhizosphere to initialise SNF (Fig. 1.5). Rhizobia are free-living soil bacteria that sense these molecules and move toward the source using chemotaxis. As the bacteria progress to the plant roots, a molecular cascade is initiated by the up-regulation of the *nod* gene cassette expression. This cassette enables the bacterium to produce and excrete Nod factor. This complex molecule is a lipooligosaccharide. The Nod factor acts as a signal to the host plant. Depending on the soil type and environmental conditions, there can be many genera of Rhizobia present in the soil. However, certain Rhizobia genera have co-evolved with their host plant. Thus the Nod factor structure is host plant specific and this signal relays to the plant whether its symbiont is present and in what density. Thus it is an indication whether or not it is feasible for the plant to initiate the changes needed for the symbiosis. A study on *Medicago truncatula* and *Sinorhizobium meliloti* investigated the performance of the symbiosis when the plants were inoculated with different strains of *Sinorhizobium meliloti* under varying conditions (Hirsch, 1992; Gage, 2004). Sulieman et al. (2013) observed that even the strain of bacteria is important to the efficiency of the symbiosis.

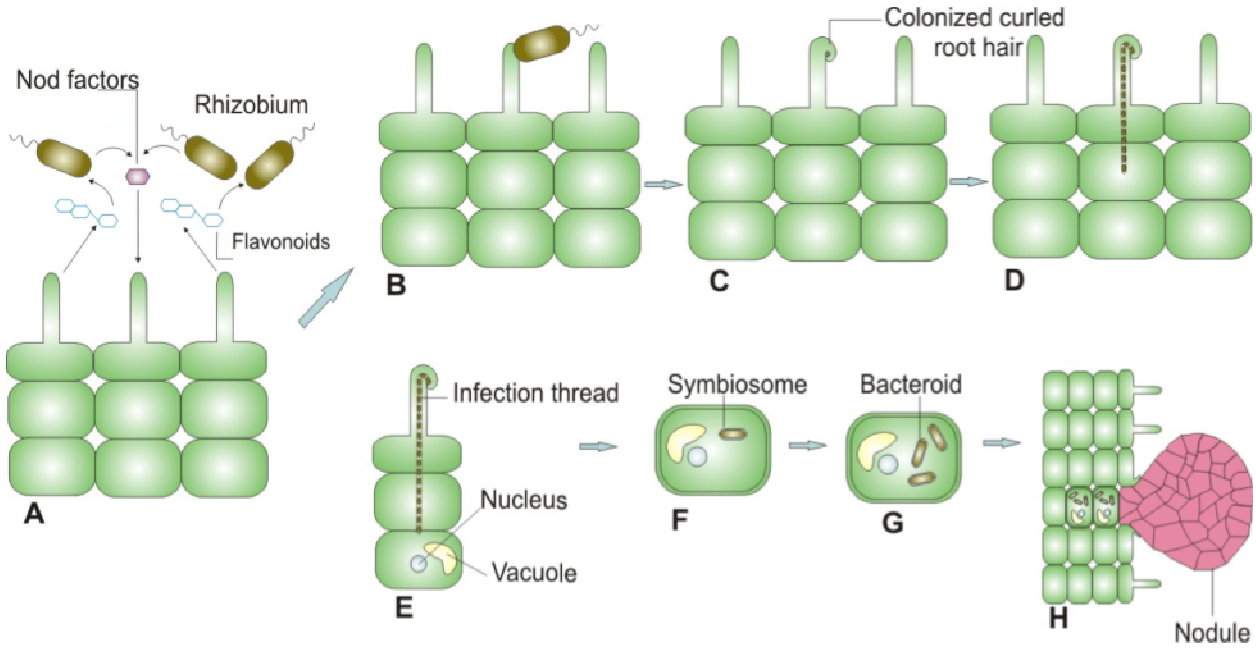

Fig. 1.5 Nodule development. (A) Nitrogen stress is sensed by the roots, flavonoids are excreted from the root system. The surrounding Rhizobia react by moving towards the host plant's root hairs while excreting Nod factors. (B) When the bacterial cells have accumulated by a root hair, a firmer bond is created. (C) The colonised root hair curls to form a "Shepherd's crook". (D) The bacteria penetrate the surface of the root hair (infection thread) and (E) increase the cortical cell division rate. (F) During the formation of the nodule, the bacteria are enveloped by the plant derived membrane where they infect the host's cells that make up the nodule itself. (G) When the nodule is formed, the bacterial cell walls are replaced so that the cells form large branched cells that are named bacteroids. (H) The organ is mature and ready to fix atmospheric nitrogen (Jensen, 2015).

If the matching Nod factor is perceived by the plant, a number of changes in the roots are initiated. Areas of the plant cell membranes become depolarised; cell division in the root cortex is enhanced; oscillations in the intracellular calcium concentrations occur; and root hair deformation can be observed 6-18 hours after inoculation (Hirsch, 1992; Gage, 2004). The bacteria then cover the host plant root system and loosely attach themselves to the root hair receptors by using the Rhicadhesin Ca^{2+} binding protein (Hirsch, 1992). The species-specific connection is then enhanced by the organisms producing lectins; and or the host plant producing cellulose fibrils towards the bacteria and the bacteria producing fimbriae towards the host. Thereafter the bacteria must infiltrate the root hair (Gage, 2004).

Infiltration is done in close proximity to the root hair tip, where the cell wall is thinner and less cross-linked; and where the deformation occurs. As the cell's tip deforms, it can take on many types of shapes, for example, spirals, corkscrews, twists and even branches. The bacteria are thus found in between the cell wall as the root hair tip bends or curls, also called the "Sheppard's crook" formation. At this weakened spot, the bacteria extends an infection thread into the root hair cell and towards the root epidermal cell. The Rhizobia

grow in the infection thread as the thread grows into the interior of the root and branches. The bacteria then exit the thread and move toward the nodule cells and enter. There, further bacterial growth and differentiation leads to the breakdown of bacterial cell walls and creates a branched colony called the bacteroid (Hirsch, 1992; Gage, 2004).

A mature nodule can be distinguished as having a pinkish hue, due to the leghemoglobin. This leghemoglobin protein is similar in structure to the animal hemo- and myoglobin proteins with similar function. Leghemoglobin, however, has a higher affinity for oxygen as it is used to regulate the microanaerobic habitat required for nitrogenase function. It is interesting to note that the apoprotein is produced from the plant genome and the heme group from the bacterial genome. Thus leghemoglobin is only produced when SNF is in place (Willey et al., 2008). The bacteroids produce either determinate or indeterminate nodules.

Determinate nodules can be found on studied legumes such as *Lotus*, *Lupinus*, *Vicia*, *Aspalathus* and *Glycine*, and are usually found on the roots of species found in the tropics. These nodules are round, do not have a persistent meristem and have a pink hue all around as they do not have nodule developmental gradients (Fig. 1.6A). Nitrogen fixation thus takes place everywhere in the nodule (Gage, 2004).

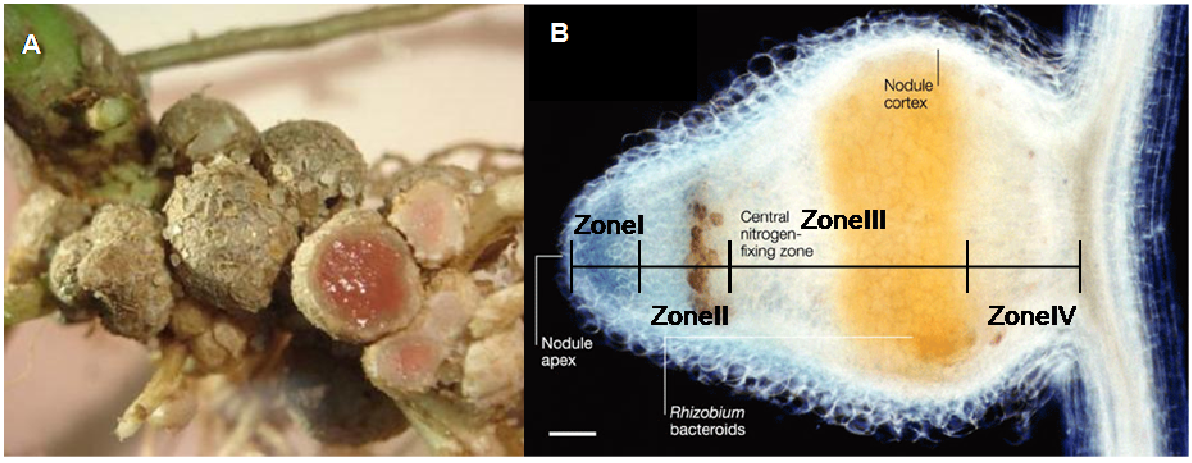

Fig. 1.6 Nodule morphology. Determinate nodules (A) have nitrogenase activity throughout the round tissue (as seen by the presence of the pink leghemoglobin) (Dean, 2009). However, indeterminate nodules (B) only have one zone actively fixing nitrogen (ZoneIII) (Dixon and Kahn, 2004).

Indeterminate nodules are found on studied species from the *Medicago*, *Pisum* and *Trifolium* genera. These nodules, however, are elongated as it is composed of four developmental zones (Fig. 1.6B). Zone I, the meristem, is the youngest part of the nodule and is situated at the tip. The meristem is where the bacterial growth occurs.

The next zone, Zone II, is adjacent to Zone I as the young bacteria infect the nodule cells and differentiate into the bacteroid. An overlapping area arises between Zone II and Zone III where the bacteroid reaches maturity. Zone III is the largest area of the nodule and can be differentiated from the other as being slightly bulged and containing the characteristic pink hue of leghemoglobin. In this zone nitrogenase is active and the fixing of nitrogen takes place. The final area is nearest to the root. Zone IV is where bacteroid senescence occurs (Gage, 2004).

Nodules can be found in clusters or individually or in combination along the main and lateral roots, depending on host plant root system architecture. Nodule size can vary from millimetres in length, such as *Medicago truncatula*, to centimetres in diameter as seen with *Phaseolus* (Gage, 2004).

As stated before, this symbiosis is sometimes critical to the host plant's survival. However owing to the strain that it causes the host, it is also regulated to suit the balance of demand and production cost. This is not the only factor that contributes to the success of the symbiosis. Other abiotic and biotic factors in combination have the ability to terminate the growth of new nodules as well as to initiate the senescence of mature actively nitrogen-fixing nodules.

Water is not only required for photosynthesis; temperature, turgor pressure and pH control; and many other processes within and around the host plant and bacteria; but also for the regulation of SNF. The amount of water in the soil can neither be too little nor too great for optimal SNF yield. A long period of drought will lead to the senescence of a large percentage of plant tissue including the mature nodules. The concentration of the free-living Rhizobia reduces as they also require water to move toward nutrients. At the other end of the spectrum, plants do not produce root hairs during times of high water saturation, thus reducing sites of infection. When the soil becomes waterlogged, it is difficult for the plant to diffuse oxygen away from the nodule and thus nitrogenase. As nitrogenase is highly sensitive to oxygen, strain is placed on the existing leghemoglobin molecules and resources are concentrated to enhance nodule oxygen permeability (Mulongoy, 1992).

As SNF is initiated as a response to plant nitrogen stress, an adequate concentration of usable nitrogen in the soil will not lead to a strong symbiosis. An increase in nitrogen content in the soil (for example when fertiliser is added to the soil) will reduce the host plant's demand for this most important nutrient. Senescence of the immature nodules is initiated and thereafter the mature nodules until the host plant balances the demand for

nitrogen with the uptake rate and SNF. It is much cheaper for the host plant to merely recruit nitrogen from the soil than to maintain the symbiosis and will thus favour the uptake pathways (Mulongoy, 1992).

Other nutrients found at high concentrations in the soil such as manganese (Mn^{2+}) and aluminium (Al^{3+}) reduces the efficiency of SNF. While a lack of calcium has the same outcome. Micronutrients also have an effect on SNF. The cofactor of nitrogenase, molybdenum, as well as boron, cobalt and copper are required for atmospheric nitrogen to be biologically fixed (Mulongoy, 1992).

If the pH of the rhizosphere surrounding the host plant root system is acidic, the growth of the plant and the symbiosis is impaired. The hydrogen ion gradient between the plant cells and the soil is reversed and thus transport channels that are dependent on this gradient do not work as effectively (Mulongoy, 1992).

The habitat in which the host plant finds itself will also determine the productivity of SNF. If the plant is found growing under mostly shady conditions, its' photosynthetic efficiency would be lower than that of a plant growing in mostly sunny conditions. Thus the shade host plant would not be able to provide the nodules with as many photosynthates as a sun host plant would be able to. Thus SNF efficiency is reduced. The regulation of nodule temperature is important for optimal enzymatic rates. This optimal temperature range differs from the species of Rhizobia that is part of the symbiosis. As Rhizobia are found across the earth, this optimal temperature range is dependent on where the species originated from. However, the general temperature range for nitrogenase *in vivo* activity is seldom under 25 ℃ or higher than 38 ℃ (Mulongoy, 1992).

The most important biotic factor to the success of SNF is whether the host plant's symbiont is present in the soil in significant numbers. If a host plant is introduced to a new habitat, such as a crop plant, it is likely that the soil must be inoculated with the specific species of Rhizobia before planting. Fields that had a plant reintroduced, such as a crop field or in habitat rehabilitation programs, might also need a reinoculation event. If the host plant is removed from an area the free-living Rhizobia cell counts decrease. However, if too many Rhizobia cells are present the plant might sense the bacteria as a pathogen and will rather defend itself against the symbiosis (Mulongoy, 1992).

Animals such as insects and nematodes can interfere with not only the development of nodules but also the rhizosphere in which they live. Other bacterial species can also infect the host plant and create non-active nodules or tumours that compete for the same

substrates as the active nodules. Non-nodulated plant neighbours compete with the host plant for nutrients, water, space and light. Non-nodulated plants might sense the accumulation of the Rhizobia to a neighbouring host plant and release secondary metabolites in order to defend itself from a possible pathogen, and thus negatively affect the nodulated plant neighbour (Mulongoy, 1992).

Grazing and harvesting amplifies defoliation of the host plants from the natural senescence rate. This reduces the host plant's ability to produce optimal levels of photosynthates and leads to lower concentrations of carbohydrates available for SNF (Mulongoy, 1992).

As it is complicated to determine the details of the configuration and action of the nitrogenase enzyme, it is also difficult to determine the cost of SNF to the host plant. It is estimated that 11-14% of the carbon from photosynthates is allocated to SNF. It is less costly to acquire NO_3^- from the soil than to maintain the symbiosis. Glycine max was used to find that 4.99 mg of carbon is used to acquire one mg of nitrogen through NO_3^- uptake, while it required 8.28 mg of carbon for every mg of nitrogen fixed via SNF. These figures vary with species and whether the legume is an ureide or amide exporter (Valentine et al., 2011). The reaction of nitrogen fixation is catalysed by nitrogenase; however, it is still a relatively slow process. Five molecules of N_2 are reduced per second. Thus the bacteroid can produce nitrogenase enzymes to such an extent that is comprises 20% of the total cell protein. This large number of active enzymes ensures that the required amount of nitrogen is fixed (Bloom, 2006). However, the cost of 16 ATP molecules per molecule of N_2 to be fixed is a high requirement for the host plant. The importance of phosphate in the reaction as well as in the enzyme itself is thus undisputed. To have nitrogen fixed the nodule needs phosphate.

1.4 Phosphate

1.4.1 Phosphorous in nature

As with nitrogen, phosphorous has a natural cycle (Fig. 1.7). It is difficult to estimate the earth's phosphorous content as it is mainly found underground. Volcanism and the uplifting of the earth's crust exposes phosphorous containing minerals such as apatite

($Ca_{10}(PO_4)_6(OHFCl)_2$). Apatite is then weathered or eroded by acids exuded by microorganisms. The "freed" phosphate (HPO_4^{2-} or $H_2PO_4^-$) is then either taken up by plants and microorganisms, chelated to metal ions found in the ground such as ferric ion (Fe^{3+}) and Al^{3+}, or washed into rivers by rain (Ruttenburg, 2003). The chelated phosphate cannot be taken up by organisms until the metal is removed (Bloom, 2006).

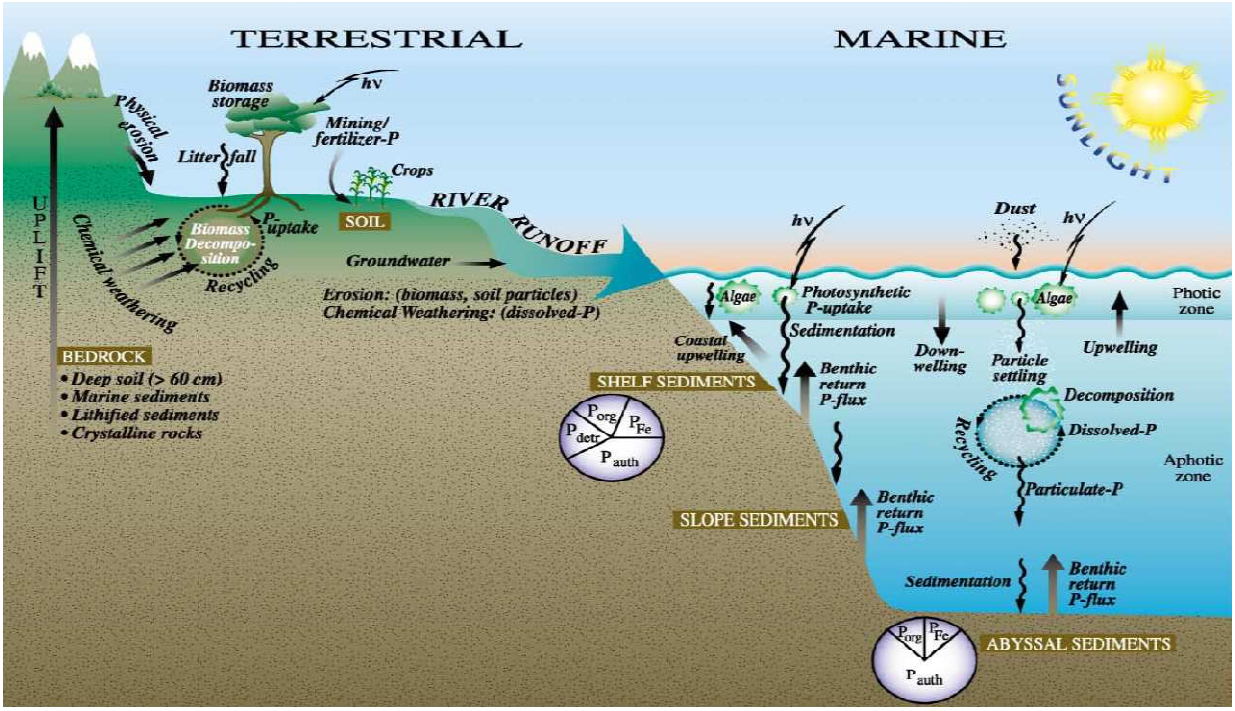

Fig. 1.7 The global phosphorous cycle starts as bedrock is moved towards the soil surface. Through weathering and erosion, phosphate is released into the soil. Plants and microorganisms use the phosphate in biochemical pathways. The remaining phosphate is either bound to metal ions or leached into rivers and the ocean. Microorganisms again use the phosphate. Decomposing organisms and phosphate containing particles drift to the ocean floor where the phosphate then becomes sediment. These sediments eventually become the bedrock that starts the cycle (Ruttenberg, 2003).

The phosphate that is absorbed is used to produce essential molecules: DNA, RNA, proteins, phospholipids, sugar phosphates, coenzymes such as nicotinamide adenine dinucleotide phosphate ($NADP^-$ and NADPH), in signalling, and more importantly nucleoside triphosphates (Bloom, 2006). As the organisms die and decompose, these organic phosphate-containing molecules are returned to the soil. Animals obtain phosphate from eating plants or herbivores. The excrement from and decomposed animals also return phosphate to the soil (Ruttenburg, 2003).

Phosphate molecules that are leached into rivers are either taken up by the organisms in the water, become sediment (phosphorite) on the bottom of the river bed or are washed

into the ocean (Wisniak, 2005). In the marine environment, phosphate is also taken up by microorganisms, algae and phytoplankton. As these single-celled organisms are eaten phosphate is taken up into the food web. Decomposed organisms and phosphate molecules that are not taken up, sink to the ocean floor where it creates sediments (phosphorite). Phosphate containing dust is blown from the land onto the surface of the ocean. The dust is taken on the ocean currents to other areas of the world where it settles (Ruttenburg, 2003; Wisniak, 2005).

As time goes on, the ocean floor is brought to the surface through volcanism and the uplifting of the earth's crust (Ruttenburg, 2003). Thus the cycle is complete.

Unfortunately, the uplift of apatite and weathering thereof is a slow process. The distribution of apatite is not equal around the world. As plants and microorganisms compete for this important nutrient it is possible that the soil can become depleted of free phosphate, especially in areas where there is little apatite deposits. The additional chelation and leaching of free phosphate add to this state.

Plants growing in these phosphate poor soils are stunted with dark green leaves. These leaves may show necrotic spots (of dead tissue) and be malformed. Similar to nitrogen deficiency, phosphate stressed plants produce thin stems with added senescence of older leaves as phosphate from these tissues is relocated to other tissues. Plants that have experienced phosphate stress during development have a tendency to mature after plants grown with an adequate supply of phosphate. Some plant species produce surplus anthocyanin molecules to add a red-purple hue to the dark green tissues. This symptom is also found with nitrogen deficiency, however, in the case of phosphate stress, it does not correlate with chlorosis (Bloom, 2006).

Crop farmers thus need to manage the resources found in their fields to secure a reliable harvest. A method of no-tilling is used to preserve the microbial ecosystem in the soil to enable faster decomposition of the remaining plant material after the harvest. Another method is to add phosphate-containing fertiliser to the soil and so artificially increasing the phosphate concentration.

1.4.2 Fertiliser

Similar to the fertilization of soil with nitrogen, excess phosphate is given to the soil as much of the mineral becomes lost before plant uptake. This creates an imbalance in the phosphorous cycle. Nitrogen and phosphate that are leached into rivers and oceans encourage the growth of algae. The algae population increases rapidly and is called an algal bloom. This leads to three possible scenarios: (i) the production and release of toxic molecules from the algae; (ii) the reduction in light reaching marine vegetation (thus the death thereof and destruction of fish food and habitat); (iii) or the decrease of oxygen in the water owing to the decomposition of the large amount of algae (Anderson et al., 2002). This results in a disturbed marine ecosystem with greater negative consequences.

Another concern is linked to the pace of apatite mining versus that of the natural sedimentation of phosphorite to later become apatite. With the difficulty of determining the amount of apatite present in the earth, the estimation of the time humankind has left until the resource is depleted is variable. However, the consensus is that at the current rate of mining, the reserve will run out between the years 2030 and 2060 (Vance, 2003; Elser and Bennett, 2011).

The lack of phosphate in fertiliser (or to any phosphate-containing products) will have a detrimental effect on not only agriculture but the food industry as well. The growing human population would require a higher level of food security in the coming years; however, this might not be met with the decline in available phosphate. As phosphate is easy to mine and process, this component of fertiliser is relatively cheap. When the mineable reserves become depleted and the nutrient becomes more difficult to come by phosphate's value will increase. Alternative methods will then be required to make phosphate available to plants to ensure food security.

1.5 Research to minimize food scarcity

The current process of obtaining nitrogen for fertiliser is expensive. This coupled to the impending increase in phosphate prices will lead to higher fertiliser prices. As these two macronutrients are needed for all crops, the small scale commercial and subsistence farmers will not be able to purchase adequate amounts of fertiliser. This will not only put

strain on their own livelihoods but will impact the food security of their families and communities.

In order to address part of this problem, research is being done to encourage the association of diazotrophic bacteria with non-legume crop species. In the 1970's and 1980's researchers began to play with this idea. Unfortunately, the technology required for this work was not yet available. By 1992, para-nodules (modified lateral roots (Francisco et al., 1993)) induced by 2,4-dichlorophenoxyacetate (2,4-D) were made on various non-legume crops. However, these types of nodules were caused by a weakening of the root tissue to enable bacterial infection in the presence of polyethene glycol (PEG) and delivered little nitrogenase activity (Kennedy and Tchan, 1992). With the boom of the "'Omics" era, new research techniques were applied in this field. The analyses of model organism genomes have found that the endosymbioses of *Frankia* and Rhizobia bacteria; and that of AM Fungi with plant roots are based on a common genetic basis in not only the legume but the non-legume species as well (Santi et al., 2013). Thus, it might only require a tweaking of the genome to enable diazotrophs that naturally colonise the rhizosphere of crop plants to become endophytes with these plant roots. Further research into this matter is yet to be done and the possibilities look promising. However, by alleviating the nitrogen problem in this way, another serious problem will arise.

The process of fixing N_2 to NH_3 with the use of nitrogenase is energetically expensive. As stated before, SNF is very dependent on the phosphate status of the host plant. By enhancing the ability of crop plants to form SNF in nitrogen-poor soils it will lead to a decrease in the need for nitrogen in fertiliser to make it cheaper and reduce possible nitrogen pollution in the rivers and oceans. However, the plants would require more phosphate than before. Fields that contain little or no phosphate would need to be supplemented with this macronutrient in fertiliser even more so than before in order to maintain SNF. If a slow release mechanism is used in the fertiliser, it will be possible for the plants to maintain SNF and decrease the probability of phosphate pollution. Unfortunately, the slow release mechanisms are expensive. Coupled with the rapid decline in mineable phosphate and the inevitable increase in the price thereof, it will become difficult for small-scale and subsistence farmers to finance such fertilisers. Additional work is thus needed to increase the efficiency of phosphate uptake and metabolism of the SNF enabled crop plants.

As stated before, legumes that are able to form a symbiosis with diazotrophs populate habitats around the world. Legumes are thus found in areas of low phosphate conditions in

the soil, such as the Cape Floristic Region in South Africa; the tropics and south-western Australia (Hidaka and Kitayama, 2013; Lambers et al., 2012). As SNF is maintained in the low level of available phosphate conditions, these legumes use combinations of adaptations to obtain phosphate from the soil, and or to regulate phosphate metabolism and transport. All plants possess the genetic information to adapt to phosphate stressed conditions; however, the ability to do so differs in the extent of their needs. It is thus important to determine the extent of adaptations used by these legumes to survive and maintain SNF during phosphate stress periods. This information can then be compared to the relevant pathways in the crop enabled with SNF; any other crop; and or other legume species that can come under threat of low available phosphate conditions (Zhu et al., 2005). The regulation of the crop's pathways can then be adapted to imitate that of the studied legume and tested to determine if the crop can survive and maintain SNF during phosphate stressed periods.

Work done on the transcriptomes of plants under phosphate stress has helped considerably towards finding focus research areas. However the transcriptome can be altered rapidly by the plant, thus the time of sampling is critical and it does not give the entire picture of what is happening in the cell. Transcriptome methodology is still expensive and might deter researchers as replications of the experiments are required over the various plant organs. When working on a plant species of which the genome has not yet been sequenced and assembled, the transcriptome is referenced according to the available genome of a close relative. Thus only giving an estimate of the plant of interest's genome activity in the cell at the time. The data must then be reanalyzed when the genome of the plant of interest becomes available. Thus physiological studies can be used to determine organ-specific responses to phosphate stress without a species-specific reference, within a relatively short amount of time and resources to ensure reproducibility. As the technology used for genome sequencing and assembly, and transcriptomics become more accessible to researchers, it can place the physiological work in context with the plant's genome and create an overall setting of tissue stress responses. Research done in this manner will lead to the understanding of legumes' ability to survive phosphate stressed conditions and maintain SNF. This can then be implemented directly to legumes in the field as well as used in developing sustainable crop practices that involve SNF.

Out of the bulk of research done on plants and phosphate stress, very little thereof focuses on legumes and SNF. Of this research, most of the effort is put into understanding the regulation of the low and high-affinity phosphate transporters on the root surface and

within the plant. These studies are mainly done on a select few model legumes such as *Glycine max* and *Medicago truncatula*. As *Glycine max* is used in agriculture and *Medicago truncatula* is closely related to *Medicago sativa* which is used in agriculture, this research can be directly implemented into the field. However, other adaptations to phosphate stress are not studied as well. These include the effect that phosphate stress has on the photosynthetic capabilities and the activity of enzymes involved with bypassing phosphate requiring metabolic steps and the assimilation of the fixed nitrogen of the legume and BNF symbiosis. Different stages of phosphate stress are also evident. Plants that are grown throughout their lifespan in phosphate poor soil respond differently than plants with induced phosphate stress, as stated before. However, specific comparisons between these scenarios and their effect on the different organs and tissues of the plant are lacking in the current literature.

1.6 References

Anderson DM, Gilbert PM, Burkholder JM. 2002. Harmful algal blooms and eutrophication: nutrient sources, composition, and consequences. Estuaries 25, 704-726.

Aykroyd WR and Doughty J. 1982. History of Legumes. In: Doughty J and Walker A (eds). Legumes in human nutrition. Rome: Food and Agriculture Organisation of the United Nations 2, 3-14.

Banfield, J. 2006. The chemistry of the main group elements. In: Kotz, JC, Treichel, PM, Weaver GC (eds). Chemistry & Chemical Reactivity, 1012-1067.

Bloom AJ. 2006. Assimilation of mineral nutrients. In: Taiz L and Zeiger E (eds). Plant Physiology. Sunderland: Sinauer Associates, Inc., 289-313.

Bloom AJ. 2006. Mineral nutrition. In: Taiz L and Zeiger E (eds). Plant Physiology. Sunderland: Sinauer Associates, Inc., 73-94.

Dean J. 2009. 'Natural' nitrogen-fixing bacteria protect soybeans from aphids. http://phys.org/news/2009-04-natural-nitrogen-fixing-bacteria-soybeans-aphids.html. Accessed October 2014.

Dixon R and Kahn D. 2004. Genetic regulation of biological nitrogen fixation. Nature Reviews Microbiology 2, 621-631.

Doyle JJ and Luckow MA. 2003. The Rest of the Iceberg. Legume diversity and evolution in a phylogenetic context. Journal of Plant Physiology 131, 900-910.

Elser J and Bennett E. 2011. A broken biogeochemical cycle. Nature 478, 29-31.

Francisco PB and Akao S. 1993. The 2,4-D-induced wheat para-nodules are modified lateral roots with structure enhanced by rhizobial inoculation. Plant and Soil 157, 121-129.

Hidaka A and Kitayama K. 2013. Relationship between photosynthetic phosphorus-use efficiency and foliar phosphorus fractions in tropical tree species. Ecology Evolution 15, 4872-4880.

Horton HR, Moran LA, Scrimgeour KG, Perry MD, Rawn JD. 2006. Amino acid metabolism. In: Carlson G (ed). Principles of Biochemistry. Upper Saddle River: Pearson Education, Inc., 520-556.

Information about the Family Leguminosae. 2006. ILDIS International Legume Database & Information Service. http://www.ildis.org/Leguminosae/. Accessed November 2015.

Judd WS and Olmstead RG. 2004. A survey of tricolpate (eudicot) phylogenetic relationships. American Journal of Botany 10, 1627-1644.

Kennedy IR and Tchan YT. 1992. Biological nitrogen fixation in non-leguminous field crops: recent advances. Plant and Soil 141, 93-118.

Kotz JC. 2006. Principles of reactivity: chemical equilibria. In: Kotz, JC, Treichel, PM, Weaver GC (eds). Chemistry & Chemical Reactivity. 756-795.

Lambers H, Cawthray GR, Giavalisco P, Kuo J, Laliberté E, Pearse SJ, Scheible WR, Stitt M, Teste F, Turner BL. 2012. Proteaceae from severely phosphorus-impoverished soils extensively replace phospholipids with galactolipids and sulfolipids during leaf development to achieve a high photosynthetic phosphorus-use-efficiency. New Phytologist 196, 1098-1108.

Lewis GP. 2005. Introduction. In: Legumes of the World. Kew, Royal Botanic Gardens, 1-20.

Mosaicco. 2015. Phsophate mining. http://www.mosaicco.com/florida/mining.htm. Assessed March 2016.

Mulongoy K. 1992. Biological Nitrogen fixation. Alley farming training manual 2, 17-20.

Rees DC, Howard JB. 2000. Nitrogenase: standing at the crossroads. Current Opinion in Chemical Biology 4, 559-566.

Ruttenburg KC. 2003. The global phosphorous cycle. In: Schlesinger WH (ed). Biogeochemistry: Treatise on Geochemistry. Amsterdam: Elsevier Science 8, 585-643.

Santi C, Bogusz D, Franche C. 2013. Biological nitrogen fixation in non-legume plants. Annuals of Botany 111, 743-767.

Sulieman S, Ha CV, Schulze J, Tran LSP. 2013. Growth and nodulation of symbiotic *Medicago truncatula* at different levels of phosphorus availability. Journal of Experimental Botany, 1-12.

Valentine AJ, Benedito VA, Kang Y. 2011. Legume nitrogen fixation and soil abiotic stress: from physiology to genomics and beyond. In: Foyer CH and Zhang H (eds). Nitrogen metabolism in plants in the post-genomic era. West Sussex: Wiley-Blackwell 42, 207-248.

Vance CP, Uhde-Stone C, Allan DL. 2003. Phosphorous acquisition and use: critical adaptations by plants for securing a nonrenewable resource. New Phytologist 157, 423-447.

Willey JM, Sherwood LM, Woolverton CJ. 2008. Microbial growth. In: Prescott, Harley, Klein (eds). Microbiology. New York: McGraw-Hill Companies, Inc., 119-147.

Willey JM, Sherwood LM, Woolverton CJ. 2008. Biogeochemical cycling and introductory microbial ecology. In: Prescott, Harley, Klein (eds). Microbiology. New York: McGraw-Hill Companies, Inc., 643-666.

Willey JM, Sherwood LM, Woolverton CJ. 2008. Microorganisms in terrestrial environments. In: Prescott, Harley, Klein (eds). Microbiology. New York: McGraw-Hill Companies, Inc., 687-716.

Wisniak J. 2005. Phosphorus-From discovery to commodity. Indian Journal of Chemical Technology 12, 108-122.

Zhu H, Choi HK, Cook DR, Shoemaker RC. 2005. Bridging model and crop legumes through comparative genomics. Journal of Plant Physiology 4, 1189-1196.

CHAPTER 2
GENERAL INTRODUCTION

2.1 Introduction

The term “model organisms” includes species that have been used in many studies because they have a certain set of characteristics. These species include organisms that directly benefit humankind and or organisms that increase the efficiency of laboratory and experimental research (Hedges, 2002). A number of species from the Legume family have these characteristics and are used in fundamental research. *Glycine max* (L.) Merrill (soybean), *Pisum sativum* L. (pea), *Phaseolus vulgaris* L. (French bean), *Lupinus* and *Medicago* are grown as foodstuff and fodder and were thus chosen as legume model organisms. These plants also have the ability to form the symbiosis with diazotrophic soil bacteria (SNF). *Lotus japonicus* L. (lotus) was first used as a model organism because of the cultural significance of the plant (Lewis, 2005). However, after the sequencing of the *L. japonicus* genome, it has become an important tool in the comparison of its determinate nodules (Chapter 1.3.3) versus the indeterminate nodules (Chapter 1.3.3) of *Medicago truncatula* (Gepts et al., 2005; Rose, 2008).

Physiological studies on legumes have been numerous in the past; however, these topics have become less popular in the last few decades. The onset of the ‘Omics era brought forward a constant increase in the affordability of generating copious amounts of data, which placed physiological studies in lesser demand. The conclusions made from the physiological and ‘Omics studies can be placed in the context with eachother to produce an overview of what is happening in the plant. As the requirements for effcient ‘Omics research is different from that of physiological studies, the ‘Omics field has its own subset of model organisms. Therefore the physiological knowledge base of these species is not as strong as that of previously studied model organisms. It is thus more challenging to place ‘Omics derived data from this model organism subset in the context of the plant system. One of the species in this ‘Omics model organism subset is the legume *Medicago truncatula*.

The following chapter aims to summarise the current knowledge of the model legume *M. truncatula*. Thereafter, two scenarios of soil phosphate content reduction are explained. The two sections will then lead to the hypothesis and aims of studying the effects of phosphate stress on nodulated *M. truncatula*. The next section discusses the parameters measured in the study in order to determine the possible plant stress. The chapter will then conclude.

2.2 *Medicago*: the model Legume

Medicago (Latin: *Medica*, or “from Media” an ancient country in the south-western area of Asia) is a genus of 87 species (Allen and Allen, 1981; Steele et al., 2010). These species are classified into the sections of Cartiensae, Platycarpae, Lupularia, Lunatae, Heynianae, Dendrotelis, Orbicularus, Geocarpae, Medicago, Hymenocarpos, Buceras and Spirocarpos (Steele et al., 2010). In the greater legume family, *Medicago* is part of the Trifolieae tribe, which is situated in the inverted repeat-lacking clade of the Papilionoideae subfamily (Fig. 1.1, p. 2) (Lewis, 2005).

2.2.1 *Medicago truncatula* origin and morphology

Medicago truncatula (barrel medic) is a Spirocarpos species native to the Mediterranean. Natural populations have been sampled in Spain, Turkey, Greece, Lebanon, France, Iraq, Italy, Syria, Morocco, Libya, Egypt, Tunisia, Iran, Jordan and Algeria; and on the islands of Cyprus Rhodes, Crete, Capri, Malta, Sardinia, Sicily, and Corsica (Lensis and Lensis, 1979; Delalande et al., 2007). It is cultivated mainly in Australia, where it serves as a forage and crop rotation plant (Choi et al., 2004).

The plant is characterised as a small (150-800 mm long), herbaceous annual (Lenis and Lensis, 1979). When growing in an environment with low sunlight and or at high plant density, the main axis is elongated. Without these stresses, the main axis forms the leaves at the neck level with short growth between nodes, thus forming a rosette (Moreau, 2006). The leaves are formed of three leaflets, as characteristic of the Trifolieae tribe. Each leaflet can be between 8-27 mm long by 7-21 mm wide with an obovate shape (oval that narrows towards the base). The apical section of each leaflet is serrated with alternating large and

smaller triangular teeth. The upper side of the leaflets has fewer hairs than the bottom side (Lensis and Lensis, 1979). Each leaflet may form an anthocyanin spot in the middle of the upper side (Moreau, 2006).

Three months after germination, yellow florets are formed that are 5-8 mm in length. The floret morphology is standard with that of the Papilionoideae subfamily, as described in the previous chapter (Section 1.2.1). After self-pollination, the florets form cylindrical coiled pods that can be 4.5-7 mm in diameter, containing one or two seeds per coil. The seeds are small and can amount to 5 grammes per 1 000 seeds (Lensis and Lensis, 1979).

Medicago truncatula forms one primary root where from all lateral roots are grown. Root architecture is highly dependent on the environment in which it is found. The optimum soil for *Medicago* is well-drained, deep, aerated with a relatively neutral pH range of 6.5 to 7.5 (Allan and Allan, 1981). If the plant experiences nutrient and or water deficiency the root architecture will change in order to enhance the probability of obtaining the required substance. *Medicago truncatula* has the ability to form root symbioses with AM fungi, when in need of water and certain nutrients; and with the nitrogen-fixing soil bacterium *Sinorhizobium meliloti* for the formation of indeterminate nodules. Nodules can be found on the primary root as well as on the lateral roots depending on the strain of nodulating bacteria and root developmental stage at the time of infection (Boualem et al., 2008). The description of AM fungi and nodulation can be found in Chapter 1 of this thesis.

2.2.2 *Medicago* uses and research

The most economically important species of the *Medicago* genus is the perennial, *M. sativa* (Gholami et al., 2014). This species is also known as alfalfa, an Arabicised Persian word that can be traced to the Iranian word for “horse fodder, “aspoasti”. Another common name for this species is lucerne, which relates to the early cultivation of *M. sativa* in Europe by the Lake Lucerne district in Switzerland (Allan and Allan, 1981). This species is the most important foraging crop in the temperate regions of the world. It is seen as the fourth highest valued crop in North America (Gholami et al., 2014). The agricultural importance of this species has led to its frequent use in experiments. Physiological studies on *M. sativa* have been used to better understand indeterminate nodules (Terpolili et al., 2008).

However, with the advent of the 'Omics era, an alternative plant was needed. *M. truncatula* was proposed as a model organism in 1990 by Barker et al. The use of *M. sativa* proved challenging in the new field as it is a perennial cross-fertilizing, autotetraploid species. *Medicago truncatula*, however, is an annual, diploid and self-fertilizing plant. These features are accompanied with *M. truncatula*'s small physical size, short generation time and ability to form symbioses with the same diazotrophic bacteria as *M. sativa* and AM fungi, made *M. truncatula* a better candidate for 'Omics studies (Gholami et al., 2014). Thus researchers are able to obtain adequate sample sizes as a larger amount of plants can be grown over more generations in a controlled area during a certain time frame. The relatively small genome ensures easier experimental design. The ~465 megabases (Mb) *M. truncatula* genome has been sequenced and refined to the latest freely available version Mt4.0 (Tang et al., 2014). As the plants can fertilize themselves, it is easier to breed plants that are homozygous for the gene(s) of interest. Choi et al. (2004) developed a range of genetic markers to create linkage maps to determine synteny between *M. truncatula* and selected legumes. They observed substantial conservation between *M. truncatula* and the diploid *M. sativa* genomes in terms of gene content and order. This enhances the suggestion of *M. truncatula* as a genetic model plant as the research done can be applied to an economically important plant with less additional experimentation than with further related organisms.

The sequencing of both *M. truncatula* and *S. meliloti* genomes have led to the development of bioinformatic tools, the Affymetrix GeneChip® *Medicago* Genome Array (http://www.affymetrix.com/catalog/131472/AFFY/Medicago+Genome+Array#1_1) for transcriptomic studies, and a manual containing protocols for the most effective methods for *M. truncatula* experimental design (http://www.noble.org/medicagohandbook/). These tools have been used to enlarge the data set on the genomic and molecular functioning of nodulation. However one cannot directly use the physiological knowledge of *M. sativa* with *M. truncatula* molecular data. Thus additional studies are required to place the molecular analyses into the greater context of the SNF system.

2.2.3 Phosphate and symbiotic nitrogen fixation

The imminent decline in mineable phosphate for the use in fertilizer is likely to result in a decrease in the yield and security of many crop species including legumes, as discussed in Chapter 1. Management of the remaining phosphate reserve combined with the

breeding or engineering of crops that obtain and utilise phosphate in a more efficient manner can reduce the impact of the possible loss of this macronutrient. Thus is it important to study how the SNF system reacts to growing and surviving in environments where phosphate is the limiting factor. This information can help to design phosphate deficiency management plans and can lead to the discovery of novel or efficient phosphate stress coping mechanisms that could be incorporated into crop plants.

The high level of synteny between *M. sativa* and *M. truncatula* and the molecular resources available make *M. truncatula* a good candidate to use as plant of interest for the study of how the SNF system reacts to phosphate stress.

A *M. truncatula* RNA-sequencing study by Cabeza et al. (2014) revealed that of the nodule genes that were significantly expressed, 7.8% were differentially expressed between two treatments of phosphate. Of these differentially expressed genes, 75.4% were downregulated in the plants that were exposed to phosphate depletion, versus the plants grown at the optimum phosphate level. Downregulated expression includes genes involved in primary and secondary metabolism, while the upregulated expression is part of the stress response. These results indicate the importance of phosphate in the plant system. The study included results of experiments done to determine the possible changes in plant growth and nodule number; the phosphate concentration in the organs; nitrogen fixation; and the amino acid and sugar composition of the nodules when the plants are grown in nutrient-depleted media. This study indicated that *M. truncatula* maintains threshold phosphate levels in the nodules, while the rest of the plant becomes phosphate depleted. The plant SNF system is thus prioritised in terms of nutrients to maintain the fixation of the macronutrient nitrogen for the plant in the hope that it will survive until phosphate is again made available.

The regulation of the plant stress response is not only based on gene level, but also with metabolite availability. A finer look at the possible changes in key enzyme activity can add to the understanding based on the Cabeza et al. (2014) study. Thus the experimental work described in this thesis aims to add to the physiological side of the research involving nodulated *M. truncatula* and phosphate stress.

2.3 Possible phosphate stressed scenarios

There are two highly probable scenarios in which crops can experience phosphate stress. In the one scenario, plants experience phosphate stress throughout the lifespan. The other scenario explains how plants have an induced phosphate starvation period of growth.

2.3.1 Phosphate-deficient lifespan

The first scenario can be described as a crop sown in a field that is phosphate poor. This can happen as the soil of the particular field has not been adequately fertilised to replenish the phosphate used by the previous vegetation and microorganisms, or chelated to metal ions, or leached out. The phosphate concentration available to the plants is not as low to completely deter growth. Soil that has not been adequately fertilised can also lack a stable source of nitrogen. Thus nodulating legume species, such as *Medicago*, will attempt to initialize and maintain SNF despite the phosphate stress. As described in Chapter 1, phosphate is required for the biosynthesis of many essential molecules used by plants. Thus the lack of optimum phosphate throughout the lifespan of the plant could have an effect on certain primary metabolic pathways. As the plant is composed of different organs that are regulated differently, it can be interesting to determine if the photosynthetic organs respond differently to the phosphate stress than the organs found below the ground surface.

The research question that can be formed from this scenario is as follows: How does below optimum phosphate level affect the photosynthesis; biomass; nitrogen and carbon content; and organic acid synthesis of below ground tissues (nodules and roots) and above ground tissues (stems and leaves) of *M. truncatula*?

The hypothesis formulated for this research question is as follows: *Medicago truncatula* grown at low phosphate will have reduced photosynthetic efficiency and biomass, and scavenges and redistributes available P_i for photosynthesis.

To test the hypothesis, *M. truncatula* can be inoculated with *S. meliloti* and grown in a sterile medium. The plants can be given a controlled nutrient solution lacking in nitrogen. The nutrient solution contains a phosphate concentration that is either low enough to produce a stressed phenotype or sufficient to ensure optimum growth of the plant. Plants

grown with the nutrient solution that supports optimum growth serve as the control group. Certain parameters that are linked to the processes listed in the research question can be evaluated experimentally. These analyses will form an understanding that can lead to the rejecting or not the rejecting the first hypothesis.

2.3.2 Induced phosphate deficiency

The second scenario looks at when plants have been sown under optimal phosphate conditions, but during their lifespan, the phosphate supply proceeds to diminish leading to a stressed phenotype. This can happen as a field had been adequately fertilised with phosphate and seeds had been sown in it. Thereafter either the population density of the crop and or microbes had utilised the available phosphate, or chelation or leaching of phosphate had taken place without it being replenished. Plants then experience an induced phosphate stress period.

As in the first scenario, phosphate stress possibly affects nodulated *M. truncatula* primary metabolism in all organs. However in this set of experiments the main organs of interest are found below the ground surface. Thus it is likely that the nitrogen fixing and assimilating tissues, the nodules and roots, experience the stressed period at different degrees.

This leads the discussion to a second research question: How does the starvation of phosphate affect: biomass, nitrogen and carbon content, organic acid synthesis and nitrogen assimilation in *M. truncatula* nodules and roots?

The following hypothesis can be formulated for the above research question: *Medicago truncatula* that has been starved of phosphate will alter organic acid carbon supply to nitrogen assimilation, differently between roots and nodules.

As with the first possible phosphate stress scenario, the plant of interest can be inoculated with *S. meliloti* and grown in similar growth media with a nutrient solution devoid of nitrogen. For the first period of time, all the plants in the experiment will be grown with the same nutrient solution containing the optimal concentration of phosphate. During the second growth period, phosphate stress can be induced to half the plant population by feeding a nutrient solution with an inadequate phosphate concentration. The remainder of the population continues growth with the optimal phosphate concentration and serves as the control group. Parameters that were studied in the first scenario on the below ground

tissues as a whole are again determined, but for the nodules and roots separately. Additional parameters such as the activity of nitrogen assimilating enzymes might give an indication on whether these organs maintain the metabolism of nitrogen when SNF is exposed to suboptimal conditions.

2.4 Parameters to be analysed

Following the two possible scenarios in which inoculated *M. truncatula* can experience phosphate stress a number of parameters can be analysed. Together these analyses could add to the molecular data available to create a better understanding of SNF maintenance during phosphate stress. The next section provides information on the parameters measured to help in rejecting or not rejecting the hypotheses set for each scenario.

2.4.1 Photosynthesis

Photosynthesis (synthesis using light) is the first pathway that comes to mind when one speaks of plants. The process harvest energy from light (photons) to drive the formation of carbohydrates (glucose; $C_6H_{12}O_6$) and oxygen (O_2) from carbon dioxide (CO_2) and water (H_2O) (Blankenship, 2006).

$$6\ CO_2 + 6\ H_2O \rightarrow C_6H_{12}O_6 + 6\ O_2$$

Photosynthesis is also linked to an electron transport system that converts the energy absorbed from the photons into chemical energy. This energy is used to drive various steps in plant metabolism. One of the molecules produced is adenosine triphosphate (ATP; $C_{10}H_{16}N_5O_{13}P_3$) that lends phosphorylation potential to reactions. While the other molecule produced is the reductant nicotinamide adenine dinucleotide phosphate (NADPH; $C_{21}H_{29}N_7O_{17}P_3$) (Hind, 1982). During phosphate stressed conditions it was found that the expression of genes that code for many of the subunits needed to produce the photosystem complexes are downregulated. In addition, the decline in available P_i to produce ATP reduces the activity of ATPase (EC 3.6.3.52) leading to the negative regulation of ribulose-1,5-bisphosphate carboxylase/oxygenase (RuBisCo, EC 4.1.1.39). It

is thus expected that the activity of photosynthesis will decline during the phosphate stressed period (Hermans et al., 2006).

In order to determine the rate at which a plant is photosynthesising, the rate at which it is exchanging CO_2 and H_2O with the atmosphere can be measured. This can be done by using the infrared gas analyser (IRGA) in a closed system. Here follows a simplified explanation of how CO_2 exchange is measured. A leaf is enclosed in a chamber that houses the calibrated analyses tubes of the IRGA. The leaf is then irradiated with a source of light that can be regulated and supplied with a set and known concentration of CO_2 at a fixed flow rate. The chamber does not allow for the air inside the chamber to escape the system, nor air from the atmosphere to enter the system. The air from the chamber is then monitored for a change in CO_2 concentration. If the air from the chamber contains less CO_2 than what is supplied to the leaf, the net reaction is favoured toward photosynthesis. If the measured CO_2 concentration is more than what is supplied, the leaf's net reaction is favoured towards photorespiration (Long, 1982). The rate of photosynthesis is calculated by the IRGA in micromoles of CO_2 per square metre per second (µmol $CO_2.m^{-2}.s^{-1}$).

By regulating the amount of light energy (photosynthetic active radiance; PAR; µmol photons.$m^{-2}.s^{-1}$) that the leaf is exposed to and measuring the stable photosynthetic rate at each PAR setting, one is able to set up a light response curve (LRC). The LRC displays photosynthetic rate as a function of PAR. From this curve, it is possible to calculate certain parameters. These include: The saturated photosynthetic rate (Pmax) as the photosynthetic rate value where the LRC reaches a plateau and thus photosynthesis is no longer limited by light, but by CO_2. The light compensation point (LCP), as the concentration of PAR where the plant crosses over from respiration to photosynthesis (the net reaction thus equals zero, or put differently, the plant respires as much as it photosynthesizes). The quantum yield (QY) is calculated from the slope of the curve as the photosynthetic rate increases above zero. The photosynthetic respiration rate (PR) indicates how much CO_2 the plant is giving off when exposed to complete darkness. The possible photosynthetic productivity (PPP) of the plant is the ratio of Pmax and PR. Another parameter can be calculated using Pmax and the concentration of P_i in the leaf tissue, called the photosynthetic phosphate use efficiency (PPUE).

When these parameters are compared between the treatments of stressed and non-stressed plants, one can determine whether it is possible for phosphate to affect the fundamental process of photosynthesis.

2.4.2 Biomass, growth allocation and relative growth rate of organs

A comparison of biomass between phosphate stressed and non-stressed plants is an indication of whether the treatment group is affected by the reduced availability of phosphate. As discussed in Chapter 1.4.1 a symptom of phosphate stress is stunted growth. This is a symptom that many crop producers would like to avoid.

The commonly used method to determine biomass is by harvesting the plant material as fresh weight (FW), placing the material in an oven until it breaks crisply when bent and then weighing the material as dry weight (DW). This method ensures that variability of the water content between plants is reduced and only the mass produced by the plant is determined. Dry weight can also be calculated by using a ratio of FW versus DW as determined by a previous sample. The DW root to shoot ratio comparison is another indication of plant phosphate stress. Plants growing in phosphate poor soils will increase root growth and surface area to try and obtain phosphate in other parts of the soil (Vance et al., 2003). The stunted growth and increase in root growth should increase the root to shoot ratio of plants under phosphate stress versus those grown in optimal conditions (Hermans et al., 2006).

As stated above it is expected that plants grown under phosphate stressed conditions increase their root systems while overall growth is stunted in comparison to the control plants. However, it is still relevant to determine the growth allocation rate (GA) of each system or organ of interest (Bazzaz, 1998). The comparison of GA between the phosphate treatments can indicate to which system or organ biomass is being allocated to at a different rate owing to the reduced availability of phosphate.

Another parameter that can be calculated using biomass is relative growth rate (RGR). This parameter is used as a fundamental measure of the production of the dry biomass of the system or organ over a certain period of time relative to the plant as a whole. Relative growth rate can be used to determine if a system or organ is increasing in biomass at a different rate at certain time points during its lifespan. This can also be compared between the phosphate stressed and non-stressed plants while keeping the time points normalised (Beadle, 1982).

2.4.3 Inorganic phosphate, δ^{13} carbon and δ^{15} nitrogen determination

With the use of an assay and isotopes the P_i, carbon and nitrogen content of plant material can be determined. These analyses can indicate the possible differences in the amount of phosphate that is available for metabolism and the proportion of biomass that consists of carbon and nitrogen, between organs or treatments (Le Roux et al., 2009).

These values can also be used to calculated certain parameters such as the PPUE (as described in section 2.4.1); the carbon and nitrogen construction cost (C_W); the specific nitrogen utilisation rate (SNUR); growth respiration rate ($R_g(t)$); and the amount of nitrogen in the plant that was fixed from the atmosphere (%NDFA). These calculations are discussed in the following section.

2.4.4 Carbon and nitrogen cost and efficiency

The calculation for C_W is used to determine the amount of carbon that is used by the plant to construct new tissue with the carbon and nitrogen available at the time. This comparison between treatments can indicate whether more carbon is needed to produce growth during phosphate stress and if it could strain the photosynthetic pathway (Mortimer et al., 2005).

The SNUR of a plant is an indication of the efficiency at which the plant uses nitrogen to produce biomass. It is presented as the amount of DW of the system or organ per nitrogen content per day. If the value is to increase for a certain treatment it indicates that more biomass is created for the same amount of nitrogen and period of time. A difference between treatments may show that adequate phosphate is required to maintain the optimal use of nitrogen to produce new tissue. This calculation done by Nielsen et al. (2001) for phosphate efficiency had been adapted for nitrogen use.

The rate of growth respiration of a system or tissue shows the amount of CO_2 that is respired by the tissue per unit of growth per day. This parameter is also an indication of the efficiency of the plant by using the nutrients available for growth. An increase in $R_g(t)$ indicates an increased loss of carbon for each unit of growth per day. Thus the efficiency of the plant is reduced. By comparing this parameter between phosphate treatments, it is possible that the amount phosphate that is available to the plant can have an effect on the carbon efficiency of growth (Peng et al., 1993).

The following parameter is used with plants that can initiate and maintain SNF. The portion of nitrogen present in the plant that was derived from the atmosphere is an indication of how efficient the plant is to assimilate nitrogen made available by SNF. As the nutrient solution did not contain nitrogen the plants used in this body of work were dependent on SNF for survival. A low %NDFA will show that the plant had relied on the nitrogen stored in the seed and the little nitrogen administered before SNF was established. As the fixation of nitrogen from the atmosphere requires a relatively large amount of energy derived from phosphate, a phosphate stressed plant would recycle the nitrogen already in the system, or try to maintain sufficient levels of phosphate in the nodules, or both (Shearer and Kohl, 1986).

From the parameters described above further nitrogen efficiency calculations can be made such as the BNF uptake efficiency; root (soil) uptake efficiency; nodule nitrogen uptake per P_i; and root nitrogen uptake per P_i.

2.4.5 Phosphoenolpyruvate carboxylase

Phosphoenolpyruvate carboxylase (PEPc; EC 4.1.1.31) is a soluble protein found in the cytoplasm of plant cells and bacteria. Phosphoenolpyruvate carboxylase catalyses the reaction of phosphoenolpyruvate (PEP; $C_3H_5O_6P$) with bicarbonate (HCO_3^-) to form oxaloacetate ($C_4H_4O_5$) and inorganic phosphate (P_i; HPO_4^{2-}):

Phosphoenolpyruvate + HCO_3^- → Oxaloacetate + P_i

By producing oxaloacetate the enzyme thus catalyses one of the anaplerotic reactions needed by the tricarboxylic acid cycle (TCA cycle). The plant also uses PEPc to regulate seed germination, root cation levels, the pH level in the vacuole, stomatal movements, and the maturing of fruit. The enzyme is involved in the transfer of reducing power of NADH and recaptures carbon from respiration. Plant species that make use of the C_4 or the Crassulacean acid metabolism (CAM) modes of photosynthesis express additional isoforms of PEPc that are adapted to the specific mode of photosynthesis. Phosphoenolpyruvate carboxylase has also been found to supply SNF with carbon thus aiding in nitrogen assimilation (Lepiniec et al., 1993; Silvera et al., 2014).

Isoforms of this protein vary as the function of PEPc varies. By the year 2002, 75 various isoforms of PEPc had been identified (Kai et al., 2003). The square structure of PEPc is owing to the “dimer-of-dimers” configuration of the four identical 95 to 116 kDa

(kilodalton) subunits. The metal cations of magnesium (Mg^{2+}) and manganese (Mn^{2+}) are cofactors for PEPc. The enzyme is activated by glucose 6-phosphate ($C_6H_{13}O_9P$) from the upstream metabolism of sucrose ($C_{12}H_{22}O_{11}$), while the allosteric inhibitors malate ($C_4H_6O_5^{2-}$) and aspartate ($C_4H_7NO_4^{1-}$) are products of downstream reactions that use oxaloacetate as a reactant. Phosphoenolpyruvate carboxylase isoforms that form part of the C_4 and CAM modes of photosynthesis are additionally regulated by light. Optimal PEPc activity is reached at a pH of 7.5-8.5 to maintain the K_m values of PEP and bicarbonate in the same order of magnitude (Lepiniec et al., 1994).

Owning to the production of P_i, it is thought that PEPc is involved in the stress response to phosphate deficiency. When the concentration of phosphate in the cell is reduced so that normal functioning is negatively affected, non-phosphorylating enzymes are induced to maintain the essential metabolism pathways. One of the essential pathways is glycolysis. Thus PEPc activity is increased in order to bypass the phosphate requiring enzyme pyruvate kinase (PK; discussed in the following section) (Rychter et al., 2015). The P_i molecule released from PEP is recycled to maintain the phosphate homoeostasis of the plant (Plaxton and Carwell, 1999). The production of oxaloacetate in roots can lead to the exudation of this negatively charged organic acid. The metal cations such as Fe^{2+} and Al^{2+} that chelate P_i in the soil and render it unavailable for plant uptake (as discussed in Chapter 1.4.1) also bind to the exuded organic acids. Therefore decreasing the probability of the metal cations to bind to applied or freed P_i in the soil and thus increasing the P_i uptake of plants and bacteria (Vance et al., 2003).

It is thus important to establish to what level *M. truncatula* uses this bypass enzyme in terms of other enzymes that are regulated during phosphate stress.

2.4.6 Pyruvate kinase

Pyruvate kinase (PK; EC 2.7.1.40) is a cytosolic enzyme found ubiquitously in all plants. It is not solely a plant protein, as it is found in all organisms that contain the Glycolytic pathway. Through the use of substrate level phosphorylation, PK activity is responsible for the direct conversion of PEP into pyruvate ($C_3H_4O_3$) (Podestá and Plaxton, 1992).

Phosphoenolpyruvate + ADP → Pyruvate + ATP

Pyruvate is transported into the mitochondrion where it is converted to acetyl-CoA ($C_{23}H_{38}N_7O_{17}P_3S$) or oxaloacetate and fed into the TCA cycle to produce substrates for

biosynthesis pathways and respiration (Oliver et al., 2008). This molecule is also the precursor to the synthesis of amino acids such as alanine ($C_3H_7NO_2$), isoleucine ($C_6H_{13}NO_2$), leucine and valine ($C_5H_{11}NO_2$) (Horton et al., 2006). The cytosolic plant PK enzyme is characterised as a heterotetramer comprised of subunits of either 56 or 57 kDa. Together the heterotetramer is approximately 250 kDa. For the reaction to commence the cations Mg^{2+} and potassium (K^+) are required. The affinity of PK to the substrates is highest in an environment where the pH is 6.5 to 7.5. Molecules that inhibit the activity of PK include oxalate ($C_2O_4^{2-}$), magnesium citrate ($C_6H_6MgO_7$) and glutamate ($C_5H_9NO_4$). Aspartate can act as an activator of PK by removing the inhibition caused by glutamate and by facilitating the binding of the substrate PEP to the enzyme's active site (Hu and Plaxton, 1996).

As pyruvate is constantly used by the cell, PK is categorized as one of the maintenance enzymes of the plant. Unless the plant is experiencing highly stressed conditions, the activity of PK will not be lower than a baseline rate (Sung et al., 1988). Under phosphate stress, the expression levels of PK genes are not different from that when not under stress (Cabeza et al., 2014). Pyruvate kinase is however in contest with other enzymes, such as PEPc (as mentioned above), for the substrates PEP and ATP. Pyruvate kinase is not the sole catalyst for the production of pyruvate. Mitochondrial NADP-malic enzyme (ME, EC 1.1.1.40) and lactate dehydrogenase are two examples of enzymes that are able to produce pyruvate in organelles or in the cytosol as needed (Drincovich et al., 2001). Thus the cell is able to function without the optimal activity of PK, as the phosphate stress condition of the plant places phosphate containing molecules such as ADP for use by other enzymes.

It is thus interesting to study the activity of PK in the context of the activity of the "bypass" enzyme, PEPc during the phosphate optimum and stressed conditions.

2.4.7 NADH-malate dehydrogenase

Malate dehydrogenase (MDH; EC 1.1.1.37) that uses NADH as reducing agent, is a cytosolic enzyme found in eukaryotic and prokaryotic cells. Cytosolic MDH in eukaryotes functions as a malate/aspartate shuttle to exchange reducing equivalent between the cytosol and the mitochondrial membranes. By catalysing the reversible reaction of reducing oxaloacetate with the coenzyme NADH to malate and NAD^+, both oxaloacetate

and malate are transported across the membranes instead of NADH and NAD^+ (Minárik et al., 2002).

Oxaloacetate + NADH ⇌ Malate + NAD^+

Malate dehydrogenase is active as a dimer of two identical subunits. Each subunit can be 39 to 35 kDa. Cytosolic MDH activity is regulated by the availability of the substrate and coenzyme. Mitochondrial MDH activity in either direction is inhibited by citrate ($C_6H_8O_7$). However, when the concentrations of malate and NAD^+ are high, citrate is an activator of the enzyme. Chloroplast NADPH-MDH enzyme activity is enhanced as the disulphide bridges in each subunit N-terminus is reduced and thus cleaved. This reduction potential is produced via the electron transport chain from photosynthesis. Thus chloroplast NADPH-MDH is indirectly regulated by the concentration of light the plant experiences (Goward and Nicholls, 1994).

As discussed above with PEPc and oxaloacetate, malate as a negatively charged organic acid is also exuded into the rhizosphere. Exuded organic acids increase the mobilisation of chelated soil phosphate, and the amenability to dephosphorylation by exuded acid phosphatases (to be discussed in the following section) and the solubility of organic phosphate. These reactions in the soil enhance the possibility of soil microorganisms and plant roots to obtain phosphate from the soil (Plaxton and Tran, 2011).

Cytosolic MDH activity is increased with the availability of the reaction's substrates. As the expression level of PEPc is increased during phosphate stress, the oxaloacetate concentration in the cytosol is also likely increased. Thus either the expression level or the activity of MDH must increase to enable the cell to metabolise the accumulated oxaloacetate. Through the sequencing of the transcriptome of *M. truncatula* nodules that have been subjected to phosphate depletion for five days, it was determined that MDH expression level remained relatively unchanged when compared to the plants that received optimal phosphate throughout the growth period (Cabeza et al., 2014). Thus it is a possibility that MDH activity is increased at the substrate level during phosphate stress. Malate is also an important source of energy and carbon to the bacteroid. It serves as the carbon skeleton for the formation of asparagine in the nodule. Asparagine is one the main amino acids that are allocated to the shoots of plants that are amide exporters, such as *M. truncatula* (Fischinger and Schulze, 2010).

The activity of MDH is the following step from PEPc to circumvent the phosphate requiring PK reaction to produce the pyruvate needed in the TCA cycle. The last enzyme in the PK "bypass" route is ME. Malic enzyme catalyses the reaction of malate in the mitochondrion to pyruvate by oxidising NAD^+ to NADH and respiring a molecule of carbon dioxide (CO_2) (Drincovich et al., 2001; Plaxton and Tran, 2011). However, ME is not discussed further in this body of work. It is thus important to determine whether the activity of MDH is influenced by a change in phosphate availability to the plant. This data can then be used in relation to that of PEPc and PK to produce an idea of the magnitude that *M. truncatula* uses this "bypass" route during phosphate stress.

2.4.8 Acid phosphatase

The Acid phosphatases (APase; EC 3.1.3.2) represent a family of soluble enzymes that are ubiquitously found in all organisms. There are a variety of these enzymes to suit every cell and every situation. The most researched APase class is the purple acid phosphatase (PAP) (Olczak et al., 2003). The essential reaction that these proteins catalyse is the hydrolysis of a phosphate monoester or anhydride to form an alcohol and P_i molecule (Vance et al., 2003; Hurley et al., 2010). Phosphate monoesters include PEP, mononucleotides, ATP, sugar phosphates and inorganic pyrophosphate (Olczak et al., 2003). These reactions can be catalysed under acidic conditions, thus the specificity of the acid phosphatase name (Hurley et al., 2010).

Phosphate monoester + $H_2O \rightleftharpoons$ Alcohol + P_i

Acid phosphatases are used by cells to remobilise internal phosphate to facilitate distribution of phosphate where needed (Hurley et al., 2010). As the pH range of most soil types is between neutral and acidic, it is favourable for APase activity. Various bacteria and plants thus secrete APases into the surrounding soil to free phosphate from organic matter. The freed phosphate can then be taken up by the organisms in the surrounding area (Rodríguez and Fraga, 1999).

Purple acid phosphatase is named after the purple-pinkish colour of isolated enzymes in a water solution. This colour is caused by a charge transfer between a tyrosine residue and the "chromophoric" Fe^{3+} ion. This Fe^{3+} ion is accompanied by either a zinc (Zn^{2+}) or a manganese (Mn^{2+}) "non-chromophoric" ion in the plant PAP binuclear metal site. There are two groups of plant PAPs. The enzymes are placed in the groups based on size.

Smaller PAPs are monomeric enzymes of about 35 kDa. These PAPs, such as AtACP5, generally hydrolyze para-nitrophenyl phosphate (pNPP, $C_6H_6NO_6P$) to para-nitrophenol (pNP, $C_6H_5NO_3$) and P_i. The larger PAPs are placed in a different group. These enzymes are generally 55 kDa and are composed of two identical monomers to form a dimer. Each monomer has a binuclear metal site with a Fe^{3+} ion and either a Zn^{2+} or Mn^{2+} ion bound. The "non-chromophoric" ion does not necessarily have to be the same in each monomer (Olczak et al., 2003).

Under phosphate deprived conditions the expression levels of APases, especially PAPs, were upregulated in *M. truncatula* (Cabeza et al., 2014). As APases free phosphate from organic molecules that are either found within the cell or in the soil, it is important to the plant to have a high concentration of these enzymes present during periods of phosphate stress. It is interesting to note that APase competes with PEPc and PK for the substrate PEP. An increase in APase activity might have some effect on the substrate availability of PEPc and APase. A look at how APase activity is affected by the change in phosphate availability of nodulated *M. truncatula* plants may indicate how the symbiosis uses these important enzymes in relation to PEPc and PK.

2.4.9 Nitrate reductase

Nitrate reductase (NR; EC 1.6.6.1) is a soluble protein found in the cytoplasm or bound to plasma membranes. It is there where nitrate (NO_3^-) is reduced by NAD(P)H to nitrite (NO_2^-), $NAD(P)^+$ and water (Kaiser et al., 2011).

$$NO_3^- + NAD(P)H \rightarrow NO_2^- + NAD(P)^+ + H_2O$$

The enzyme itself is comprised of two identical subunits forming a dimer. Each subunit is about 100 kDa with an active site where e^- are donated from NAD(P)H and another active site for the reduction of NO_3^-. The C-terminal (carbon terminal) of each subunit contains the flavin adenine dinucleotide (FAD) cofactor. The next domain is connected by a "hinge" and contains the heme-Fe. Another domain is connected to the heme-Fe domain with a flexible "hinge" and the molybdenum-molybdopterin (Mo-MPT) cofactor (Kaiser et al., 2011).

The NR enzyme can be inactivated by phosphorylation on a serine residue located on the hinge between the heme-Fe domain and the Mo-MPT domain and the binding of a NR inhibitor protein (NIP) (Kaiser and Huber, 2001). Nitrate reductase is also inhibited by the

binding of tungsten (W) to the Mo-MPT co-factors (Adamakis et al., 2012). If the enzyme is found in the photosynthetically active region of the plant, it was found that NR activity is increased when exposed to light and the sugars produced by photosynthesis (Kaiser and Huber, 2001). Nitrate reductase is also capable of reducing NO_2^- further to nitrogen oxide (NO). This reaction uses molecular oxygen as e^- donor. This reaction is competitively by NO_3^- as and is not as prominent as the above-mentioned reaction (Kaiser and Huber, 2001; Kaiser et al., 2011).

Nitrite is further reduced to NH_4^+ by the enzyme nitrite reductase (EC 1.7.7.1). To reduce NO_3^- to NH_4^+ in this manner, a cell uses the equivalent of 10 ATP molecules (Bloom, 2011).

As discussed before (Chapter 1.3.1), NO_3^- can be readily absorbed by plant roots from the soil. The nitrogen atom is reduced until it forms NH_4^+. Thereafter it is assimilated into an amino acid and used where needed throughout the plant. The primary route for NO_3^- to enter this pathway is through NR. Nodulated legumes depend on SNF to provide nitrogen for assimilation. However, as mentioned before, SNF requires a relatively large amount of energy to function. If NO_3^- is available, the plant would rather absorb and metabolise it to NH_4^+, as this route requires about 36% less energy than SNF (Bloom, 2011). As the legumes in this study will not be fed NO_3^-, it will be interesting to see whether NR activity will be affected by the availability of phosphate under constant SNF conditions.

2.4.10 Glutamine synthetase

Glutamine synthetase (GS; EC 6.3.1.2) is an enzyme that can be found in the cytoplasm (GS1 form) and in plant plastids (GS2 form) (Lea and Miflin, 2011). Through substrate level phosphorylation glutamate ($C_5H_8NO_4$) is made into the active intermediate γ-glutamyl phosphate ($C_5H_{10}O_7P$). Ammonium is then deprotonated and assimilated into the intermediate to form glutamine ($C_5H_{10}N_2O_3$) and P_i (Bloom, 2011).

Glutamate + ATP → γ-glutamyl phosphate + ADP

γ-glutamyl phosphate + NH_4^+ → Glutamine + H^+ + P_i

Glutamine synthetase is made up of identical subunits (38-40 kDa each in GS1 and 44-45 kDa each in GS2) that form two pentameric rings that sit face-to-face. This configuration produces ten active sites between subunits' N-terminal and C-terminal found

across the rings (Seabra et al., 2013). Regulation of GS activity is similar to that of NR described above (Lea and Miflin, 2011). Co-factors of the enzyme include cobalt ion (Co^{2+}), Mn^{2+} and Mg^{2+} (Bloom ,2006).

Ammonium ions can also be absorbed via the roots from the soil. As NO_3^- is soluble in water, this nitrogen source can be leached from the soil when it rains or flooding occurs. Thus NH_4^+ is sometimes the most abundant nitrogen source other than SNF. The assimilation of absorbed NH_4^+ is also less expensive in terms of energy than to first reduce NO_3^- to NH_4^+. Plants can prefer NH_4^+ as a source of nitrogen and use GS to metabolise it to keep the cellular concentration below toxic (Bloom, 2011). As NH_4^+ is first deprotonated before the reaction can start, NH_3^+ from SNF is used by GS to start nitrogen assimilation pathway (Seabra et al., 2013).

Glutamine synthetase works in cohort with the enzyme glutamate synthase, or glutamine:2-oxoglutarate aminotransferase (GOGAT; EC 1.4.1.14). Glutamate synthase produces two glutamate molecules from the reaction of glutamine, 2-oxoglutarate (α-ketoglutarate; $C_5H_6O_5$), NADH and H^+ in the roots. By using the GS/GOGAT system the plant can assimilate one NH_4^+ molecule into two molecules of amino acids (glutamate) by only using the energy equivalent of two ATP molecules (Bloom, 2011).

The GS/GOGAT system requires phosphate to help catalyse the assimilation of NH_4^+/NH_3^+. The scenario of a nodulated legume planted in soil containing low phosphate levels could have an effect on the activity of this first step in the assimilation of the most important nutrient to plant life.

2.4.11 Aspartate aminotransferase

After nitrogen has been assimilated into glutamine and glutamate transamination reactions incorporate it into other amino acids. One of these transaminating enzymes is aspartate aminotransferase (AAT; EC 2.6.1.1). This cytosolic and plastidic enzyme catalyses the reversible formation of aspartic acid (aspartate; $C_4H_7NO_4$) and 2-oxoglutarate from glutamate and oxaloacetate (Bloom, 2006).

Glutamate + Oxaloacetate ⇌ Aspartate + 2-oxoglutarate

Aspartate aminotransferase in the plastid is a dimer of two identical monomer subunits. The subunits are approximately 45 kDa and when dimerized produce two active sites

(Del la Torre et al., 2014). All aminotransferases require pyridoxal 5'-phosphate, the active form of vitamin B_6 (PLP; $C_8H_{10}NO_6P$) as a coenzyme (Wilkie et al., 1996; Horton et al., 2006).

Oxaloacetate is produced by PEPc as carbon is fixed. Aspartate is used in the malate/aspartate shuttle of cytosolic MDH as described earlier in this chapter. This amino acid as the receptor of glutamine's amide nitrogen via the catalysis by asparagine synthetase (AS; EC 6.3.5.4). This irreversible reaction requires ATP and yields the amino acid asparagine ($C_4H_8N_2O_3$) (Horton et al., 2006). Legume amide exporters use asparagine as the main amino acid to transport from the nodules to the shoots (Sprent, 2009; Bloom, 2011). Aspartate is also the precursor to threonine ($C_4H_9NO_3$), lysine ($C_6H_{14}N_2O_2$) and methionine ($C_5H_{11}NO_2S$) (Horton et al., 2006). The 2-oxoglutarate is used by GOGAT to produce more glutamate.

Aspartate aminotransferase is thus an essential enzyme in the biosynthesis of not only aspartate but many other amino acids. As AAT relies on products from PEPc for the forward reaction, it might compete with MDH. However, the forward reaction product is required with the product of MDH to enable the transport of reducing equivalents across the membranes of organelles (Wilkie et al., 1996). The reverse reaction of AAT is also used by the plant to produce glutamate when the GS/GOGAT system is not as effective. Reports of significantly increased asparagine levels in *M. truncatula* shoots during phosphate stress have been made by Sulieman et al. (2013). The increase of this amino acid is thought to be a signal from the shoots to down regulate the activity of nitrogen fixation in the nodules. It is thus interesting to measure the activity of AAT during phosphate stress as it will impact on PEPc, MDH GOGAT and AS activities.

2.4.12 Glutamate dehydrogenase

NAD(H)-glutamate dehydrogenase (GDH; EC 1.4.1.2) is a protein found in the mitochondria, while NADP(H)-GDH is found in the chloroplast (Turano et al., 1997). This enzyme catalyses the synthetic reaction of the amination of 2-oxoglutarate and the catabolic reaction of deaminating glutamate (Loulakakis and Roubelakis-Angelakis, 1991).

$$\text{Glutamate} + H_2O + NAD(P)^+ \rightleftharpoons \text{2-oxoglutarate} + NH_3^+ + NAD(P)H + H^+$$

Glutamate dehydrogenase structure varies depending on the tissue it is found in. Two different subunits (α- and β-polypeptides) assemble in different ratios to create the

hexameric structure. The α-polypeptide has a molecular weight of 43.0 kDa, while the β-polypeptide is slightly smaller at 42.5 kDa (Dubois et al., 2003).

With this variation in structure, it is difficult to determine the specific function of GDH. The structure type formed of the enzyme in particular tissues is regulated by the expression levels of the α- and β-polypeptide genes (Labboun et al., 2009). Two strong hypotheses for the main function of GDH have been put forward. The one hypothesis argues that GDH's main function is to oxidise glutamate to provide carbon skeletons to GOGAT and the TCA cycle, and has no or little nitrogen assimilation activity. The GS/GOGAT system is thus seen as the major pathway to the assimilation of NH_3^+. Under nitrogen stress or in senescing tissues, however, GDH activity is increased. This second hypothesis suggests that GDH may form part of the reassimilation of nitrogen in dying cells to be transported to young or growing tissue. Glutamate dehydrogenase can in this way be complimentary to the GS/GOGAT system (Robinson et al., 1991; Turano et al., 1997). A hypothesis that is less frequently reported questions whether GDH is rather a stress monitoring protein by sensing the redox status of each tissue (Dubois et al., 2003).

As GDH competes for substrates with GS, GOGAT and AAT (in both directions of the catalysis) and is also associated with stress response. Thus it will be interesting to determine whether GDH changes the rate of the anabolic and or catabolic reactions during phosphate stress and how the possible change compares to the other enzymes in nitrogen metabolism.

2.5 Conclusion

The analyses of the parameters described above on the tissues of *M. truncatula* that had been inoculated with the nitrogen-fixing soil microorganism *S. meliloti* and grown under the two described possible phosphate stressed conditions could enrich the current information regarding SNF and its ability to survive and maintain function under nutrient stress.

With this background in mind, the following main hypothesis was set up: Lifelong and induced phosphate stress in *M. truncatula* will induce metabolic phosphate recycling and saving in the above and below ground organs, to affect the efficiency of carbon and nitrogen metabolism.

The main hypothesis was built on the hypotheses for the two possible phosphate stressed scenarios as described in section 2.3. These being: *Medicago truncatula* grown at low phosphate will have reduced photosynthetic efficiency and biomass, and scavenges and redistributes available P_i for photosynthesis (section 2.3.1). And: How does the starvation of phosphate affect: biomass, nitrogen and carbon content, organic acid synthesis and nitrogen assimilation in *M. truncatula* nodules and roots? (section 2.3.2).

2.6 References

Adamakis IDS, Panteris E, Eleftheriou EP. 2012. Tungsten toxicity in plants. Plants 2, 82-99.

Allen ON and Allen EK. 1981. The Leguminosae. In: Allen ON (ed). The Leguminosae. A source book of characteristics, uses and nodulation. London: Macmillan Publishers, 3-706.

Barker DG, Bianchi S, Blondon F, Datteé Y, Duc G, Essad S, Flament P, Gallusci P, Génier G, Guy P, Muel X, Tourneur JD, Huguet T. 1990. *Medicago truncatula*, a model plant for studying the molecular genetics of the Rhizobium-legume symbiosis. Plant Molecular Biology Reporter 8, 40-49.

Bazzaz FA. 1998. Allocation of resources in plants: state of science and critical questions. In: Bazzaz FA and Grace J (eds). Plant resource allocation. San Diego: Physiological Ecology Series of Academic Press, 1-37.

Beadle SP. 1982. Plant growth analysis. In: Coombs J and Hall DO. Techniques in bioproductivity and photosynthesis. Oxford: Pergamon Press 20-25.

Blankenship RE. 2006. Photosynthesis: the light reactions. In: Taiz L and Zeiger E (eds). Plant Physiology. Sunderland: Sinauer Associates, Inc., 125-158.

Bloom AJ. 2006. Assimilation of mineral nutrients. In: Taiz L and Zeiger E (eds). Plant Physiology. Sunderland: Sinauer Associates, Inc., 289-313.

Bloom AJ. 2011. Energetics of nitrogen acquisition. In: Foyer CH and Zhang H (eds). Nitrogen metabolism in plants in the post-genomic era. West Sussex: Wiley-Blackwell 42, 63-81.

Boulalem A, Laporte P, Jovanovic M, Laffont C, Plet J, Combier J, Niebel A, Crespi M, Frugier F. 2008. MicroRNA166 controls root and nodule development in *Medicago truncatula*. The Plant Journal 54, 876-887.

Cabeza RA, Liese R, Lingner A, Von Stiegiltz I, Neumann J, Salinas-Riester G, Pommerenke C, Dittert K, Schulze J. 2014. RNA-seq transcriptome profiling reveals that *Medicago truncatula* nodules acclimate N_2 fixation before emerging P deficiency reaches the nodules. Journal of Experimental Botany 65, 6035-6048.

Choi H, Kim D, Uhm T, Limpens E, Lim H, Mun J, Kalo P, Penmetsa RV, Seres A, Kulikova O, Roe BA, Bisseling T, Kiss GB, Cook DR. 2004. A sequence-based genetic map of *Medicago truncatula* and comparison of marker colinearity with *M. sativa.* Genetics 166, 1463-1502.

Del la Torre F, Cañas RA, Pascual MB, Avila C, Cánovas FM. 2014. Plastidic aspartate aminotransferases and the biosynthesis of essential amino acids in plants. Journal of Experimental Biology 65, 5527-5534.

Delalande M, Greene S, Hughes S, Nair R, Huguet T, Aouani ME, Prosperi JM. 2007. Wild accessions / populations. In: Mathesius U, Journet EP, Sumner LW (eds). The *Medicago truncatula* Handbook, 1-27.

Drincovich MF, Casati P, Andreo CS. 2001. NADP-malic enzyme from plants: a ubiquitous enzyme involved in different metabolic pathways. Federation of European Biochemical Societies Letters 490, 1-6.

Dubois F, Tercé-Laforgue T, Gonzalez-Moro M, Estavillo J, Sangwan R, Gallais A, Hirel B. 2003. Glutamate dehydrogenase in plants: is there a new story for an old enzyme? Plant Physiology and Biochemistry 41, 565-576.

Fischinger SA and Schulze J. 2010. The importance of nodule CO_2 fixation for the efficiency of symbiotic nitrogen fixation in pea at vegetative growth and during pod formation. Journal of Experimental Botany 61, 2281–2291.

Gepts P, Beavis WD, Brummer EC, Shoemaker RC, Stalker HT, Weeden NF, Young ND. 2005. Legumes as a model plant family. Genomics for food and feed report of the cross-legume advances through Genomics conference. Plant Physiology 137, 1228–1235.

Gholami A, De Geyter N, Pollier J, Goormachtigab S, Goossens A. 2014. Natural product biosynthesis in *Medicago* species. Natural Product Report 31, 356-380.

Goward CR and Nicholls DJ. 1994. Malate dehydrogenase: a model for structure, evolution, and catalysis. Protein Science 3, 1883-1888.

Hedges SB. 2002. The origin and evolution of model organisms. Nature Reviews Genetics 3, 838-849.

Hind G. 1982. Photosynthetic energy conversion. In: Coombs J and Hall DO (eds). Techniques in bioproductivity and photosynthesis. Oxford: Pergamon Press, 112-117.

Hermans C, Hammond JP, White PJ, Verbruggen N. 2006. How do plants respond to nutrient shortage by biomass allocation? Trends in Plant Science 11, 610-617.

Horton HR, Moran LA, Scrimgeour KG, Perry MD, Rawn JD. 2006. Amino acid metabolism. In: Carlson G (ed). Principles of Biochemistry. Upper Saddle River: Pearson Education, Inc., 520-556.

Hu Z and Plaxton WC. 1996. Purification and characterization of cytosolic Pyruvate Kinase from leaves of the Castor Oil Plant. Archives of Biochemistry and Biophysics 333, 298-307.

Hurley BA, Tran HT, Marty NJ, Park J, Snedden WA, Mullen RT, Plaxton WC. 2010. The dual-targeted purple acid phosphatase isozyme AtPAP26 is essential for efficient acclimation of *Arabidopsis* to nutritional phosphate deprivation. Journal of Plant Physiology 153, 1112-1122.

Kaiser WM and Huber SC. 2001. Post-translational regulation of nitrate reductase: mechanism, physiological relevance and environmental triggers. Journal of Experimental Biology 52, 1981-1989.

Kaiser WM, Planchet E, Rümer S. 2011. Nitrate reductase and nitric oxide. In: Foyer CH and Zhang H (eds). Nitrogen metabolism in plants in the post-genomic era. West Sussex: Wiley-Blackwell 42, 127-145.

Labboun S, Tercé-Laforgue T, Roscher A, Bedu M, Restivo FM, Velanis CN, Skopelitis DS, Moshou PN, Roubelakis-Angelakis KA, Suzuki A, Hirel B. 2009. Resolving the role of plant glutamate dehydrogenase. I. *in vivo* real time nuclear

magnetic resonance spectroscopy experiments. Plant and Cell Physiology 50, 1761-1773.

Le Roux MR, Khan S, Valentine AJ. 2009. Nitrogen and carbon costs of soybean and lupin root systems during phosphate starvation. Symbiosis 48, 102-109.

Lea PJ and Miflin BJ. 2011. Nitrogen assimilation and its relevance to crop improvement. In: Foyer CH and Zhang H (eds). Nitrogen metabolism in plants in the post-genomic era. West Sussex: Wiley-Blackwell 42, 1-40.

Lesins KA and Lesins L.1979. Subgenus Spirocarpus. In: Junk D (ed). Genus *Medicago* (Leguminosae). A taxogenetic study. Hague: Kluwer Academic Publishers Group, 140-215.

Lepiniec L, Keryer E, Philippe H, Gadal P, Crétin C. 1993. Sorghum phosphoenolpyruvate carboxylase gene family: structure, function and molecular evolution. Plant Molecular Biology 21, 487-502.

Lepiniec L, Vidal J, Chollet R, Gadal P, Crétin C. 1994. Phosphoenolpyruvate carboxylase: structure, regulation and evolution. Plant Science 99, 111-124.

Lewis GP. 2005. Introduction. In: Legumes of the World. Kew, Royal Botanic Gardens, 1-20.

Long SP. 1982. Measurement of photosynthetic gas exchange. In: Coombs J and Hall DO. Techniques in bioproductivity and photosynthesis. Oxford: Pergamon Press, 25-34.

Loulakakis KA and Roubelakis-Angelakis KA. 1991. Plant NAD(H)-glutamate dehydrogenase consists of two subunit polypeptides and their participation in the seven isoenzymes occurs in an ordered ratio. Journal of Plant Physiology 97, 104-111.

Minárik P, Tomáškova N, Kollárová M, Antálik M. 2002. Malate dehydrogenases – structure and function. General Physiology and Biophysics 21, 257-265.

Moreau D. 2006. Morphology, development and plant architecture of *M. truncatula*. In: Mathesius U, Journet EP, Sumner LW (eds) The *Medicago truncatula* handbook, 1-6.

Mortimer PE, Pérez-Fernández MA, Valentine AJ. 2005. Mycorrhizal C costs and nutritional benefits in developing grapevines. Mycorrhiza 15, 159-165.

Nielsen KL, Eshel A, Lynch JP. 2001. The effect of phosphorous availability on the carbon economy of contrasting common bean (*Phaseolus vulgaris* L.) genotypes. Journal of Experimental Botany 52, 329-339.

Olczak M, Morawiecka B, Wątorek W. 2003. Plant purple acid phosphatases — genes, structures and biological function. Acta Biochimica Polonica 50, 1245-1256.

Oliver SN, Lunn JE, Urbanczyk-Wochniak E, Lytovchenko A, Van Dongen JT, Faix B, Schmälzlin E, Fernie AR, Geigenberger P. 2008. Decreased expression of cytosolic pyruvate kinase in potato tubers leads to a decline in pyruvate resulting in an *in vivo* repression of the alternative oxidase. Plant Physiology 148, 1640-1654.

Peng S, Eissenstat DM, Graham JH, Williams K, Hodge NC. 1993. Growth depression in mycorrhizal citrus at high-phosphorous supply. Journal of Plant Physiology 101, 1063-1071.

Plaxton WC and Carswell MC. 1999. Metabolic aspects of the phosphate starvation in plants. In: Lerner HR (ed). Plant responses to environmental stresses: from phytohormones to genome reorganisation. London: CRC Press, 349-372.

Plaxton WC and Tran HT. 2011. Metabolic adaptations of phosphate-starved plants. Plant Physiology 156, 1006-1015.

Podestá FE and Plaxton WC. 1992. Plant cytosolic pyruvate kinase: a kinetic study. Biochimica et Biophysica Acta 1160, 213-220.

Robinson SA, Slade AP, Fox GG, Phillips R, Ratcliffe RG, Stewart GR. 1991. The role of glutamate dehydrogenase in plant nitrogen metabolism. Journal of Plant Physiology 95, 509-516.

Rodríuez H and Fraga R. 1999. Phosphate solubilising bacteria and their role in plant growth promotion. Biotechnology Advances 17, 319-339.

Rose RJ. 2008. *Medicago truncatula* as a model for understanding plant interactions with other organisms, plant development and stress biology: past, present and future. Functional Plant Biology 35, 253-264.

Rychter AM and Szal B. 2015. Alternative pathways and phosphate and nitrogen nutrition. In: Gupta KJ, Mur LAJ, Neelwarne (eds). Alternative respiratory pathways in higher plants. Chichester: John Wiley & Sons, Ltd, 53-74.

Seabra AR, Silva LS, Carvalho HG. 2013. Novel aspects of glutamine synthetase (GS) regulation revealed by a detailed expression analysis of the entire GS gene family of *Medicago truncatula* under different physiological conditions. BioMed Central Plant Biology 13, 1-15.

Shearer GB and Kohl DH. 1986. N_2-fixation in field settings: estimates based on natural ^{15}N abundance. Australian Journal of Plant Physiology 13, 699-756.

Silvera K, Winter K, Rodriguez BL, Albion RL, Cushman JC. 2014. Multiple isoforms of phosphoenolpyruvate carboxylase in the Orchidaceae (subtribe Oncidiinae): implications for the evolution of crassulacean acid metabolism. Journal of Experimental Botany 65, 3632-3636.

Sprent JI. 2009. Development and functioning of nodules. In: Sprent JI (ed). Legume nodulation: a global perspective. West Sussex: Wiley-Blackwell 1, 79-94.

Steele KP, Ickert-Bond SM, Zarre S, Wojciechowski MF. 2010. Phylogeny and character evolution in *Medicago* (Leguminosae): Evidence from analyses of plastid *trnK*/*matK* and nuclear *GA3ox1* sequences. American Journal of Botany 97, 1142-1155.

Sung S-J, Xu S, Galloway D-P, Black CM. 1988. A reassessment of glycolysis and gluconeogenesis in higher plants. Physiologia Plantarum 72, 650-654.

Tang H, Krishnakumar V, Bidwell S, Rosen B, Chan A, Zhou S, Gentzbittel L, Childs KL, Yandell M, Gundlach H, Mayer KFX, Schwartz DC, Town CD. 2014. An improved genome release (version Mt4.0) for the model legume *Medicago truncatula*. BioMed Central Genomics 15, 312-326.

Terpolili JJ, O'Hara GW, Tiwari RP, Dilworth MJ, Howieson JG. 2008. The model legume *Medicago truncatula* A17 is poorly matched for N_2 fixation with the sequenced microsymbiont *Sinorhizobium meliloti* 1021. New Phytologist 179, 62-66.

Turano FJ, Thakkar SS, Fang T, Weisemann JM. 1997. Characterization and expression of NAD(H)-dependent glutamate dehydrogenase genes in *Arabidopsis*. Journal of Plant Physiology 113, 1329-1341.

Vance CP, Uhde-Stone C, Allan DL. 2003. Phosphorous acquisition and use: critical adaptations by plants for securing a nonrenewable resource. New Phytologist 157, 423-447.

Wilkie SE, Lambert R, Warren MJ. 1996. Chloroplastic aspartate aminotransferase from *Arabidopsis thaliana*: an examination of the relationship between the structure of the gene and the spatial structure of the protein. Biochemical Journal 319, 969-976.

CHAPTER 3
WHAT ARE THE BELOW GROUND CARBON COSTS OF PHOSPHATE STRESS IN *MEDICAGO TRUNCATULA*?

3.1 Summary

The availability of phosphate for plant uptake can limit the yield of natural and agricultural systems. As legumes that have established symbiosis with *Rhizobium* have an additional phosphate sink, the nodule, these plants are at a disadvantage when grown under phosphate-limited conditions. Thus adaptations to survive under phosphate stress may vary between tissues that have different functions in the plant. In this study, the physiological adaptations to phosphate stress in the above and below ground organs of nodulated *Medicago truncatula* Gaertner were tested. *Medicago truncatula* (A17) seedlings were inoculated with *Sinorhizobium meliloti* 1026 and grown in quartz sand. The growing plants were fed full strength Long Ashton nutrient solution with either 0.010 mM (stressed, low phosphate, LP) or 0.500 mM (control, high phosphate, HP) phosphate concentrations. Nodulated *Medicago truncatula* grown under constant LP conditions had a compromised photosynthesis system. Alternative growth allocation during LP was observed between the different organs. The content of inorganic phosphate, carbon and nitrogen in these plants were also lower during LP. Strategies of phosphate management differed between above and below ground plant tissues. The above ground tissues saved phosphate by the use of glycolytic “bypass” enzymes to scavenge phosphate and lower the plant’s dependence on adenosine-triphosphate required metabolism. Whereas the below ground tissues recycled phosphate from phosphate monoesters in the cell via acid phosphatase activity. The different phosphate management systems that were found in *Medicago truncatula* could lead to further research in the agricultural application of phosphate to legume crops for efficient yield production.

3.2 Introduction

Phosphate is one of the most limiting nutrients to plant growth. It is an essential element as its best-known attribute is in the process of energy generation. Furthermore, phosphate is used in photosynthesis; redox reactions; the synthesis and stability of membranes; the synthesis of nucleic acids; signalling; in the regulation of enzyme activity; carbohydrate metabolism; respiration; nitrogen fixation; glycolysis; and other processes (Vance et al., 2003). Plants obtain phosphate via root uptake in the forms of dihydrogen phosphate ($H_2PO_4^-$) or monohydrogen phosphate (HPO_4^{2-}) ions. On average the concentration of inorganic phosphate (P_i) in the soil is 1 to 2 µM, however, $H_2PO_4^-$ and HPO_4^{2-} concentration may vary from 0.1 to 10 µM (Kochian et al., 2004, Vance et al., 2003). These phosphate ions can be bound to metal ions such as aluminium and iron in acidic soils or calcium in alkaline soils (Kochian et al., 2004; Nautiyal et al., 2000). Most plant species are unable to take up bound P_i directly, and P_i chelation thus leads to phosphate deficient soil conditions. Under such conditions, if free inorganic soil phosphate is not increased via fertilisation, or if the existing bound P_i is not released, most plant species would tend to experience phosphate stress and reduced yields. Increasing phosphate concentration via fertilisation of crops is economically inefficient for farmers because crops utilise only up to 30% of the added nutrient. The remainder is taken up by the microbiome, chelated or leached from the rhizosphere by rain or irrigation (López-Arredondo et al., 2014).

Inorganic phosphate limitation is particularly relevant for farmers of legume crops. Legumes are second to the cereal grains as the world's most important crops, nutritionally and economically (O'Rourke et al., 2014). On the one hand legume farmers require less nitrogen in the fertiliser owing to the ability of many leguminous plants to form a symbiosis with the soil nitrogen fixing bacteria of Rhizobia. However, in exchange for this important nutrient, the bacteroid is a strong sink for photosynthates as well as phosphate (Sulieman and Tran, 2015). Thus legume farmers require phosphate application strategies that will release this non-renewable nutrient into the rhizosphere over an extended time. Unfortunately, these strategies are more expensive than the standard fertiliser, thus making it especially unavailable to small-scale farmers (Vance et al., 2003). Another approach is to determine the strategies used by legume crop plants to adapt to phosphate stress in order to develop appropriate soil and P_i management strategies.

Different crops respond to phosphate stress in diverse combinations of adaptations. Species-specific adaptations include different levels of enhanced uptake or acquisition of P_i, and the conservation of phosphate allocation and use in the whole plant (Vance et al., 2003). Thus different crop species and even varieties require individualised soil and fertilisation management strategies to obtain optimal yields.

Phosphate stress affects the entire plant; however few studies have been done to compare the adaptive strategies of the photosynthetic versus non-photosynthetic tissues. These distinct tissue types have different nutrient requirements and could, therefore, induce conflicting demands with respect to the optimal phosphate concentration in the soil medium. This study aims to elucidate what differences that might exist between the physiological response to a constant phosphate stress by the below and above ground tissues of the crop model legume, *Medicago truncatula* Gaertner.

3.3 Materials and Methods

3.3.1 Plant material

Seeds of the experimental *M. truncatula* (A17) line (The Samuel Roberts Noble Foundation, USA) were chemically scarified following the protocol described in the Medicago Handbook (Garcia et al., 2006). Seedlings were randomly selected and planted in 15 cm plastic pots containing quartz sand. The potted plants were placed in a temperature controlled, North-facing greenhouse (Natuurwetenskappe Building, Stellenbosch). Nutrient solution (50 ml) was administered on a Monday and Friday, while plants were watered with 50 ml of distilled water on a Wednesday. *Sinorhizobium meliloti* strain 1026 (The Samuel Roberts Noble Foundation, USA) was prepared for growth on the day of potting the *M. truncatula* seedlings. Preparation of bacteria and inoculation of the seedlings was done following the protocol provided in the Medicago Handbook (Journet et al., 2006). A modified Long Ashton nutrient solution (Smith et al., 1983) was prepared for every treatment (Macronutrients: 1.50 mM $MgSO_4.7H_2O$, 2.00 mM K_2SO_4, 4.00 mM $CaCl_2.2H_2O$; Micronutrients: 0.165 mM solution of 0.139 mM H_3BO_3, 0.021 mM $MnSO_4.4H_2O$, 0.002 mM $ZnSO_4.7H_2O$, 0.003 mM $CuSO_4.5H_2O$, 0.0003 mM $Na_2MoO_4.2H_2O$; Iron: 0.022 mM FeEDTA; Good's buffer: 0.100 mM MES). For the first three feedings 0.500 mM $(NH_4)_2SO_4$ was added to the

nutrient solution to ensure that plants do not experience nitrogen stress until biological nitrogen fixation (BNF) is sufficiently activated. The pH of the nutrient solution was adjusted to range between 5.8 and 6.0.

Two treatments were made, each with a varied concentration of phosphate ($NaH_2PO_4 \cdot 2H_2O$): 0.500 mM (optimum) and 0.010 mM (stressed). Plants fed with the solution containing 0.500 mM phosphate served as the control and are further referred to as HP (High Phosphate). Plants that were fed with the solution containing 0.010 mM phosphate served as the treatment group and are further referred to as LP (Low Phosphate).

3.3.2 Photosynthesis

At five weeks after potting, three plants of each treatment were used to determine possible differences in photosynthetic efficiency between treatments.

The LI-COR LI-6400 XT Portable Photosynthesis System (LI-COR Biosystems, USA) was used for all measurements. Measurements were done between 10:00 and 16:00. The youngest fully opened leaf was used from each plant. The following parameters were logged: photosynthetic rate (A) as µmol $CO_2.m^{-2}.s^{-1}$; stomatal conductance (g_s) as mol $H_2O.m^{-2}.s^{-1}$; intercellular CO_2 concentration (C_i) as µmol $CO_2.mol^{-1}$ air and transpiration rate (E) as mmol $H_2O.m^{-2}.s^{-1}$.

The reference CO_2 input was set at 400 µmol $CO_2.s^{-1}$. Leaf temperature was set to 25 ℃. While the air flow rate was 500 µmol air.s^{-1}. The photosynthetic active radiance (PAR) was set to 50 µmol photons.$m^{-2}.s^{-1}$, a leaflet was inserted into the chamber and after 5 min or when the C_i reading was stable, five consecutive readings of the above-mentioned parameters were taken. Measurements were repeated for each of the following PAR settings: 100; 250; 350; 450; 650; 850; 1 050; 1 300; 1 500 and 0 µmol photons.$m^{-2}.s^{-1}$. The leaf used was harvested, fresh weight (FW) measured, leaf area was determined, dried and the dry weight (DW) measured.

A light response curve (LRC) was set up for each treatment and the saturated photosynthetic rate (Pmax); light compensation point (LCP); quantum yield (QY); photosynthetic respiration rate (PR); photosynthetic phosphate use efficiency (PPUE); and the possible photosynthetic productivity (PP) were calculated. Pmax is designated as the photosynthetic rate value where the LRC reaches a plateau. The LCP is the amount of

PAR where the plant crosses over from respiration to photosynthesis (photosynthetic rate equals zero). The QY is calculated as the slope of the graph while photosynthesis increases. The photosynthetic respiration rate indicates how much CO_2 the plant is giving off during darkness (PAR equals zero). The efficiency at which the plant uses inorganic phosphate (P_i) during photosynthesis (PPUE) was calculated as Pmax per mM of P_i present per m^2 of the leaf. Possible photosynthetic productivity is determined as the ratio of Pmax and PR.

3.3.3 Harvest

At ten weeks after potting plants were harvested (end point harvest). Plants organs were separated as leaves, stems, roots and nodules. The organs were weighed (as FW) and stored at -80 ℃. The material of five plants was pooled to create eight samples of each organ for the HP treatment and seven samples of each organ for the LP treatment. Further analysis compared the below ground tissues (BG) to the above ground tissues (AG).

3.3.4 Biomass

The measured FW of each plant was converted to DW values by using the ratio of FW:DW obtained from the initial harvest. The calculated DW was used to determine the growth allocation (GA) of BG and AG as done using the equation (eqn) below (Bazzaz, 1998). The calculation of this parameter was completed by determining the whole plant relative growth rate (RGR). The relative growth rate was also calculated for BG and AG.

Eqn 3.1 $GA = \frac{df}{dt} = RGR \left(\frac{\partial \text{-} Br}{Bt}\right)$

The fraction for the allocation of new biomass of each organ is calculated from the RGR as milligramme dry weight gained per gramme dry weight of the plant per day. The symbol ∂ shows the new biomass produced during the time the plant had grown. Br is the organ biomass, while Bt is the total plant biomass.

The root to shoot ratio indicates if the plant is under nutrient stress and was calculated for each treatment.

3.3.5 Inorganic phosphate (P_i) concentration and acid phosphatase activity

The determination of P_i for the BG and AG tissues was done using the molybdate blue method as described by Nanamori et al. (2004). Below ground and above ground tissues of three samples per treatment were weighed out to 50 mg and ground into a fine paste with liquid nitrogen before continuing with the method. Chemicals were scaled down as the starting material was reduced in comparison with Nanamori et al. (2004). The concentration of P_i was calculated as the sample absorbance at 820 nm relative to a P_i standard curve and per mg FW. Blank reactions contained incubated assay buffer without the sample.

The acid phosphatase (APase; EC 3.1.3.2) extraction and assay were modified from Hurley et al. (2010). The protein was extracted in the following buffer: 20 mM sodium acetate (pH 5.6); 1 mM EDTA; 1 mM dithiothreitol; 5 mM thiourea; 1% (w/v) insoluble polyvinylpyrrolidone and one complete protease inhibitor cocktail (Roche) tablet per 50 ml buffer. A homogenate of one part tissue with two parts of ice cold extraction buffer (w/v) was made. The homogenate was then centrifuged at 15 000x*g* at 4 ℃ for 10 min. The supernatant was used as the cr ude protein extract. The APase assay was done using this crude extract. The assay mixture contained 50 mM sodium acetate (pH 5.6); 5 mM PEP; 10 mM $MgCl_2$; 0.2 mM NADH and 3 U of lactate dehydrogenase (LDH). The blank mixture contains all the reagents except PEP. Of the crude extract, 30 µl was added to the reaction mixture in a total volume of 250 µl. Absorbance was then measured at 340 nm as the oxidation of NADH at 25 °C for 5 min.

Enzyme activity was defined as the amount of µmol substrate consumed per g FW per minute.

3.3.6 δ^{13} Carbon and δ^{15} nitrogen analysis

Harvested material was dried in a drying oven, set to 50 ℃, until material could easily break. The material was then milled using a tissue lyser at 20 Hz for 3 min. The steel balls were removed and sent to the Archeometry Department, at the University of Cape Town. Analysis of the material included the determination of the δ^{13} carbon and δ^{15} nitrogen ratios. The isotopic ratios were calculated from the equation:

Eqn 3.2 $\delta = 1\,000‰ \left(\frac{R_{sample}}{R_{standard}}\right)$

as R represents the molar ratio of the heavy and light isotopes of the sample and standard used as explained by Farquhar et al. (1989). An average of 2.046 mg DW per sample was placed into a Fisons NA 1500 (Series 2) CHN analyser (Fisons Instruments SpA, Milan, Italy) and combusted. The isotope values were determined by a Finnigan Matt 252 mass spectrophotometer (Finnian MAT GmbH, Bremen, Germany) using a CHN analyser connected to the mass spectrometer via a Finnigan MAT Conflo control unit.

3.3.7 Carbon and nitrogen cost and efficiency calculations

The carbon and nitrogen content of the tissues were calculated from the isotope analyses.

The carbon and nitrogen construction cost (C_W) for each treatment was calculated following Peng et al. (1993) and modified by Mortimer et al. (2005):

Eqn 3.3 $C_w = \left(C + \frac{k\mathrm{N} \times 180}{24}\right)\left(\frac{1}{0.89}\right)\left(\frac{6000}{180}\right)$

as C_W represents the construction cost to produce new tissue (mmol carbon.g^{-1} DW), C shows the concentration of carbon in the sample (mmol carbon.g^{-1} DW), *k* is the nitrogen substrate reduction state as used in the analysis (*k* = -3, NH_3), N is the organic content of nitrogen in the sample (mmol nitrogen.g^{-1} DW) (Williams et al., 1987). The fraction of the tissue construction cost which provides reductant that is not incorporated into biomass is represented by the constant (1/0.89) (Williams et al., 1987; Peng et al., 1993), while the fraction (6000/180) changes the units from g glucose.g^{-1} DW to mmol carbon.g^{-1} DW.

The amount of nitrogen the nodulated plants had derived from the atmosphere (%NDFA) was calculated following Shearer and Kohl (1986):

Eqn 3.4 $\%\mathrm{NDFA} = 100\left(\frac{\delta^{15}\,\text{nitrogen}_{\,\text{Reference plant}} - \delta^{15}\,\text{nitrogen}_{\,\text{Sample}}}{\delta^{15}\,\text{nitrogen}_{\,\text{Reference plant-B}}}\right)$

with *Triticum aestivum* L. used as the Reference plant and the B-value (0.12‰) was the δ^{15} nitrogen of nodulated *Lens culinaris* Medikus grown with a nitrogen-free nutrient solution. Both *T. aestivum* and *L. culinaris* were grown under the same greenhouse conditions as the samples.

From the %NDFA calculation, the efficiency of the nodules to fix atmospheric nitrogen and the efficiency of the roots obtaining nitrogen from the initial nutrient solution feeds were calculated per treatment.

The nitrogen phosphate use efficiency was determined as the ratio of nitrogen content to the P_i concentration in the below and above ground tissues.

3.3.8 Organic acid synthesising enzyme activity

The activity of enzymes involved in the organic acid bypass pathways was determined for the BG and AG tissues. The BG and AG tissues of three samples per treatment were weighed out to 50 mg per assay to be done and ground into a fine paste with liquid nitrogen. Protein extraction for phosphoenolpyruvate carboxylase (PEPc; EC 4.1.1.31); pyruvate kinase (PK; EC 2.7.1.40); and NADH-malate dehydrogenase (MDH; EC 1.1.1.37) was modified to what was described by Ocaña et al. (1996). The extraction buffer comprised of 100 mM Tris-HCl (pH 7.8); 1 mM EDTA; 5 mM dithiothreitol; 20% (v/v) ethylene glycol; 2% (w/v) insoluble polyvinylpyrrolidone and one complete protease inhibitor cocktail (Roche) tablet per 50 ml buffer. Of the ground tissue, one part was added to four parts (w/v) extraction buffer. The homogenate was centrifuged at 3 500x*g* and 4 ℃ for 8 min. The supernatant was carefully removed and centrifuged at 30 000x*g* for 20 min. The remaining supernatant is the protein crude extract.

The assay of PEPc was determined by the oxidation of NADH as measured by Ocaña et al. (1996). The assay mixture comprised of 100 mM Tris (pH 8.5); 5 mM $MgCl_2$; 5 mM $NaHCO_3$; 4 mM phosphoenolpyruvate (PEP); 0.20 mM NADH; and 5 U of MDH. The blank assay mixture had all the reagents except for PEP and sample. Of the crude extract, 30 µl was added to the reaction mixture in a total volume of 250 µl. The absorbance was then measured at 340 nm as the oxidation of NADH at 25 ℃ for 5 min.

The activity of PK was measured as done by McCloud et al. (2001). The assay mixture was 75 mM Tris-HCl (pH 7.0); 5 mM $MgCl_2$; 20 mM KCl; 1 mM ADP; 3 mM PEP; 0.18 mM NADH and 3 U rabbit muscle lactate dehydrogenase (LDH). Two blank mixtures were made. The first had all the reagents except for ADP; while the second had all the reagents except for PEP. The absorbance was measured the same as that of PEPc.

The NADH-dependent MDH assay was done as by Appels and Haaker (1988). This assay mixture constisted of 25 mM potassium phosphate (KH_2PO_4) buffer; 0.2 mM NADH and 0.4 mM oxaloacetate (pH 7.4). Oxaloacetate was prepared fresh at each time of conducting the assay. The blank assay contained all reagents except oxaloacetate. The absorbance was measured the same as that of PEPc.

Enzyme activity was defined as the amount of µmol substrate consumed per g FW per minute.

3.3.9 Statistics

Data and calculations were entered into the program Microsoft® Office Excel 2007 (Microsoft Corporation, 2006). The Student's t-Tests and Duncan's New Multiple Range tests were run using Super-ANOVA (Statsgraphics Version 7, 1993).

3.4 Results

3.4.1 Photosynthesis

The LRC (Fig. 3.1A) for *M. truncatula* grown under phosphate stress was lower than the control. The saturated photosynthetic rate (Fig. 3.1B) of LP was significantly reduced. While the LCP (Fig. 3.1C) was increased as more light was required for the plant to reach equilibrium between photosynthesis and respiration rates. The QY (Fig. 3.1D) under LP was reduced thus less CO_2 was fixed per photon energy. During LP conditions photosynthetic respiration (Fig. 3.1E) was increased. The photosynthetic phosphate use efficiency (Fig. 3.1F) indicated that LP plants fixed more µmol CO_2 per mM P_i than during optimal conditions. However, the possible photosynthetic productivity (Fig. 3.1G) was significantly reduced under phosphate stress.

3.4.2 Biomass, relative growth rates and growth allocation

Biomass values for the BG and AG organs grown under LP were significantly reduced (Fig. 3.2A). The RGR for these tissues were also reduced, however, the RGR of the BG tissues were significantly higher than that of the AG tissues (Fig. 3.2B). This was also evident in the allocation of growth (Fig. 3.2C) to the roots and nodules during LP.

3.4.3 P_i concentration and acid phosphatase activity

The P_i concentration in LP plants was greatly reduced to those grown in optimal conditions (Fig. 3.3A). In the phosphate stressed plants, more P_i was found in the AG tissues than in the BG tissues, however not significant (Fig. 3.3A). The hydrolysis of phosphate monoesters to release P_i was significantly increased during phosphate stress, especially in the BG tissues (Fig. 3.3B).

3.4.4 Carbon and nitrogen cost and efficiency

The carbon and nitrogen content (Table 3.1) was significantly reduced when nodulated *M. truncatula* is grown under phosphate stress. However, the carbon cost of producing new tissue (Table 3.1) had not chanced as the treatment changed. The percentage of nitrogen in the plant that is derived from BNF (Table 3.1) was significantly increased when the plant was under stress. The stressed nodules acquired significantly more nitrogen (Table 3.1) from the initial feedings that contained nitrogen than the roots and the control organs. The BG organs of the stressed plants contained more nitrogen per P_i unit (Table 3.1) than the AG tissues and of the control organs.

3.4.5 Organic acid synthesising enzyme activity

M. truncatula grown under phosphate stress reduced PEPc activity (Fig. 3.4A) in the BG tissues, while it was more active in the AG tissues. The similar trend was observed for PK (Fig. 3.4B) that competes for the same substrate as PEPc. However, PK activity was significant for the AG tissues. The production of malate by MDH (Fig. 3.4C) was not significantly affected by the phosphate deficiency.

3.5 Discussion

The adaptability of crops to low phosphate conditions will influence the level of food security of the world in the current century (Vance et al., 2003). For legume crops that have a relatively high requirement for phosphate in order to maintain BNF function, it is important to know how the AG and BG tissues manage this nutrient stess. The *M. truncatula* in this study that had only a limited amount of available phosphate employed different strategies of phosphate management within the tissues that were located above or below the ground surface.

The availability of phosphate directly influences photosynthesis (Kondracka and Rychter, 1997). Not only is it used to drive the fixation of CO_2 in the form of ATP, it is also used to produce the enzymatic machinery and membranes where the reaction takes place. The photosynthesis of the LP plants was significantly reduced as the plant does not have enough resources to produce leaves (Pieters et al., 2001). The observed increase in the rate of photorespiration can be used by the plant to raise the level of free P_i in the cell. This could have been a result of the hydrolysation of 2-phosphoglycolate to glycolate and P_i by phosphoglycolate phosphatase in the chloroplast (Buchanan and Wolosiuk, 2006). It is important to note that nodulated *M. truncatula* fixed more molecules of CO_2 per mM of P_i under phosphate stress than under optimal conditions. This observed increase in P_i use efficiency was also seen in plants native to phosphate poor soils, such as the tropics, the Cape Floristic Region in South Africa and south-western Australia (Hidaka and Kitayama, 2013; Lambers et al., 2012).

The observed increase in the growth allocation and relative growth rate in the LP plants by the BG tissues could have been to increase the root surface area to scavenge the soil for unused P_i. The relative growth rate was reduced in the AG tissues of these phosphate stressed plants to possibly enable the oganism to sustain the root's requirement of carbon skeletons from photosynthesis. An increased root to shoot ratio is a typical strategy seen in phosphate stressed plants as the root surface area is increased to obtain P_i from the soil.

The P_i concentration in the BG and AG tissues were reduced under phosphate stress, as expected. However, P_i was distributed evenly between the tissues. It appears that the AG P_i management strategy may have been more efficient as the ratio of P_i concentrations in AG versus BG was higher during phosphate stress as compared to optimal phosphate

conditions. This indicates that the AG strategy of phosphate conservation may have benefited the observed increases in photosynthetic phosphate use efficiency. These results are contradictory with what was found by Abolzadeh et al. (2010) in *Lupinus albus*. In this legume the phosphate stressed leaf to root ratio was higher than under optimal conditions, however the ratios themselves were under one, indicating that the roots contained more phosphate. Thus further research is to be done to clarify this result.

The reduced biomass of the stressed plants can be linked to the observed change in carbon and nitrogen content as described by Nielsen et al. (2001). With the observed low P_i concentration in the tissues and the low photosynthesis rate, the stressed *M. truncatula* had fewer resources to produce new tissue. As it was not significantly more expensive in terms of carbon to produce new biomass irrespective of phosphate conditions, it is possible that *M. truncatula* cuold recycle carbon from the TCA cycle or other processes during phosphate stress. However, the nodules were highly nitrogen efficient during phosphate stress as seen from the increases in nitrogen uptake and %NDFA. This trend is also evident in the increase in the amount of nitrogen per P_i specifically in the phosphate stressed BG tissues.

In the cell's cytosol, PEPc and PK compete for the use of PEP to produce oxaloacetate and pyruvate respectively. Irrespective of treatment or tissue, PEPc activity in nodulated *M. truncatula* is significantly higher than that of PK. Whilst the same trend is seen for PK as PEPc, PK activity is not significantly different between treatments or tissues. Pyruvate synthesis could be sustained via LDH or the oxidation of malate via mitochondrial malic enzyme (EC 1.1.1.19). Sung et al. (1988) suggested that the kinases involved in the classic glycolysis pathway, including PK, act as a function of the plant's maintenance system. Thus the activity of these enzymes remains relatively constant owing to a decrease in sensitivity to environmental conditions.

The production rate of oxaloacetate via PEPc is increased in the AG tissues under phosphate stress. Under the same conditions, the production rate of malate via cytosolic MDH is also increased. Malate is synthesised from oxaloacetate that is produced either from PEPc or from aspartate via aspartate aminotransferase (EC 2.6.1.1). Sulieman et al (2013) described an accumulation of malate in *M. truncatula* nodules under phosphate stress. Cytosolic malate, citrate, glutamate and aspartate are inhibitors of PEPc (Moraes and Plaxton, 2000). While the malate produced can be transported to the mitochondrion to produce citrate, or to the vacuole to be stored and regulate pH. Malate and citrate can also be exported by the BG tissues to the soil in order to free chelated P_i. Citrate accumulation

in nodules under phosphate stress was also noted by Sulieman et al. (2013). The negative charge of malate and citrate competes with phosphate to bind with the positively charged metal ions of aluminium, iron and calcium. Thus unbound P_i is less likely to chelate, as the positive ions are already bound to the exuded organic acids. The plant is then able to take up P_i as the root surface area increases. The export of malate and citrate places strain on the carbon skeleton pool from photosynthates. Thus the reduced activity of BG PEPc may be a malate feedback inhibition to conserve carbon skeletons for other processes in the cell (Moraes and Plaxton, 2000). The increase of AG PEPc and MDH activities may be attributed to the need to sustain carbon skeleton intermediates of the TCA cycle while conserving the available phosphate.

The activity of APase indicates the redistribution of P_i within tissues or from anhydrides derived from senescing tissues. APase enzymes are also exported from the BG tissues to hydrolyse phosphate monoesters found in the soil (Wang et al., 2011). However, only internal APase activity was determined in this study. The activity of APase is not only higher under phosphate stress; it is also significantly higher than PEPc and PK activities. As APase can also hydrolyse PEP to form pyruvate and thus competes with PEPc and PK. The highest APase activity is found BG, where P_i redistribution is required not only for the growth of the root surface area but the sustained activity of nitrogen fixation of the nodules.

3.6 Conclusion

During phosphate deficiency from germination, nodulated *M. truncatula* that relies solely on BNF as nitrogen source needs to use the available phosphate efficiently to maintain photosynthesis, growth and BNF. Although there were typical phosphate stressed induced morphological changes, the most striking adaptations were the alteration of phosphate management in the different tissues. In this regard, the above ground tissues conserved the available phosphate via metabolic bypass reactions, associated with the PEP-derived organic acid synthesis. In contrast to this, the below ground tissues engaged in more phosphate recycling via APases in order to make more phosphate available for metabolic reactions.

3.7 Figures and Table

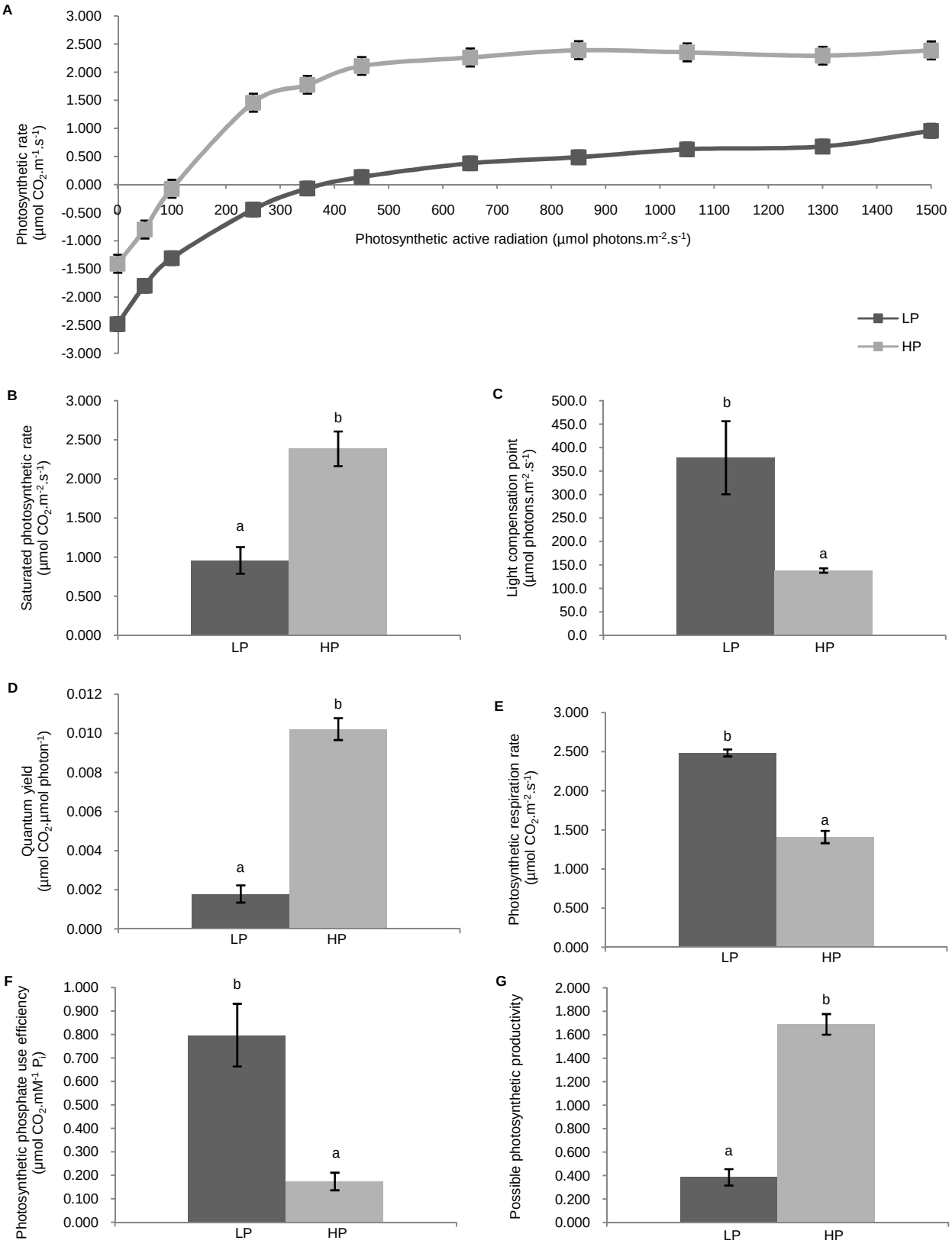

Fig. 3.1 Light response curve (A), saturated photosynthetic rate (B), light compensation point (C), quantum yield (D), photosynthetic respiration rate (E), photosynthetic phosphate use efficiency (F) and the possible photosynthetic productivity (G) for *M. truncatula* grown under LP (0.010 mM) and the control (0.500 mM). Values represent means (n = 3), while the bars represent standard error. The different letters symbolise the significant difference ($P \leq 0.05$).

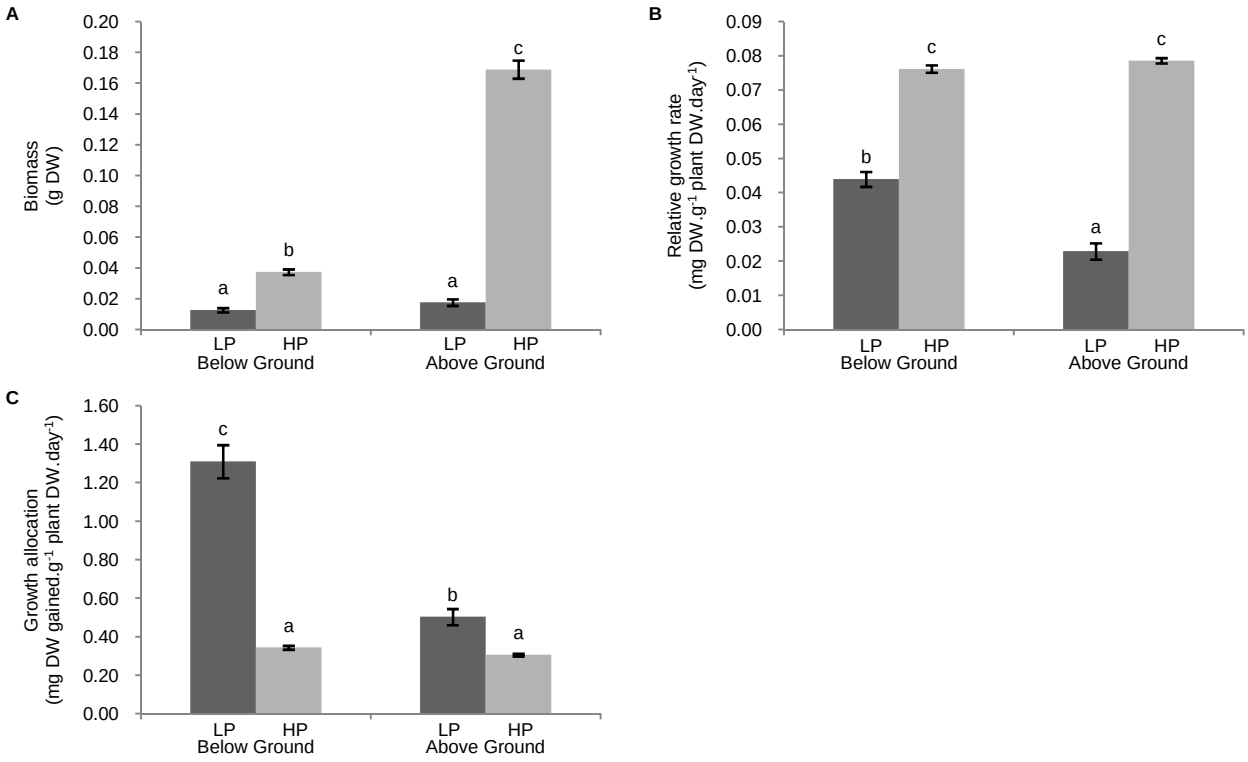

Fig. 3.2 Biomass (A), relative growth rates (B) and growth allocation (C) of below and above ground tissues grown under LP (0.010 mM) and the control (0.500 mM). Values represent means (n = 7), while the bars represent standard error. The different letters symbolise the significant difference ($P \leq 0.05$).

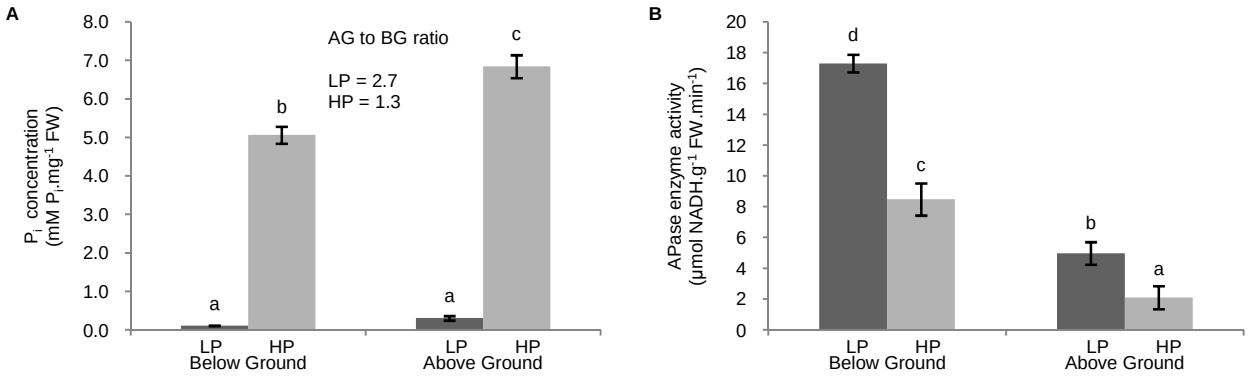

Fig. 3.3 P_i concentration and the ratios of P_i concentration in the AG to BG tissues based on treatment (A) and APase activity (B) of BG and AG tissues grown under LP (0.010 mM) and the control (0.500 mM). Values represent means (n = 3), while the bars represent standard error. The different letters symbolise the significant difference ($P \leq 0.05$).

Table 3.1 Nutrient content; carbon tissue construction cost; fraction of nitrogen derived from the atmosphere; nitrogen acquisition efficiency; and nitrogen phosphate use efficiency of phosphate stressed (0.010 mM ; LP) and control (0.500 mM; HP) *M. truncatula*. Values represent means (n = 3). The different letters symbolise the significant difference ($P \leq 0.05$).

	LP		HP	
Nutrient content mmol nutrient in plant				
Carbon	0.948 [a]	± 0.005	6.447 [b]	± 0.118
Nitrogen	0.043 [a]	± 0.001	0.319 [b]	± 0.031
Construction cost mmol carbon.g^{-1} plant DW				
C_W	1087 [a]	± 7.791	1077 [a]	± 12.59
%NDFA	73.11 [a]	± 0.633	54.04 [b]	± 3.052
Nitrogen acquisition efficiency mmol nitrogen gained.mg^{-1} tissue DW				
Nodules	3.420 [b]	± 0.034	0.082 [a]	± 0.009
Roots	0.031 [a]	± 0.001	0.026 [a]	± 0.003
Nitrogen phosphate use efficiency mmol nitrogen.mg^{-1} plant DW per mM P_i. mg^{-1} organ FW				
Below Ground	386.8 [b]	± 23.66	63.50 [a]	± 7.775
Above Ground	149.7 [b]	± 28.04	46.39 [a]	± 2.664

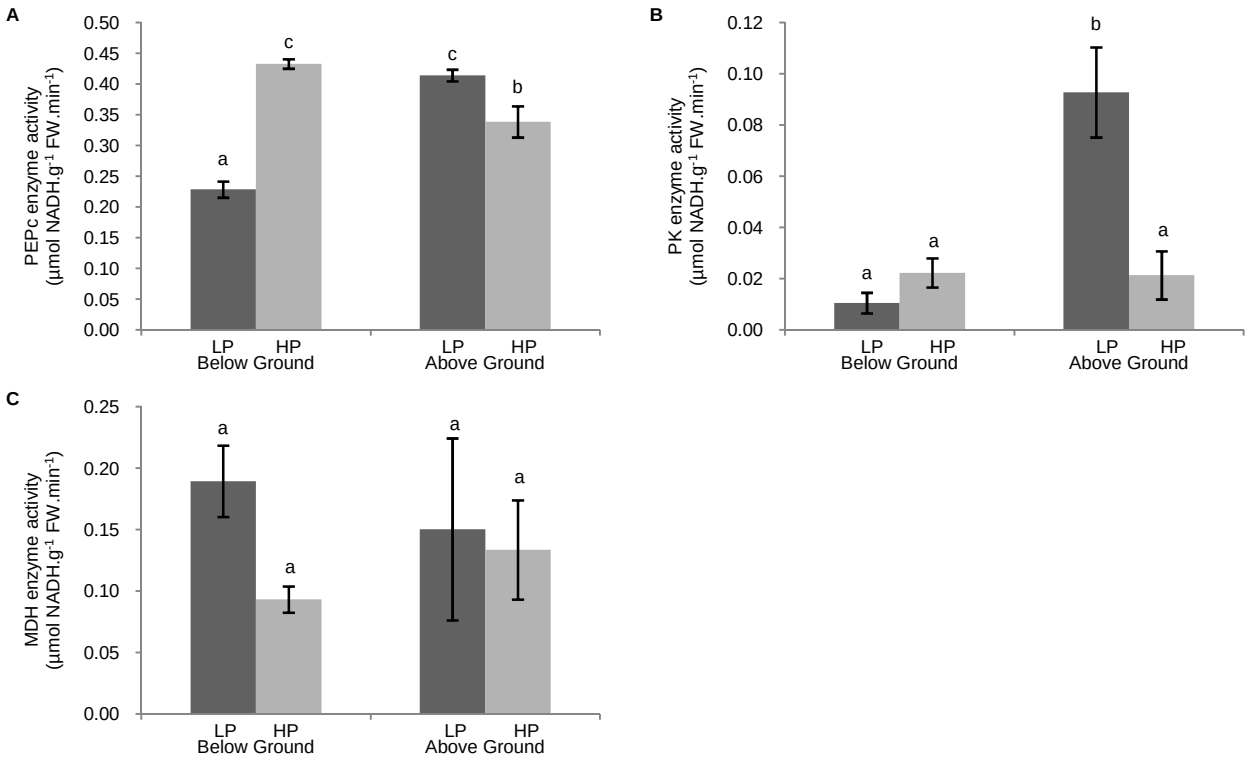

Fig. 3.4 The enzyme activities of PEPc (A), PK (B) and MDH (C) for BG and AG tissues grown under LP (0.010 mM) and the control (0.500 mM). Values represent means (n = 3), while the bars represent standard error. The different letters symbolise the significant difference ($P \leq 0.05$).

3.8 References

Abdolzadeh A, Wang X, Veneklaas EJ, Lambers H. 2010. Effects of phosphorus supply on growth, phosphate concentration and cluster-root formation in three Lupinus species. Annals of Botany 105, 365-374.

Appels MA and Haaker H. 1988. Identification of cytoplasmic nodule-associated forms of malate dehydrogenase involved in the symbiosis between *Rhizobium leguminosarum* and *Pisum sativum*. European Journal of Biochemistry 171, 515-522.

Buchanan BB and Wolosiuk RA. 2006. Photosynthesis: carbon reactions. In: Taiz L and Zeiger E (eds). Plant Physiology, fourth edition. Sunderland: Sinauer Associates, Inc., 160-195.

Bazzaz FA. 1998. Allocation of resources in plants: state of science and critical questions. In: Bazzaz FA and Grace J (eds). Plant resource allocation. San Diego: Physiological Ecology Series of Academic Press, 1-37.

Farquhar GD, Ehleringer JR, Hubick KT. 1989. Carbon isotope discrimination and photosynthesis. Annual Review of Plant Physiology Plant Molecular Biology 40, 503-537.

Garcia J, Barker DG, Journet E-P. 2006. Seed storage and germination. In: Mathesius U, Journet EP, Sumner LW (eds). The *Medicago truncatula* Handbook.

Hidaka A and Kitayama K. 2013. Relationship between photosynthetic phosphorus-use efficiency and foliar phosphorus fractions in tropical tree species. Ecology Evolution 15, 4872-4880.

Hurley BA, Tran HT, Marty NJ, Park J, Snedden WA, Mullen RT, Plaxton WC. 2010. The dual-targeted purple acid phosphatase isozyme AtPAP26 is essential for efficient acclimation of Arabidopsis to nutritional phosphate deprivation. Journal of Plant Physiology 153, 1112-1122.

Journet E-P, de Carvalho-Niebel F, Andriankaja A, Huguet T, Barker DG. 2006. Rhizobial inoculation and nodulation of *Medicago truncatula*. In: Mathesius U, Journet EP, Sumner LW (eds). The *Medicago truncatula* Handbook.

Kochian LV, Hoekenga OA, Pineros MA. 2004. How do plants tolerate acid soils? Mechanisms of aluminium tolerance and phosphorous efficiency. Annual Review of Plant Biology 55, 459-493.

Kondracka A and Rychter AM. 1997. The role of P_i recycling processes during photosynthesis in phosphate-deficient bean plants. Journal of Experimental Botany 48, 1461-1468.

Lambers H, Cawthray GR, Giavalisco P, Kuo J, Laliberté E, Pearse SJ, Scheible WR, Stitt M, Teste F, Turner BL. 2012. Proteaceae from severely phosphorus-impoverished soils extensively replace phospholipids with galactolipids and sulfolipids during leaf development to achieve a high photosynthetic phosphorus-use-efficiency. New Phytologist 196, 1098-1108.

López-Arredondo DL, Leyva-González MA, González-Morales SI, López-Bucio J, Herrera-Estrella L. 2014. Phosphate nutrition: improving low-phosphate tolerance in crops. Annual Review of Plant Biology 65, 95-123.

McColud SA, Smith RG, Schuller KA. 2001. Partial purification and characterization of pyruvate kinase from plant fraction of soybean root nodules. Physiologia Plantarum 111, 283-290.

Moraes T and Plaxton WC. 2000. Purification and characterization of phosphoenolpyruvate carboxylase from *Brassica napus* (rapeseed) suspension cell cultures. European Journal of Biochemistry 267, 4465-4476.

Mortimer PE, Pérez-Fernández MA, Valentine AJ. 2005. Mycorrhizal C costs and nutritional benefits in developing grapevines. Mycorrhiza 15, 159-165.

Nanamori M, Shinano T, Wasaki J, Yamamura T , Rao IM, Osaki M. 2004. Low phosphorus tolerance mechanisms: phosphorus recycling and photosynthate partitioning in the tropical forage grass, Brachiaria hybrid cultivar Mulato compared with Rice. Plant and Cell Physiology 45, 460-469.

Nautiyal CS, Bhadauria S, Kumar P, La Hl, Mondal R, Verma D. 2000. Stress induced phosphate solubilisation in bacteria isolated from alkaline soils. Federation of European Microbiological Societies Microbiology Letters 182, 291-296.

Nielsen KL, Eshel A, Lynch JP. 2001. The effect of phosphorous availability on the carbon economy of contrasting common bean (*Phaseolus vulgaris* L.) genotypes. Journal of Experimental Botany 52, 329-339.

Ocaña A, Cordovilla MDP, Lluch C. 1996. Phosphoenolpyruvate carboxylase in root nodules of *Vica faba*: partial purification and properties. Physiologia Plantarum 97, 724-730.

O'Rourke JA, Bolon YT, Bucciarelli B, Vance CP. 2014. Legume genomics: understanding biology through DNA and RNA sequencing. Annuals of Botany 113, 1107-1120.

Peng S, Eissenstat DM, Graham JH, Williams K, Hodge NC. 1993. Growth depression in mycorrhizal citrus at high-phosphorous supply. Journal of Plant Physiology 101, 1063-1071.

Pieters AJ, Paul MJ, Lawlor DW. 2001. Low sink demand limits photosynthesis under P_i deficiency. Journal of Experimental Botany 52, 1083-1091.

Shearer GB and Kohl DH. 1986. N_2-fixation in field settings: estimates based on natural ^{15}N abundance. Australian Journal of Plant Physiology 13, 699-756.

Smith GS, Johnston M, Cornforth IF. 1983. Comparison of nutrient solutions for growth of plants in sand culture. New Phytologist 94, 537-548.

Sulieman S and Tran L-SP. 2015. Phosphorus homeostatis in legume nodules as an adaptive strategy to phosphorus deficiency. Plant Science 239, 36-43.

Sulieman S, Van Ha C, Schulze J, Tran L-S P. 2013. Growth and nodulation of symbiotic *Medicago truncatula* at different levels of phosphorus availability. Journal of Experimental Botany 64, 2701-2712.

Sung S-J, Xu S, Galloway D-P, Black CM. 1988. A reassessment of glycolysis and gluconeogenesis in higher plants. Physiologia Plantarum 72, 650-654.

Vance CP, Uhde-Stone C, Allan DL. 2003. Phosphorous acquisition and use: critical adaptations by plants for securing a nonrenewable resource. New Phytologist 157, 423-447.

Wang L, Li Z, Qian W, Guo W, Gao X, Huang L, Wang H, Zhu H, Wu J-W, Wang D, Liu D. 2011. The Arabidopsis Purple Acid Phosphatase AtPAP10 is predominantly associated with the root surface and plays an important role in plant tolerance to phosphate limitation. Journal of Plant Physiology 157, 1283-1299.

Williams K, Percival F, Merino J, Mooney HA. 1987. Estimation of tissue construction cost from heat of combustion and organic nitrogen content. Plant, Cell and Environment 10, 725-734.

CHAPTER 4
PHOSPHATE STARVATION IN *MEDICAGO TRUNCATULA* AFFECTS NITROGEN METABOLISM

4.1 Summary

Biological nitrogen fixation efficiency is limited by phosphate supply. Legume species, such as *Medicago truncatula* Gaertner, which can form a symbiosis with nitrogen-fixing bacteria *Rhizobia,* must manage the available phosphate supply in order to survive and maintain the symbiosis. This study focused on the effect that induced phosphate-limited conditions could have on the efficiency of biological nitrogen fixation. *Medicago truncatula* (A17) seedlings were inoculated with *Sinorhizobium meliloti* 1026 and grown in quartz sand. The seedlings were fed full strength Long Ashton nutrient solution containing 0.500 mM phosphate until plants were mature. Thereafter a period of phosphate stress was induced by lowering the applied phosphate concentration to 0.010 mM. Analysis of the below ground organs, the nodules and roots, indicated alternative growth strategies during phosphate stress. Allocation of inorganic phosphate was concentrated to the nodules, while the carbon and nitrogen content were reduced. Available phosphate management strategies were also different between the organs as the nodules employed glycolytic “bypass” enzymes to save phosphate, while the roots struggled to maintain enzyme activities. Under induced phosphate stress conditions nodules relied on glutamine synthetase to produce an amide to export as nitrogen source for the rest of the plant. The roots recycled this amino acid to maintain growth rate and function. The alternative strategies in phosphate management as used by the separate below ground organs indicated an interesting set of adaptations of nodulated legumes to phosphate stress.

4.2 Introduction

Nitrogen is the most limiting nutrient to plant growth. It is used by the plant to produce nucleotides to nucleic acids; hexoamines, amines, amino acids to proteins and enzymes; and coenzymes. Nitrogen's versatility as part of oxidation-reduction reactions makes it a major element in plant metabolism and biogeochemical cycles (Bloom, 2006; Bloom, 2011). Although nitrogen makes up 78% of the Earth's atmosphere, plants cannot metabolise it as dinitrogen gas (N_2). It must first be fixed into either nitrate (NO_3^-) or ammonium (NH_4^+) to enter the biochemical cycle. The soil nitrogen fixing bacteria of Rhizobium are able to fix N_2 into ammonia (NH_3^+) as free-living cells or as part of a symbiotic nitrogen fixation system with various legume species (Valentine et al., 2011). This symbiosis is beneficial to the host plant as it receives important NH_3^+ molecules that are assimilated into either uriedes or amides for plant metabolism. In exchange, the bacteria are housed within a specialised plant organ, the nodule, and is dependent on the host for nutrition especially photosynthates and phosphate. Thus the nodule is a strong carbon and phosphate sink (Le Roux et al., 2009).

As with nitrogen, phosphate is abundant in the soil; however the concentration of soil phosphate that is available for plant uptake (mineralised and not chelated) is very low (Vance.et al., 2003). Phosphate enters the roots via diffusion and creates a depletion shell in the rhizosphere. Thereafter, active transport of constitutive low and induced high-affinity uptake systems are required to sustain the plants need for phosphate (Hinsinger, 2001). If further depletion of the phosphate reserve occurs the plant will sense that it is under phosphate stress and induce mechanisms to enhance phosphate uptake and or optimise the efficiency of phosphate use that is already in the tissues (Hinsinger, 2001; Vance et al., 2003). Adaptations to enhance uptake include increased growth rate of the roots and root hairs; changes in root architecture such as the angle of lateral root formation and possible proteoid root formation; initiation of symbiosis with arbuscular mycorrhizal fungi; the exudation of organic acids or enzymes into the soil to free bound phosphate; or increasing the expression of phosphate transporters (Schachtman et al., 1998). While optimising the efficiency of phosphate use includes remobilisation of internal orthophosphate (P_i); reduced growth rate of above ground tissues; the upregulation of alternative respiration pathways; or the increase in activity of "by-pass" enzymes for the steps in the metabolism of carbon that require P_i (Vance et al., 2003). An additional challenge for nodulated plants

is maintaining nodule homoeostasis during phosphate stress conditions (Sulieman and Tran, 2015). However, different plant species use different combinations of adaptations to survive the phosphate stress period. Thus different crops need to be managed accordingly. Of the phosphate that is applied to the soil in the form of fertiliser, up to 20% is found in the first harvest, while the remainder is bound within the soil (Vance et al., 2003). If the phosphate is not released for the following crop, the yield will not be at an optimum.

Nitrogen assimilation from soil uptake or BNF requires organic carbon skeletons. Since it is known that organic acid metabolism can be altered during phosphate stress, the goal of this study was to determine whether phosphate stress-induced changes in organic acid metabolism, affects nitrogen metabolism in below ground organs.

Thus this study aimed to elucidate the changes in growth, and carbon and nitrogen metabolism enzyme activities in *M. truncatula* nodules and roots separately after a period of induced phosphate stress.

4.3 Materials and Methods

4.3.1 Plant material

Medicago truncatula (A17) seeds (The Samuel Roberts Noble Foundation, USA) were chemically scarified as described in the Medicago Handbook (Garcia et al., 2006). Germinated seeds were selected and planted in 15 cm plastic pots containing quartz sand and placed in a temperature controlled, North-facing greenhouse (Natuurwetenskappe Building, Stellenbosch). During the growth period the plants received 50 ml of nutrient solution (as decribed below) on Mondays and Fridays. The same volume of distilled water was administered to each plant on Wednesdays. Liquid cultures of *Sinorhizobium meliloti* strain 1026 (The Samuel Roberts Noble Foundation, USA) were prepared for growth on the same day as the *M. truncatula* seedlings were planted. The preparation and maintainance of the bacterial cultures and the sunsequent inoculation of the *M. truncatula* seedlings were preformed following the protocol as provided in the Medicago Handbook (Journet et al., 2006). Each treatment received freshly prepared modified Long Ashton nutrient solution (Smith et al., 1983) constisting of macronutrients

(1.50 mM $MgSO_4.7H_2O$, 2.00 mM K_2SO_4, 4.00 mM $CaCl_2{\cdot}2H_2O$), micronutrients (0.165 mM solution of 0.139 mM H_3BO_3, 0.121 mM $MnSO_4.4H_2O$, 0.002 mM $ZnSO_4.7H_2O$, 0.003 mM $CuSO_4.5H_2O$, 0.0003 mM $Na_2MoO_4.2H_2O$), iron (0.022 mM FeEDTA) and Good's buffer (0.100 mM MES). In order to reduce the occurance of nitrogen stess in the young plants 0.500 mM $(NH_4)_2SO_4$ was added to the nutrient solution. After the first three feedings, no additional nitrogen was added to the nutrient solution as biological nitrogen fixation (BNF) was activated. The pH of the prepared nutrient solution was adjusted to range between 5.8 and 6.0.

In order to simulate the phosphate stressed condition two nutrient solution treatments were prepared, each with a varied concentration of phosphate ($NaH_2PO_4{\cdot}2H_2O$): (optimum) 0.500 mM and (stressed) 0.010 mM. The sample plants that were fed with the solution containing 0.500 mM phosphate served as the control goup and are further referred to as HP (High Phosphate). After seven weeks of growth until the harvest, half of the plants were fed a nutrient solution containing 0.010 mM phosphate and served as the stressed treatment group further referred to as LP (Low Phosphate).

4.3.2 Harvest

The sample plants were harvested at ten weeks after being potted before any flower buds had developed (end point harvest). The plant organs were separated on ice into leaves, stems, roots and nodules. The organs were immediately weighed (as FW) and stored at -80 ℃ until further use. The organ mater ial of plants from the same treatment was pooled to reduce variance between sample plants. As five plants were pooled to create one sample the HP treatment group consisted of eight pooled samples and the LP treatment consisted of seven samples of each organ. Further analysis compared the nodules to the roots.

4.3.3 Biomass

The plant material from the initial harvest was dried and weighed. A ratio of FW versus DW was calculated for each organ and used to convert the FW of the sample plants to DW. These calculated DW values were subsequently used to determine the growth allocation (GA) of nodules and roots by also calculating the whole plant relative growth

rate (RGR) as in the equation (eqn) below (Bazzaz, 1998). The relative growth rates of the nodules and roots were also calculated.

Eqn 4.1 $GA = \frac{df}{dt} = RGR \left(\frac{\partial \text{- Br}}{Bt}\right)$

The fraction for the allocation of new biomass of each organ is calculated from the RGR as milligramme dry weight gained per gramme dry weight of the plant per day. The symbol ∂ shows the new biomass produced during the time the plant had grown. Br is the organ biomass, while Bt is the total plant biomass.

In addition, the root to shoot ratios of the sample plants were calculated to determine whether the plants were under nutrient stress.

4.3.4 Inorganic phosphate (P_i) concentration and acid phosphatase activity

In order to have an indication of the levels of available free phosphate in the plant material, the P_i concentrations in the nodules and roots were determined by using the molybdate blue method as described by Nanamori et al. (2004). The organ tissues in question of three samples per treatment were weighed out to 50 mg each. Thereafter, the material was treated with liquid nitrogen and ground into a fine paste before continuing with the protocol. The concentration of P_i per tissue was calculated as the sample absorbance at 820 nm relative to a P_i standard curve and per mg of FW. The control blank reactions contained incubated assay buffer without the addition of sample extract.

The acivity of the acid phosphatases (APase; EC 3.1.3.2) can be measured by using the method decribed by Hurley et al. (2010). For this study the extraction and assay protocols were modified from the Hurley et al. (2010) paper. The proteins were extracted in a buffer solution containing 20 mM sodium acetate (pH 5.6), 1 mM EDTA, 1 mM dithiothreitol, 5 mM thiourea, 1% (w/v) insoluble polyvinylpyrrolidone and one complete protease inhibitor cocktail (Roche) tablet for every 50 ml of buffer solution. A homogenate was solution was produced of one part sample tissue to two parts of ice cold extraction buffer (w/v). The homogenate was then centrifuged at 15 000x*g* at 4 ℃ for 10 min. The resultant supernatant was removed and used as the crude protein extract. The following APase assay was done using this crude extract. The assay mixture contained 50 mM sodium acetate (pH 5.6), 5 mM phosphoenolpyruvate (PEP), 10 mM $MgCl_2$, 0.2 mM NADH and 3 U of lactate dehydrogenase (LDH). The blank mixture that served as the control contained all the assay buffer reagents except PEP. Of the

crude protein extract, 30 µl was added to the reaction mixture to make a total volume of 250 µl. The absorbance of each assay was measured at 340 nm as the oxidation of NADH at 25 ℃ for 5 min. The enzyme's activity was defin ed as the amount of µmol substrate consumed per g FW per minute.

4.3.5 δ^{13} Carbon and δ^{15} nitrogen analysis

The plant material from three samples per treatment was dried at 50 ℃. The dry material was then milled using a tissue lyser at 20 Hz for 3 min until it was a fine power. The three steel balls were carefully removed and the powered material was sent to the Archeometry Department, at the University of Cape Town. The analysis included the determination of the δ^{13} carbon and δ^{15} nitrogen ratios in the samples. These isotopic ratios were calculated from the equation:

Eqn 4.2 $\delta = 1\,000‰ \left(\frac{\mathrm{R_{sample}}}{\mathrm{R_{standard}}}\right)$

as R represents the molar ratio of the heavy and light isotopes of the sample and the standard used in the experiment as explained by Farquhar et al. (1989). An average of 2.046 mg DW per sample was placed into a Fisons NA 1500 (Series 2) CHN analyser (Fisons Instruments SpA, Milan, Italy) and combusted. The isotope values were determined by a Finnigan Matt 252 mass spectrophotometer (Finnian MAT GmbH, Bremen, Germany) using a CHN analyser connected to the mass spectrometer via a Finnigan MAT Conflo control unit.

4.3.6 Carbon and nitrogen cost and efficiency calculations

From the isotopic ratios obtained from the isotope analyses the carbon and nitrogen content of the tissues could be calculated.

The carbon cost to construct new tissue (C_W) for each treatment was calculated following the equation described by Peng et al. (1993) as modified by Mortimer et al. (2005):

Eqn 4.3 $\mathrm{C_w} = \left(\mathrm{C} + \frac{k\mathrm{N} \times 180}{24}\right)\left(\frac{1}{0.89}\right)\left(\frac{6000}{180}\right)$

as C_W represents the construction cost to produce new tissue (mmol carbon.g^{-1} DW), C shows the concentration of carbon in the sample (mmol carbon.g^{-1} DW), *k* is the nitrogen substrate reduction state (*k* = -3, NH_3), N as the organic content of nitrogen in the sample (mmol nitrogen.g^{-1} DW) (Williams et al., 1987). The fraction of the tissue construction cost which provides reductant that is not incorporated into biomass is represented by the constant (1/0.89) (Williams et al., 1987; Peng et al., 1993), while the fraction (6000/180) changes the units from g glucose.g^{-1} DW to mmol carbon.g^{-1} DW.

The uptake rate of nitrogen by the below ground tissues, nodules and roots were calculated by multiplying the nitrogen content found in each organ with the respective growth rate. Thus it indicates the mol nitrogen that was taken up per mg of the organ's DW per day.

The specific nitrogen utilisation rate (SNUR) (g DW.mg^{-1} nitrogen.day^{-1}) is an indication of the amount of DW the plant had gained with the nitrogen it had absorbed as modified from Nielsen et al. (2001):

Eqn 4.4 $$\mathrm{SNUR} = \left(\frac{W - W_1}{t_2 - t_1}\right)\left(\frac{\ln(N_2) - \ln(N_1)}{N_2 - N_1}\right)$$

where N_2 is the nitrogen content of the sample (mmol nitrogen.g^{-1} sample DW), N_1 is the nitrogen content of the initial harvest sample (mmol nitrogen.g^{-1} sample DW), t_2 is the number of days the sample plant was grown, t_1 is the number of days the initial harvest sample plant was grown, W_2 is the DW (g) of the sample tissue (nodules, roots or below ground tissues), and W_1 is the DW (g) of the initial harvest sample tissue (nodules, roots or below ground tissues accordingly).

Growth respiration rate ($R_g(t)$) as mmol CO_2 respired.g^{-1} new tissue gained DW.day^{-1} is calculated as by Peng et al. (1993):

Eqn 4.5 $$R_g(t) = C_t - \Delta W_c$$

where C_t represents the carbon needed to construct new tissue (mmol CO_2.g^{-1} new tissue.day^{-1}). C_t was calculated as the plant growth rate (g new tissue DW.day^{-1}) multiplied by the construction cost of making the new tissue (previously calculated as C_W). ΔW_C indicated the change in root content (mmol CO_2.g^{-1} new tissue.day^{-1}). This was calculated by multiplying the plant carbon content with the plant growth rate.

The percentage of nitrogen present in the plant tissue that had been derived from the atmosphere (%NDFA) and thus by BNF was calculated following the equation described by Shearer and Kohl (1986):

Eqn 4.6 $$\%\mathrm{NDFA} = 100\left(\frac{\delta^{15}\,\mathrm{nitrogen}_{\,\mathrm{Reference\ plant}} - \delta^{15}\,\mathrm{nitrogen}_{\,\mathrm{Sample}}}{\delta^{15}\,\mathrm{nitrogen}_{\,\mathrm{Reference\ plant}} - \mathrm{B}}\right)$$

with *Triticum aestivum* L. used as the Reference plant and the B-value (0.12‰) was the δ^{15} nitrogen ratio of nodulated *Lens culinaris* Medikus grown with a nitrogen-free nutrient solution. Both *T. aestivum* and *L. culinaris* sample plants were grown under the same greenhouse conditions as the samples of interest.

By using the values generated from the %NDFA calculation, the efficiency of the nodules to fix atmospheric nitrogen and the efficiency of the roots to obtain nitrogen from the initial nutrient solution applications were calculated for each treatment.

4.3.7 Organic acid synthesising enzyme activity

Nodule and root activities of two enzymes involved in the organic acid bypass pathways and one housekeeping enzyme were determined as follows. Nodule and root material of three samples per treatment were weighed out to 50 mg per assay performed. As done in the molybdate blue protocol to determine sample P_i concentration, the weighed out tissues was ground into a fine paste using liquid nitrogen. The extraction protocol for phosphoenolpyruvate carboxylase (PEPc; EC 4.1.1.31), pyruvate kinase (PK; EC 2.7.1.40) and NADH-malate dehydrogenase (MDH; EC 1.1.1.37) was modified in this study to what was originally described by Ocaña et al. (1996). The extraction buffer comprised of 100 mM Tris-HCl (pH 7.8); 1 mM EDTA; 5 mM dithiothreitol; 20% (v/v) ethylene glycol; 2% (w/v) insoluble polyvinylpyrrolidone and one complete protease inhibitor cocktail (Roche) tablet per 50 ml of buffer prepared. Of the cold fine tissue paste, one part (50 mg) was added to four parts (w/v) extraction buffer. The resultant homogenate wass centrifuged for 8 min at 3 500x*g* and 4 ℃. The supernatant was carefully removed and it was centrifuged at 30 000x*g* for 20 min. The supernatant from the second spin step was used further as the crude protein extract.

The assay to determine the activity of PEPc was performed by monitoring the oxidation of NADH as measured by Ocaña et al. (1996). The assay mixture comprised of 100 mM Tris (pH 8.5); 5 mM $MgCl_2$; 5 mM $NaHCO_3$; 4 mM PEP; 0.20 mM NADH; and

5 U of MDH. The control blank assay mixture contained all the assay buffer reagents except for PEP and sample supernatant. Of the crude protein extract, 30 µl was added to the reaction mixture to produce a total volume of 250 µl. The absorbance of the liquid was then measured continuously at 340 nm at 25 ℃ for 5 min.

The activities of PK in the respective tissues were measured as described by McCloud et al. (2001). The assay mixture contained 75 mM Tris-HCl (pH 7.0); 5 mM $MgCl_2$; 20 mM KCl; 1 mM ADP; 3 mM PEP; 0.18 mM NADH and 3 U rabbit muscle LDH. For this assay two control blank mixtures were made. The first blank mixture contained all the assay mixture reagents except for ADP; while the second contained all the assay mixture reagents except for PEP. The absorbancies of the respective liquids were measured in the same manner as that of PEPc.

The protocol as described by Appels and Haaker (1988) was used to assay the NADH-dependent MDH activities in nodule and root tissues. This assay mixture was made of 25 mM potassium phosphate (KH_2PO_4) buffer; 0.2 mM NADH and 0.4 mM oxaloacetate (pH 7.4). The oxaloacetate solution was freshly prepared for each experiment performed. The control blank assay contained all the assay reagents except for oxaloacetate. The absorbancies of the assay liquid were measured the same as that of PEPc assay.

Enzyme activity was defined as as done with the APase assay described above.

4.3.8 Nitrogen assimilating enzyme activity

Nitrogen assimilating enzyme activities were also determined for the nodules and roots. Nodules and roots of three samples per treatment were weighed out to 50 mg per assay to be done and ground into a fine paste with liquid nitrogen. Crude protein extraction for nitrate reductase (NR; EC 1.6.6.1); glutamine synthetase (GS; EC 6.3.1.2); aspartate aminotransferase (AAT; EC 2.6.1.1); and glutamate dehydrogenase (GDH; EC 1.4.1.2) was done according to El-Shora and Ali (2011). The extraction mixture contained: 50 mM KH_2PO_4 buffer (pH 7.5); 2 mM EDTA; 1.5% (w/v) soluble casein; 2 mM dithiothreitol; 1% (w/v) insoluble PVPP; and one complete protease inhibitor cocktail (Roche) tablet per 50 ml buffer. One part material was added to 10 parts extraction buffer. The homogenate was centrifuged at 3 000x*g* for 5 min at 4 ℃. The supernatant was

collected and centrifuged at 15 000x*g* for 40 min at 4 ℃. The collected supernatant was used as crude protein extract.

The activity of NR was determined by measuring the concentration of nitrite using a modified method from Kaiser and Lewis (1984). The assay mixture contained 100 mM KH_2PO_4 buffer (pH 7.5); 100 mM KNO_3; 2 mM NADH; and 100 µl crude protein extract to make a final volume of 1 ml. The mixtures were incubated 30 ℃ for 30 min. The reaction was stopped by adding 500 µl of the stop solution (1% (w/v) of sulphanilamide in 1.5 M hydrochloric acid and 0.02% (w/v) of n-l-naphthyl-ethylenediamine dihydrochloride) to each sample. Samples were centrifuged at 500*xg* for 5 min. The concentration of nitrite produced was determined by measuring the absorbance at 540 nm. The blank measurement contained assay mixture and stop solution without any protein extract added.

The GS activity assay was done by modifying the method by Kaiser and Lewis (1984). The reaction contained 2.0 mM imidazole (pH 7.2); 1.8 mM $MgSO_4$; 240 µM hydroxylamine; 3.68 mM glutamic acid; and 720 µM ATP to 100 µl crude protein extract to a final volume of 1 ml. The mixtures were incubated at 28 ℃ for 15 min. Thereafter 500 µl of ferric chloride reagent (245 mM trichloroacetic acid, 118 mM ferric chloride and 500 mM hydrochloric acid) was added to each sample to stop the reaction. Samples were centrifuged 500*xg* for 10 min. The absorbance was measured at 540 nm to determine the concentration of γ-glutamyl hydroxamate produced by GS. The extinction coefficient of γ-glutamyl hydroxamate was taken as 850 $M^{-1}cm^{-1}$ (Krasnikov et al., 2009). The blank measurement contained assay mixture and stop solution without any protein extract added.

The assay for AAT activity was performed as described by Khadri et al. (2006). The assay mixture contained 50 mM Tris-HCl buffer (pH 8.0); 4 mM $MgCl_2$; 10 mM aspartate; 0.2 mM NADH; and 1 mM 2-oxoglutarate (α-ketogluturic acid). This assay was also carried out as with PEPc. The blank measurement contained assay mixture without a crude protein extract.

The activity of GDH was done as described by Glevarec et al. (2004). For the aminating reaction the oxidation of NADH was monitored in the following assay mixture: 100 mM Tris-HCl buffer (pH 8.0); 1 mM $CaCl_2$ (pH 8.0); 13 mM 2-oxoglutarate (α-ketogluturic acid); 50 mM $(NH_4)_2SO_4$ and 0.25 mM NADH. The deamination reaction contained 100 mM Tris-HCl buffer (pH 9.0); 1 mM $CaCl_2$ (pH 9.0); 33 mM glutamic acid and 0.25 mM NAD^+. The

reduction of NAD^+ was monitored. The reactions were measured as done with PEPc while the blank contained assay mixture without protein extract.

4.3.9 Statistics

The data and calculations generated from the above mentioned exmeriments were entered into the program Microsoft® Office Excel 2007 (Microsoft Corporation, 2006). The Student's t-Test and the Duncan's New Multiple Range test were run using Super-ANOVA (Statsgraphics Version 7, 1993) to determine possible significant changes in parameters between the treatments and or tissues.

4.4 Results

4.4.1 Biomass, relative growth rates and growth allocation

The biomass of nodules was significantly reduced when plants have been starved of phosphate (Fig. 4.1A). Data that is not shown indicated that the root to shoot ratio was significantly higher during LP to confirm that the plants were experiencing phosphate stress. Growth was slower in the nodules during phosphate stress (Fig. 4.1B); however, the allocation of growth (Fig. 4.1C) was not significant across tissues or treatments.

4.4.2 P_i concentration and acid phosphatase activity

The level of P_i was greater in nodules during phosphate starvation, while the root P_i concentration had decreased (Fig. 4.2A). The activity of APase was reduced during phosphate starvation; however, it was only significant in the roots (Fig. 4.2B).

4.4.3 Carbon and nitrogen cost and efficiency

After an induced phosphate stress period nodulated *M. truncatula* had shown a significant decrease in carbon (Fig. 4.3A) and nitrogen (Fig. 4.3B) content. It was also less expensive, in terms of carbon, to construct new tissue under phosphate stress (Fig. 4.3C). The rate at which nitrogen was taken up via the below ground tissues as a whole

(Fig. 4.3D), nodules (Fig. 4.3E) and roots (Fig. 4.3F) were significantly reduced as the plants experienced phosphate deficiency, as this tendency was also observed in the utilisation of nitrogen by the plant (Fig. 4.3G). The growth respiration rate (Fig. 4.3H) was decreased as the tempo of producing new tissues was reduced under phosphate stress. The percentage of nitrogen in the plant that was derived from the atmosphere (Fig. 4.3I) was significantly lower when under stress than *M. truncatula* grown under optimum conditions. The nitrogen uptake efficiency from BNF (Fig. 4.3J) and the soil (Fig. 4.3K) were reduced under phosphate stress, however, it was only significantly so from BNF. The nodules of stressed *M. truncatula* had lower nitrogen uptake efficiency to the P_i concentration (Fig. 4.3L) in the tissues than under optimum conditions. However the roots had higher nitrogen uptake efficiency to the P_i concentration (Fig. 4.3M) in the tissue under phosphate stress, but it is not significant. The nitrogen uptake efficiency to the P_i concentration of the stressed nodules was significantly lower than that of the stressed roots.

4.4.4 Organic acid synthesising enzyme activity

Under induced phosphate stress the nodules increased PEPc activity, while the root activity was reduced (Fig. 4.4A). PK activity (Fig. 4.4B) had decreased in the nodules and had remained relatively the same in the roots tissues during the stressed period. The production of malate through cytosolic MDH was significantly increased in the nodules, while the roots remained relatively constant. The activity of MDH was significantly greater in the roots than in the nodules (Fig. 4.4C).

4.4.5 Nitrogen assimilating enzyme activity

Nitrate reductase activity (Fig. 4.5A) was significantly reduced in the nodules under LP, while a similar propensity was seen in the roots' NR activity, but it was not significant. The production of glutamine by GS was increased in the nodules and roots during phosphate starvation, but again only significantly so in the nodules. The activity of GS was not significantly different between the nodules and roots (Fig. 4.5B). Glutamate produced from AAT activity (Fig. 4.5C) was significantly reduced in nodules, however, only a small reduction was seen in roots. AAT activity was greater in the nodules than the roots, thus this enzyme's main site of work may be the nodules. Except for the deamination in roots,

the activity of GDH (Fig. 4.5D and Fig. 4.5E) was less when the level of phosphate in the soil was reduced. The significant reduction of the aminating reaction in both the nodules and roots to the level of the deaminating reaction under optimal conditions may also be an indicator of phosphate stress. However, the enzyme's two reactions ware not significantly different in either the nodules or roots under phosphate stress.

4.5 Discussion

Under induced phosphate stress nodulated *M. truncatula* nodules and roots employed different strategies to survive the period of nutrient deficiency. The nodule tissues saved phosphate by relying on bypass enzymes and GS to divert metabolism to pathways that require less ATP. The roots, however, reduced carbon metabolism and recycle glutamine to survive the stress period.

Without the supplementation of phosphate into the soil, the plant creates a depletion zone around its root system (Balzergue et al., 2013). The phosphate-starved plant must then employ strategies to not only survive the starvation but also to scavenge for available soil and intercellular phosphate (Vance et al., 2003).

As nodules are strong phosphate sinks, it is important for *M. truncatula* to maintain nodule homoeostasis even under stress conditions (Qin et al., 2012; Sulieman and Tran, 2015). In this study, the reduction in relative growth rate and constant growth allocation indicated that the stressed plant would rather maintain the existing tissue than to produce significantly more from the onset of starvation. Root parameters remained constant over the stressed period. The significant increase in the root to shoot ratio in the stressed plants may show that the photosynthetic tissues were also maintained with little additional growth (Nanamori et al., 2004). The significant reduction of P_i found in the roots may have been relocated to the nodules to be used as a reserve for BNF if the starvation continues or root P_i was used for root growth (Kang et al., 2014; Sulieman and Tran, 2015).

The reduction seen in the carbon and nitrogen content of the phosphate stressed plants could be related to the decline in tissue growth and growth rates. However, the carbon needed to construct new tissue was also reduced during phosphate stress. This could be that the stressed plants were optimising the amount of carbon used to maintain established tissue and recycle carbon skeletons rather than to produce additional tissue.

The lower rate of growth respiration was also a sign of slower growth and use of carbon in producing new tissue during the phosphate stressed period. It appeared that carbon cost for growth competed with the carbon cost of BNF. This result was also observed in phosphate-starved *Glycine max* by Le Roux et al. (2009) indicating that nodule tissues act as strong carbon sinks during phosphate stress. Although no nitrogen was supplied to either treatment after the nodules were established, traces of nitrogen could still have been found in the quartz sand. This nitrogen was absorbed by the below ground tissues as the plants matured. From the time point that the low phosphate condition was induced, these plants had a decline in the rate of nitrogen uptake via the nodules and roots. This could be that the reaction to induced phosphate stress did not support the adaptations for acquiring nitrogen of low concentrations from the growth medium as was done with adequate phosphate feeding. The utilisation rate of the acquired nitrogen was also reduced during the induced phosphate stress period and may lead to reduced growth and nitrogen assimilation (Magadlela et al., 2014). The portion of nitrogen in the plant that was derived from BNF was also reduced and could be as a result of fewer nitrogenase enzymes (EC 1.19.6.1) present per plant. The nodule number and biomass had declined during the induced phosphate stressed period thus reducing the efficiency of BNF (Valentine et al., 2011). As the nodule tissue acted as a strong phosphate sink, strain was placed on the entire plant to allocate sufficient phosphate to the nodules to support BNF (Sulieman and Tran, 2015). However, under phosphate stress the nodules were not as effective as the roots in utilising the amount of nitrogen taken up to the concentration of P_i in the tissue. This might be that the nitrogen assimilated by the bacteroid was transported into the root cytoplasm at a fast rate as the P_i is allocated from the root to the nodule tissue (Sulieman et al., 2013).

The increased activity for PEPc and MDH within the nodules under phosphate stress indicated that the nodules are using the phosphate bypass pathway as observed by Le Roux et al. (2009) in Lupinus. Transcriptome studies done on *M. truncatula* nodules under phosphate stress by Cabeza et al. (2014) found a significant upregulation of nodule PEPc genes. PEPc activity was increased from its function to produce oxaloacetate for nitrogen assimilation and the TCA cycle; to also free P_i from PEP (Nanamori et al., 2004). MDH activity was thus also increased to metabolise the oxaloacetate pool into malate for nitrogen assimilation, to feed back into the TCA cycle and possible export into the soil to free P_i for plant uptake. MDH activity is also significantly higher than PEPc, but not less than APase activity (Le Roux et al., 2009). Thus the nodules use APase predominantly to dephosphorylate PEP and MDH for nitrogen assimilation or export (Nanamori et al., 2004).

Cabeza et al. (2014) also indicated the significant increase in nodule phosphatase transcription when plants were no longer fed with phosphate.

Phosphate stressed roots indicated a change in PEPc and APase activity, which were reduced. As in the nodules, APase activity was higher than PEPc and was the main competitor for PEP. Root MDH activity was higher than the nodule MDH activity. Thus the roots may be the main organ for malate export to the soil irrespective of phosphate status.

Nitrogen assimilation in the nodules and roots was well regulated. As no nitrate was supplied to the plants after BNF was established, the reduction in NR activity in the nodules may be attributed to fewer enzymes present in the organ. Under phosphate stress any unnecessary protein is degraded and the amino acids used where needed. The increase in GS activity and decrease of the aminating GDH reaction in the nodules indicate that the available ammonium from BNF and concentrated phosphate are used to increase glutamine production (El-Shora and Ali, 2011). The synthesis of aspartate is facilitated by the transfer of the amino group from glutamate to oxaloacetate via AAT activity (Khadri et al., 2006). Stable carbon isotope analysis of carbon dioxide assimilated via PEPc and photosynthesis is used to determine the level of aspartate produced. However, in this study, the rate of the reverse reaction was measured. Thus we assumed that the reverse reaction could be used as an indicator of the enzyme's activity as a whole. The reduced activity of AAT in the nodules during phosphate stress could have led to reduced synthesis of asparagine. This export amino acid is produced from aspartate, glutamine and ATP via asparagine synthetase (EC 6.3.5.4) (Pathirana et al., 1997). The phosphate stressed plant can reduce the need for ATP by not producing asparagine and rather use glutamine as the main amino acid for export. This was supported by the increase in nodule GS activity. Phosphate stress studies indicate that asparagine is the most abundant amino acid in the nodules and the phloem of *M. truncatula* (Cabeza et al., 2014, Sulieman et al., 2013). However, asparagine concentration decreased in the nodules but increased in the phloem. Thus the regulation of the amino acid synthesis in the nodules could be dependent on the level of phosphate stress perceived by the photosynthetic tissues. Sulieman et al. (2013) suggested that asparagine is a shoot derived stress signal for the nodules to decrease nitrogenase activity. The observed reduction of the aminating reaction of GDH could also be attributed to the decrease in the production of 2-oxoglutarate from AAT and the use thereof by the TCA cycle to produce citrate (Kwinta and Cal, 2005). The root nitrogen assimilating enzymes used in this study retained a constant rate irrespective of the treatment, except for the aminating GDH

reaction. The slower aminating GDH reaction rate increaseD the availability of NAD(P)H as reduction power for other metabolic processes (Kwinta and Cal, 2005). As the GDH activities were constant under phosphate stress irrespective of the organ, it is possible that the translation of GDH proteins was reduced in the below ground tissues or that after the onset of phosphate stress, GDH enzymes were degraded in the nodules and roots. Cabeza et al. (2014) did not identify changes in the expression of nitrogen assimilating enzyme genes in the nodules.

4.6 Conclusion

During phosphate starvation upon induction at maturity, the nitrogen assimilation was distinctly altered in roots and nodules of *M. truncatula*. Under induced LP conditions nodules rely on glutamine synthetase to produce an amide to export as nitrogen source for the rest of the plant. In contrast, the roots recycle this amino acid in order to maintain growth rate and function. Phosphate management strategies are also different between the organs as the nodules employ glycolytic “bypass” enzymes to save phosphate, while the roots struggle to maintain enzyme activities.

4.7 Figures

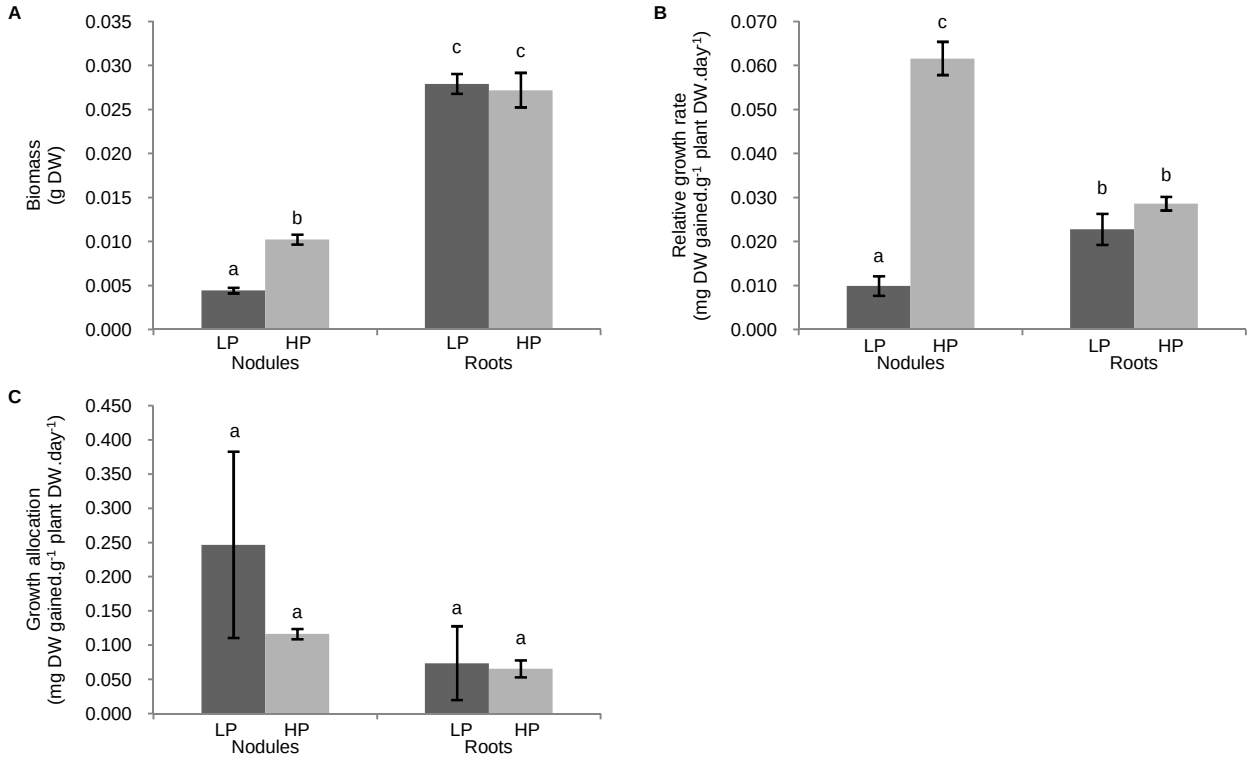

Fig. 4.1 Biomass (A), relative growth rates (B) and growth allocation (C) of *M. truncatula* nodules and roots starved of phosphate (0.010 mM) and the control (0.500 mM). Values represent means (n = 5), while the bars represent standard error. The different letters symbolise the significant difference ($P \leq 0.05$).

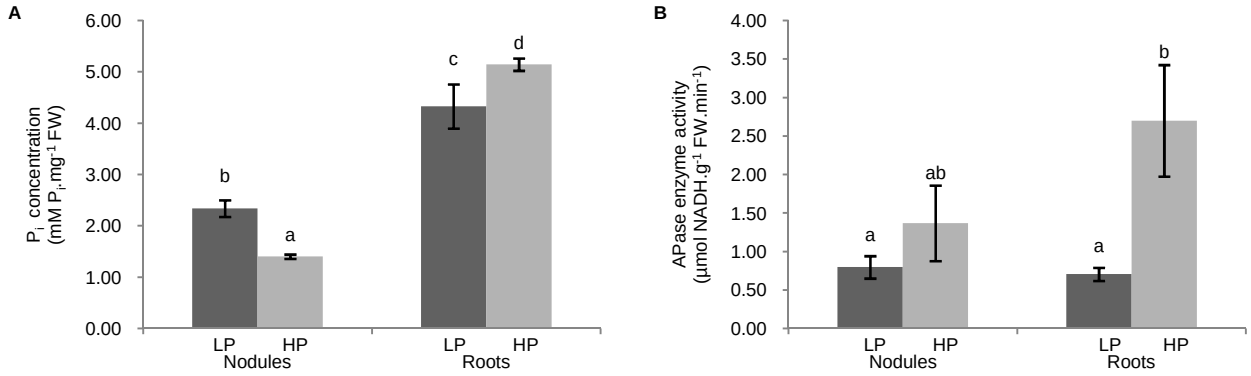

Fig. 4.2 P_i concentration (A) and APase activity (B) values in *M. truncatula* nodules and roots grown under LP (0.010 mM) and the control (0.500 mM). Values represent means (n = 3), while the bars represent standard error. The different letters symbolise the significant difference ($P \leq 0.05$).

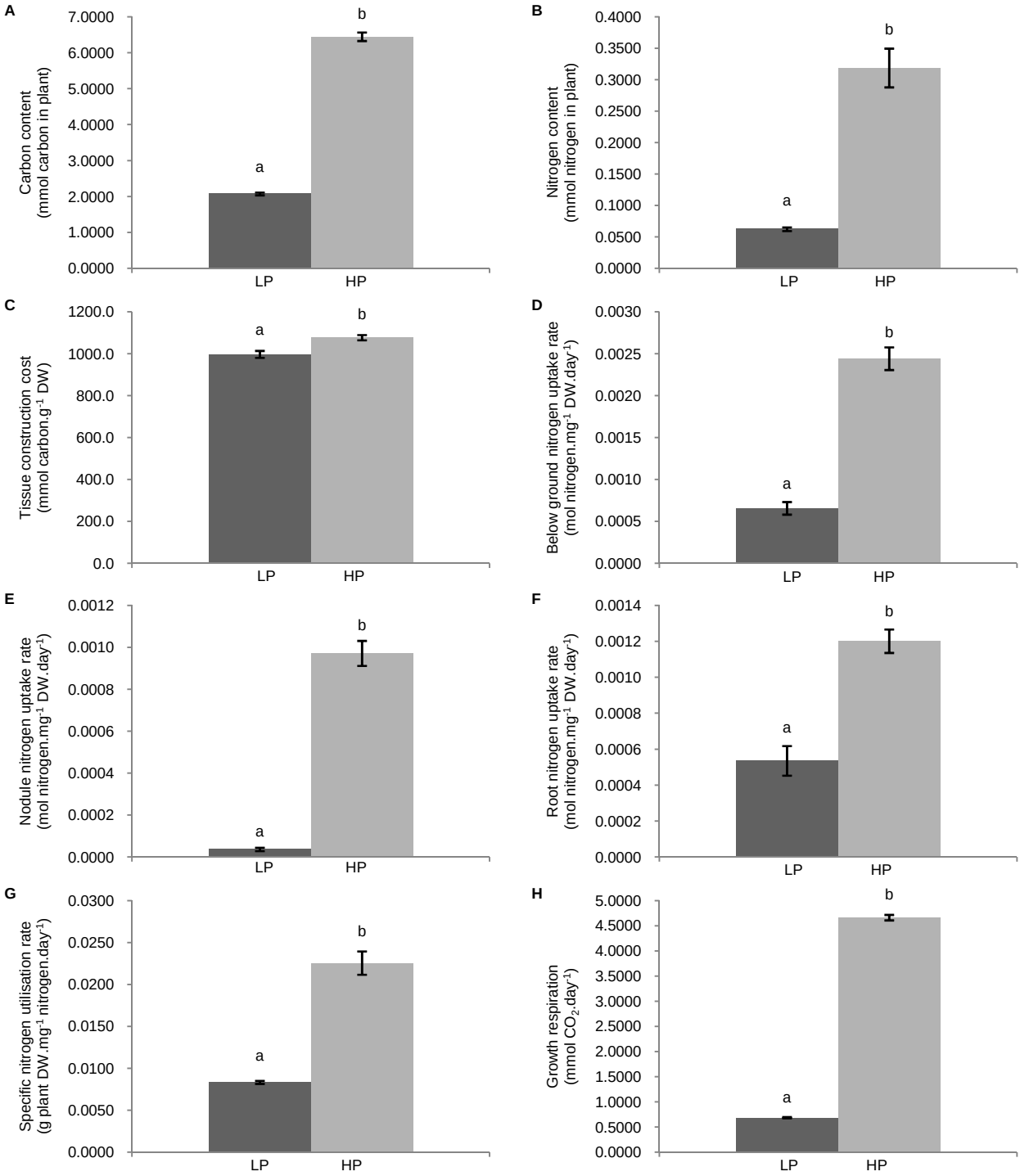

Fig. 4.3 The carbon and nitrogen content (A and B, respectively); tissue construction cost (C) and the nitrogen uptake rates of the below ground tissue (D), nodules (E) and roots (F); the specific nitrogen utilisation rate (G) and growth respiration rate (H) of phosphate-starved (0.010 mM) and the control (0.500 mM) *M. truncatula*. Values represent means (n = 3), while the bars represent standard error. The different letters symbolise the significant difference ($P \leq 0.05$).

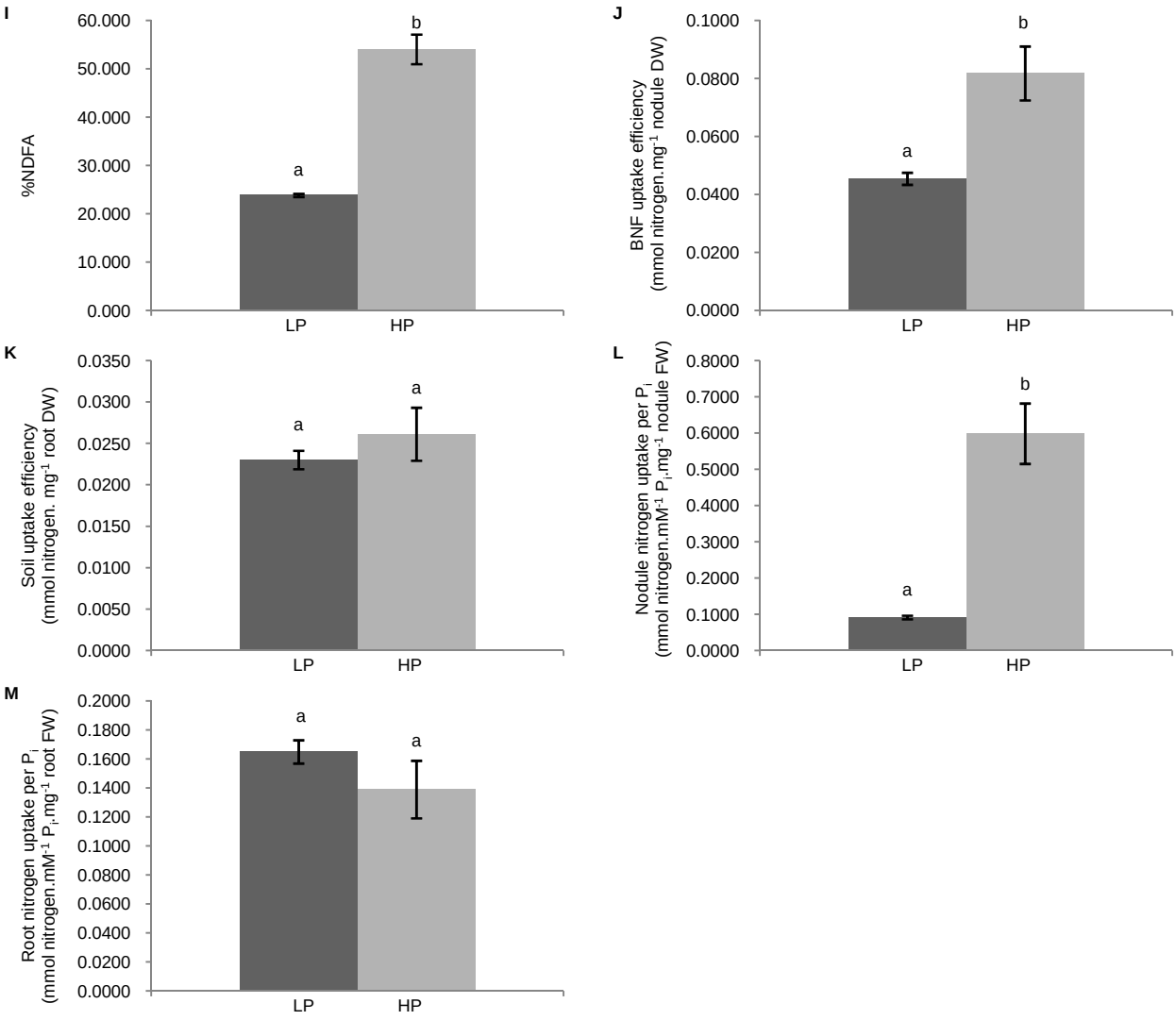

Fig. 4.3 continued. The percentage of nitrogen derived from the atmosphere (I); the nitrogen uptake efficiency from BNF (J), soil (K); and the ratio of nitrogen content to P_i concentration in nodules (L) and roots (M) of phosphate-starved (0.010 mM) and the control (0.500 mM) *M. truncatula*. Values represent means (n = 3), while the bars represent standard error. The different letters symbolise the significant difference ($P \leq 0.05$).

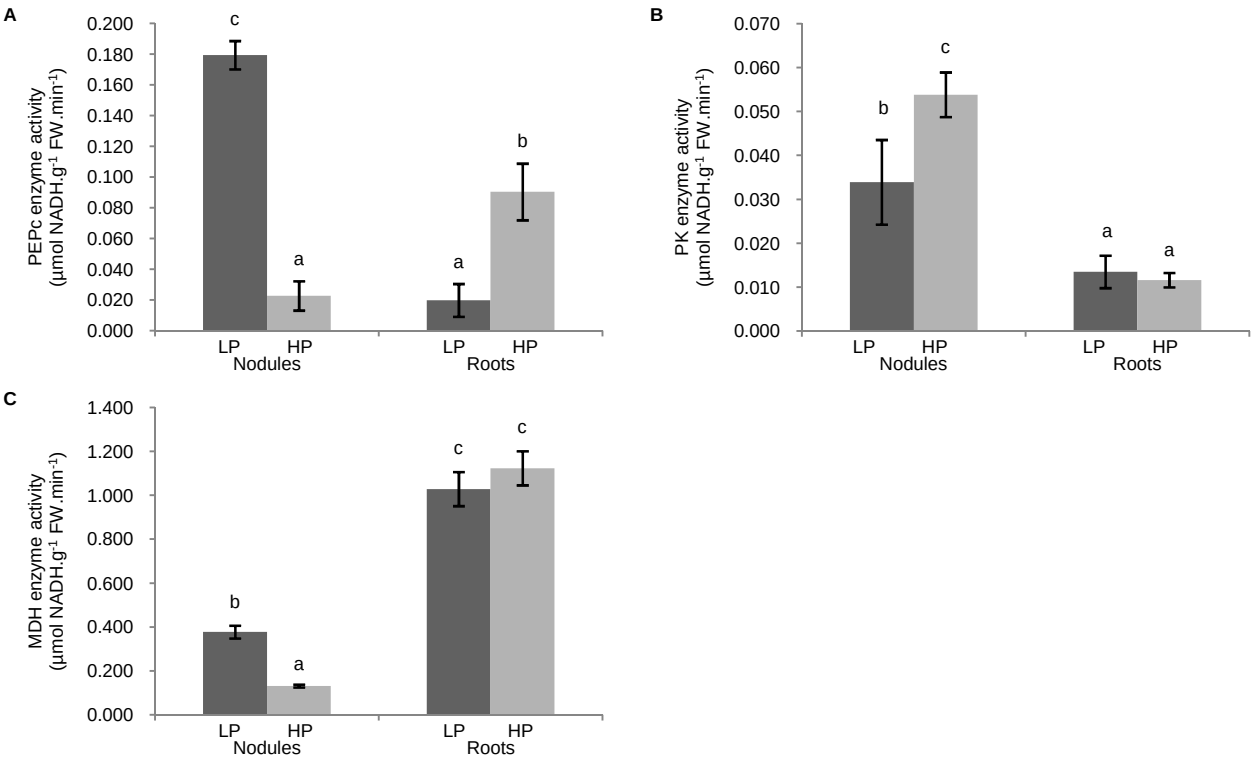

Fig. 4.4 The enzyme activities of PEPc (A), PK (B) and MDH (C) of phosphate-starved (0.010 mM) and the control (0.500 mM) *M. truncatula* nodules and roots. Values represent means (n = 3), while the bars represent standard error. The different letters symbolise the significant difference ($P \leq 0.05$).

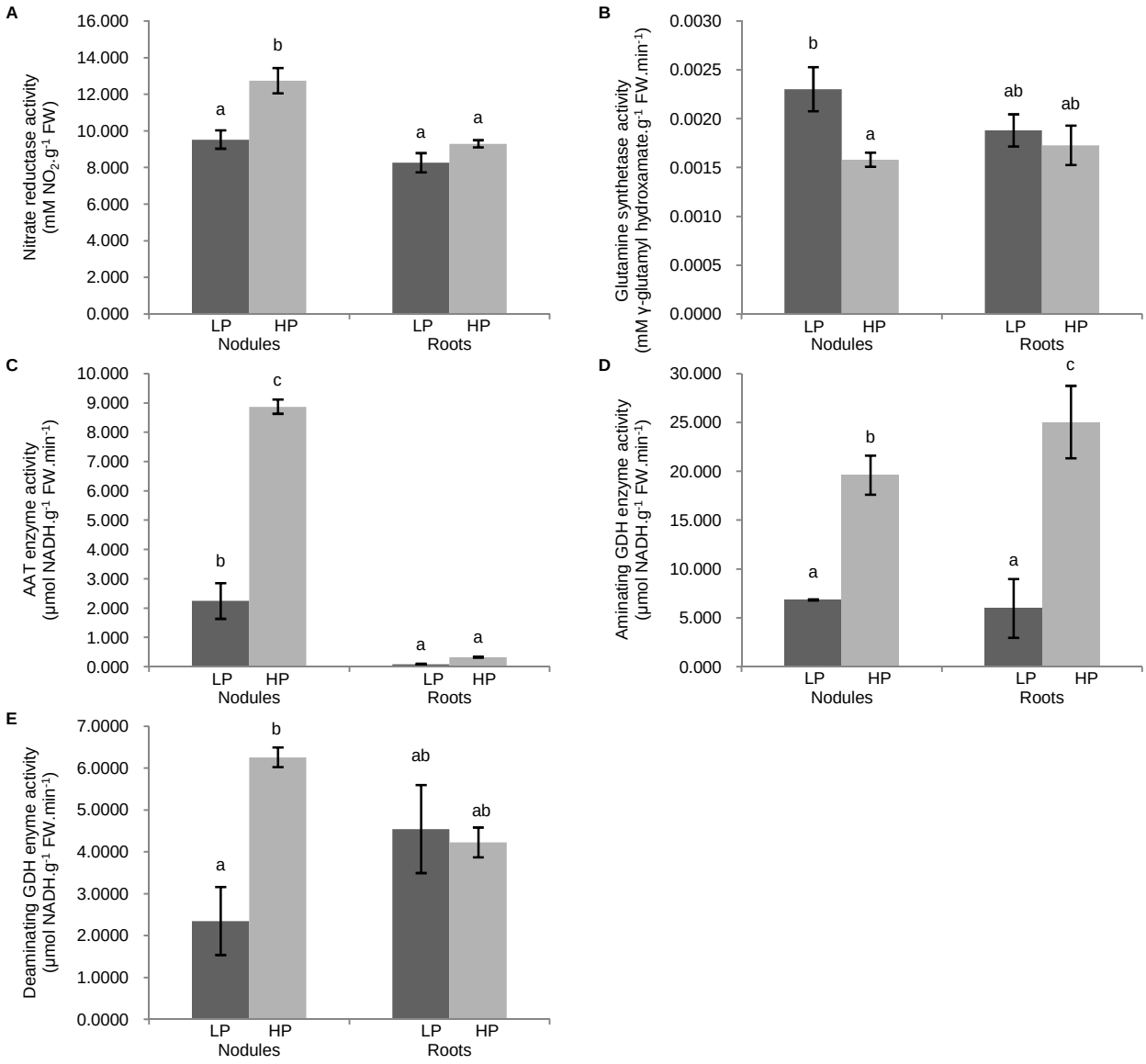

Fig. 4.5 The enzyme activities of NR (A), GS (B), AAT (C) and the aminating and deaminating reactions of GDH (D and E, respectively) in nodules and roots of phosphate-starved (0.010 mM) and the control (0.500 mM) *M. truncatula*. Values represent means (n = 3), while the bars represent standard error. The different letters symbolise the significant difference ($P \leq 0.05$).

4.8 References

Appels MA and Haaker H. 1988. Identification of cytoplasmic nodule-associated forms of malate dehydrogenase involved in the symbiosis between *Rhizobium leguminosarum* and *Pisum sativum*. European Journal of Biochemistry 171, 515-522.

Balzergue C, Chabaud M, Barker Bécard G, Rochange SF. 2013. High phosphate reduces host ability to develop Arbuscular Mycorrhizal symbiosis without affecting root calcium spiking responses to the fungus. Frontiers in Plant Science 4, 1-15.

Bazzaz FA. 1998. Allocation of resources in plants: state of science and critical questions. In: Bazzaz FA and Grace J (eds). Plant resource allocation. San Diego: Physiological Ecology Series of Academic Press, 1-37.

Bloom AJ. 2006. Mineral nutrition. In: Taiz L and Zeiger E (eds). Plant Physiology. Sunderland: Sinauer Associates, Inc., 75-93.

Bloom AJ. 2011. Energetics of nitrogen acquisition. In: Foyer CH and Zhang H (eds). Nitrogen metabolism in plants in the post-genomic era. West Sussex: Wiley-Blackwell 42, 63-81.

Cabeza RA, Liese R, Lingner A, Von Stiegiltz I, Neumann J, Salinas-Riester G, Pommerenke C, Dittert K, Schulze J. 2014. RNA-seq transcriptome profiling reveals that *Medicago truncatula* nodules acclimate N_2 fixation before emerging P deficiency reaches the nodules. Journal of Experimental Botany 65, 6035-6048.

El-Shora HE and Ali AS. 2011. Changes in activities of nitrogen metabolism enzymes cadmium stressed Marrow seedlings. Asian Journal of Plant Sciences 10, 117–124.

Farquhar GD, Ehleringer JR, Hubick KT. 1989. Carbon isotope discrimination and photosynthesis. Annual Review of Plant Physiology Plant Molecular Biology 40, 503-537.

Garcia J, Barker DG, Journet E-P. 2006. Seed storage and germination. In: Mathesius U, Journet EP, Sumner LW (eds). The *Medicago truncatula* Handbook.

Glevarec G, Bouton S, Jaspard E, Riou M-T, Cliquet J-B, Suzuki A, Limami AM. 2004. Respective roles of the glutamine synthetase/glutamate synthase cycle and glutamate

dehydrogenase in ammonium and amino acid metabolism during germination and post-germinative growth in the model legume *Medicago truncatula*. Planta 219, 286-297.

Groat RG and Vance CP. 1981. Root nodule enzymes of ammonia assimilation in Alfalfa (*Medicago sativa* L.). Plant Physiology 67, 1198-1203.

Hinsinger P. 2001. Bioavailability of soil inorganic P in the rhizosphere as affected by root induced chemical changes: a review. Plant and Soil 237, 173-195.

Hurley BA, Tran HT, Marty NJ, Park J, Snedden WA, Mullen RT, Plaxton WC. 2010. The dual-targeted purple acid phosphatase isozyme AtPAP26 is essential for efficient acclimation of Arabidopsis to nutritional phosphate deprivation. Plant Physiology 153, 1112-1122.

Journet E-P, de Carvalho-Niebel F, Andriankaja A, Huguet T, Barker DG. 2006. Rhizobial inoculation and nodulation of *Medicago truncatula*. Mathesius U, Journet EP, Sumner LW (eds). In: The *Medicago truncatula* Handbook.

Kaiser JJ and Lewis OAM. 1984. Nitrate reductase and glutamine synthetase activity in leaves and roots of nitrate-fed *Helianthus annuus* L. Plant and Soil 77, 127-130.

Kang J, Yu H, Tian C, Zhou W, Li C, Jiao Y, Liu D. 2014. Suppression of photosynthetic gene expression in oots is required for sustained root growth under phosphate deficiency. Journal of Plant Physiology 165, 1156–1170.

Khadri M, Tejera NA, Lluch C. 2006. Alleviation of salt stress in Common Bean (*Phaseolus vulgaris*) by exogenous abscisic acid supply. Journal of Plant Growth and Regulation 25,110-119.

Krasnikov BF, Nostramo R, Pinto JT, Cooper AJL. 2009. Assay and purification of ω-amidase/Nit2, a ubiquitously expressed putative tumor suppressor that catalyzes the deamidation of the α-keto acid analogues of glutamine and asparagine**.** Analytical Biochemistry 391, 144-150.

Kwinta J and Cal K. Effects of salinity stress on the activity on glutamine synthetase and glutamate dehydrogenase in Triticale seedlings. Polish Journal of Environmental Sciences 14, 125-130.

Le Roux MR, Khan S, Valentine AJ. 2009. Nitrogen and carbon costs of soybean and lupin root systems during phosphate starvation. Symbiosis 48, 102-109.

Magadlela A, Kleinert A, Dreyer LL, Valentine AJ. 2014. Low-phosphorous conditions affect the nitrogen nutrition and associated carbon costs of two legume tree species from a Mediterranean-type ecosystem. Australian Journal of Botany 62, 1-9.

McColud SA, Smith RG, Schuller KA. 2001. Partial purification and characterization of pyruvate kinase from plant fraction of soybean root nodules. Physiologia Plantarum 111, 283-290.

Mortimer PE, Pérez-Fernández MA, Valentine AJ. 2005. Mycorrhizal C costs and nutritional benefits in developing grapevines. Mycorrhiza 15, 159-165.

Nanamori M, Shinano T, Wasaki J, Yamamura T , Rao IM, Osaki M. 2004. Low phosphorus tolerance mechanisms: phosphorus recycling and photosynthate partitioning in the tropical forage grass, Brachiaria hybrid cultivar Mulato compared with Rice. Plant and Cell Physiology 45, 460-469.

Nielsen KL, Eshel A, Lynch JP. 2001. The effect of phosphorous availability on the carbon economy of contrasting common bean (*Phaseolus vulgaris* L.) genotypes. Journal of Experimental Botany 52, 329-339.

Ocaña A, Cordovilla MDP, Lluch C. 1996. Phospho*enol*pyruvate carboxylase in root nodules of *Vica faba*: partial purification and properties. Physiologia Plantarum 97, 724-730.

Pathirana MS, Samac DA, Roeven R, Yoshioka H, Vance CP, Gantt JS. 1997. Analyses of phosphoenolpyruvate carboxylase gene structure and expression in alfalfa nodules. The Plant Journal 12, 293-304.

Peng S, Eissenstat DM, Graham JH, Williams K, Hodge NC. 1993. Growth depression in mycorrhizal citrus at high-phosphorous supply. Journal of Plant Physiology 101, 1063-1071.

Qin L, Zhao J, Tian J, Chen L, Sun Z, Guo Y, Lu X, Gu M, Xu G, Liao H. 2012. The high-affinity phosphate tansporter GmPT5 regulates phosphate transport to nodules and nodulation in Soybean. Journal of Plant Physiology 159, 1634-1643.

Schachtman DP, Reid RJ, Ayling SM. 1998. Phosphorus uptake by plants: from soil to cell. Journal of Plant Physiology 116, 447-453.

Shearer GB and Kohl DH. 1986. N_2-fixation in field settings: estimates based on natural ^{15}N abundance. Australian Journal of Plant Physiology 13, 699-756.

Smith GS, Johnston M, Cornforth IF. 1983. Comparison of nutrient solutions for growth of plants in sand culture. New Phytologist 94, 537-548.

Sulieman S and Tran L-SP. 2015. Phosphorus homeostasis in legume nodules as an adaptive strategy to phosphorus deficiency. Plant Science 239, 36-43.

Sulieman S, Van Ha C, Schulze J, Tran L-SP. 2013. Growth and nodulation of symbiotic *Medicago truncatula* at different levels of phosphorus availability. Journal of Experimental Botany 64, 2701-2712.

Valentine AJ, Benedito VA, Kang Y. 2011. Legume nitrogen fixation and soil abiotic stress: from physiology to genomics and beyond. In: Foyer CH and Zhang H (eds). Nitrogen metabolism in plants in the post-genomic era. West Sussex: Wiley-Blackwell 42, 207-248.

Vance CP, Uhde-Stone C, Allan DL. 2003. Phosphorous acquisition and use: critical adaptations by plants for securing a nonrenewable resource. New Phytologist 157, 423-447.

Williams K, Percival F, Merino J, Mooney HA. 1987. Estimation of tissue construction cost from heat of combustion and organic nitrogen content. Plant, Cell and Environment 10, 725-734.

CHAPTER 5
GENERAL DISCUSSION

5.1 Research goal

The goal of this body of work was to increase the current knowledge base on the adaptability of a legume-rhizobia symbiosis to an environment of below optimum phosphate levels.

5.2 Chapter discussion

Chapter 1 described Leguminosae as one of the most important plant families to the environment and to human and herbivore nutrition. This diverse family's ability to form a symbiosis with soil diazotrophic bacteria enables these plant species to grow in environments where soil nitrogen is scarce. The chapter then further explained the role of nitrogen in the environment. The process of the fixation of atmospheric nitrogen by the soil diazotrophic bacteria and the symbiosis formed with legumes were also discussed. The requirement of a relatively large amount of energy in the form of ATP to complete the biological fixation of atmospheric nitrogen leads to the discussion of the role of phosphate in the environment. Phosphate, as with nitrogen, is found as a macronutrient in artificial fertilisers. However, the current mineable phosphate reserves are estimated to become depleted in the current century. The decline of phosphate in fertilisers will reduce yield for all crops, but will have a greater impact on the legume grain crops. It is thus important to determine how these crops could metabolically react to insufficient levels of available phosphate. A nodulating legume species that is either used a crop or is closely related to one can be used as a plant of interest.

The following chapter explored the possibility of using *M. truncatula* Gaertner as the plant of interest for such a study. Although is not used as a crop worldwide, it is related to the important foraging species *M. sativa* L. The *M. truncatula*-*S. meliloti* SNF system has

become an important model in 'Omics research. Thus the genomic and transcriptomic studies on the plant and SNF system are well underway. However, information on how this particular SNF system reacts to different scenarios of phosphate stress is still lacking.

Two research questions were thus formulated for probable scenarios in which phosphate stress can manifest in crop fields. The first involved the effect that phosphate stress would have on photosynthesis; and biomass, nutrient content and activities of certain organic acid synthesising enzymes and phosphatases. These analyses were done on plant tissues found above and below the soil surface. The study plants were inoculated with *S. meliloti* and grew in a suboptimum phosphate environment throughout their lifespan this research was looked at in Chapter 3. The second question formulated involved a more specified approach to induced phosphate stress on the below ground tissues of inoculated *M. truncatula*. Again biomass, nutrient content and organic acid synthesising enzymes and phosphatases were studied but were combined with enzymes that are part of the nitrogen assimilation pathway. Chapter 4 described these experiments in more detail.

Chapter 2 provided further background on the specific parameters analysed in order to determine whether the hypotheses formulated could be rejected or failed to be rejected. Chapters 3 and 4 encompass the experimental work done to answer the two posed research questions respectively.

The first stress scenario (Chapter 3) concluded that the rate and efficiency of photosynthesis were reduced if the plant of interest was grown under constant phosphate stress. However, the significant increase in phosphate use efficiency during photosynthesis was a good adaptive strategy against the stress condition. The expected reduction of biomass and increase of allocation of growth to the roots was seen in the lifelong stressed plants. It was interesting to note how the different tissues reacted to phosphate stress. The increase in the synthesising of oxaloacetate in the above ground tissues by PEPc might be an indication that the plant was trying to recycle carbon lost via the increased respiration rate during severe stress. The significant increase in malate production in the below ground tissues could be that these tissues were maintaining SNF by increasing production of this source of nodule energy. However, both the above and below ground tissues relied on the recycling of phosphate to maintain growth, and photosynthesis and SNF respectively. Increases in malate production and the activity of APases in below ground tissues could also have led to their export into the rhizosphere in order to make more soil phosphate available to the plant. The increase in nitrogen to P_i ratio in the stressed below ground organs was another indication of how important the

nitrogen deprived legume values the maintenance of SNF. These findings indicated that although overall biomass and photosynthesis were reduced, the efficiency of using phosphate in these processes was significantly increased. Thus the hypothesis formed in Chapter 2.3.1 failed to be rejected.

The second scenario (Chapter 4) involved the induction of phosphate stress on inoculated *M. truncatula* after a growth period of optimum phosphate supply. This set of experiments was only done on the below ground tissues, the nodules and roots separately. It seems that the allocation of new growth was slowly directed to the nodules during the induced stress period. Nodule biomass and number were reduced, however, the increased root to shoot ratio still indicated that the plants were experiencing phosphate stress. Although the biomass contained less carbon and nitrogen, there was more P_i found in stressed nodules and less P_i in the roots. Combined with the reduction of carbon cost to produce new tissue and the increased nitrogen efficiency, it seems that the stressed plants were using these scarce macronutrients at a higher efficiency than what the control plants needed to. The increased organic acid synthesis rates in the nodules can contribute to the increased nutrient use efficiency. While the activity of APase was high relative to the other enzyme activities studied in this work, the reduction in activity in the below ground tissues under phosphate stress was contradictory to the result in the first stress scenario. Thus indicating that the stage of development at which phosphate stress is experienced is also a determinate of how SNF manages the stress. The changes in nitrogen assimilating enzyme activities in the stressed nodules are interesting. The root activities for the same enzymes were relatively stable. As studies decribed by Cabeza et al., (2014) and Sulieman and Tran (2015) did not detect a change in the expression of nodule nitrogen assimilating enzyme-encoding genes, this result from the activities should be further examined. From the overall analyses, it seems that nodulated *M. truncatula* optimises its use of the available nutrients to enable it to maintain its tissues and survive the stress period until phosphate is sufficiently available again. From this study, it indicates that the nodules had induced a number of phosphate stress managing strategies, while the roots also adapted to the stress, however, less significantly. We have thus failed to reject the hypothesis formulated for this part of the work.

When these findings are compared to responses to phosphate stress observed in other legume species (Table 5.1), the annual *M. truncatula* photosynthetic response is consistent with those in the family. The nodules favour conserving phosphate in most species as the efficiency of nitrogen fixation consistently decreases.

5.3 Research limitations and future work

As with any experimental study, there are some limitations and recommendations for the future to address this body of work. The lack of a CO_2 response curve meant that certain functions of photosynthesis such as the maximum electron transport capacity at saturated PAR and the maximum ratio of RuBisCo carboxylation could not be calculated for this work. The possible difference in the photosynthetic production rate of ATP can indicate how much of this energy can be utilised by SNF.

Not all of the organic acid synthesising, APases and nitrogen assimilating enzyme activities were analysed in this work. The addition of ME, secreted APases, GOGAT, AS, nitrogenase and glycolytic enzyme activities would further enhance the understanding of how SNF manages phosphate stress in these key metabolic pathways. Further purification of the enzymes is advised as the activity measured can then be determined for each specific isoform.

The small physical size of the plant organs proved to be a limitation in this study as the enzyme assays had to be scaled down to accommodate this. It also meant that no assays could be done using the crude extracts to determine the protein concentration. The calculations were thus normalised to the FW per sample used to make the crude extract from. For future studies, it is advised that the Bradford method is used for the determination of protein content in each sample analysed. The activity of each enzyme or isoform can then be represented in a clearer manner as one unit of FW may not have the same amount of the protein of interest between samples.

Organic acids and certain APases are excreted into the soil to bind to or free phosphate. It will be interesting to compare the changes in the organic acid synthesising enzymes and APases activities to the possible changes in the amount of organic acids and APases found in the rhizosphere under phosphate stress.

An analysis of the membrane lipid composition could indicate whether the stressed nodulated *M. truncatula* replaces the phosphate in these lipids with sulphate. This not only frees phosphate to be used in metabolism, but it could weaken the membranes.

Table 5.1 Effect of phosphate stress on photosynthesis rate; metabolic efficiency; phosphate recycling; and biological nitrogen efficiency in legume species.

Species	Type of starvation & duration	Organ of interest	Effect of phosphate stress				Reference
			Photosynthesis	Metabolic	Recycling	BNF	
Glycine max	Induced 14 days	Nodules & roots	Decrease	Increase nodule phosphate conservation & amino acid synthesis	Not applicable	Decrease	Le Roux et al., 2009
Lupinus albus	Deficiency 30 days	Nodules & roots	Decrease	Not applicable	Not applicable	No effect	Thuynsma et al., 2014
Lupinus angustifolius	Induced 14 days	Nodules & roots	No effect	Increase nodule phosphate conservation & amino acid synthesis	Not applicable	No effect	Le Roux et al., 2009
Medicago sativa	Deficiency 54 days	Nodules	Not applicable	Decrease malate & asparagine content	Not applicable	Decrease	Sulieman et al., 2013
Medicago truncatula	Deficiency 51 days	Above ground & below ground	Decrease	Increase in above ground reliance	Increase in below ground reliance	Increase	Chapter 3
	Induced 23 days	Nodules & roots	Not applicable	Increase nodule phosphate conservation & glutamine synthesis	Decrease in roots	Decrease	Chapter 4
Vigna mungo	Induced 20 days	Nodules	Decrease	Not applicable	Not applicable	Decrease	Chaudhary et al., 2008
Virgilia divaricata & *Virgilia oroboides*	Deficiency 70-80 days	Nodules & roots	Decrease	Decreased nodule ureide export; increased root glutamine production	Not applicable	Decrease	Magadlela et al., 2014; Magadlela et al., 2015;
Virgilia divaricata	Deficiency 50 days	Nodules & roots	Not applicable	Not applicable	Increase in nodules	Not applicable	Vardien et al., 2015

As there were different results observed for the organs studied in the two stress scenarios it could be beneficial to follow the development of the changes in metabolism. These differences included the %NDFA, carbon contruction cost and some enzyme activities. This can be done by harvesting material at more than two intervals throughout the stressed period. These comparisons will give a timeframe and sequence to how the SNF metabolism adapts to phosphate stress.

5.4 Conclusion

A decline in the availability of phosphate in fertiliser will lead to a decline in crop yields. Yet with the knowledge of how a certain crop is adapted to a reduction in available phosphate in its rhizosphere farmers, plant breeders, plant biotechnologists and plant physiologists can plan the most effective use of the soil and nutrients to enable a sustainable crop yield. This body of work attributes to the accumulation of knowledge by indicating that the organs of plants differ in their adaptive strategies to different phosphate stress scenarios.

If the levels of available phosphate and nitrogen in the soil are low when the *M. truncatula* seeds are sown, these plants will germinate and form a symbiosis with *S. meliloti*. With the added phosphate sink of the nodule tissues, *M. truncatula* concerves this nutrient in the above ground tissues, while it is recycled within the tissues found below the ground surface.

If the soil had adequate phosphate available until *M. truncatula* maturity but low levels of nitrogen, the symbiosis with *S. meliloti* will also be initiated. However, if the level of available phosphate decreases, the nodules will try to concerve the phosphate within the tissue to produce glutamine for export as nitrogen source to the rest of the plant.

It is thus interesting to note the differences in the metabolic management employed by the tissues under different scenarios of phosphate stress. Additional studies are required to better understand these reactions of *M. truncatula* and SNF to phosphate stress to enable researchers to efficiently help farmers to increase food security during times of phosphate shortages.

5.5 References

Cabeza RA, Liese R, Lingner A, Von Stiegiltz I, Neumann J, Salinas-Riester G, Pommerenke C, Dittert K, Schulze J. 2014. RNA-seq transcriptome profiling reveals that *Medicago truncatula* nodules acclimate N_2 fixation before emerging P deficiency reaches the nodules. Journal of Experimental Botany 65, 6035-6048.

Chaudhary MI, Adu-Gyamfi JJ, Saneoka H, Nguyen NT, Suwa R, Kanai S, El-Shemy HA, Lightfoot DA, Fujita K. 2008. The effect of phosphorus deficiency on nutrient uptake, nitrogen fixation and photosynthetic rate in mashbean, mungbean and soybean. Acta Physiologiae Plantarum 30, 537-544.

Le Roux MR, Khan S, Valentine AJ. 2009. Nitrogen and carbon costs of soybean and lupin root systems during phosphate starvation. Symbiosis 48, 102-109.

Magadlela A, Kleinert A, Dreyer LL, Valentine AJ. 2014. Low-phosphorus conditions affect the nitrogen nutrition and associated carbon costs of two legume tree species from a Mediterranean-type ecosystem. Australian Journal of Botany 62, 1-9.

Magadlela A, Kleinert A, Steenkamp ET, Valentine AJ. 2015. Variable P supply affects N metabolism in a legume tree, *Virgilia divaricata*, from nutrient-poor Mediterranean-type ecosystems. Functional Plant Biology 43, 1-11.

Sulieman S, Schulze J, Tran LSP. 2013. Comparative analysis of the symbiotic efficiency of *Medicago truncatula* and *Medicago sativa* under phosphorus deficiency. International Journal of Molecular Sciences 14, 5198-5213.

Sulieman S and Tran L-SP. 2015. Phosphorus homeostasis in legume nodules as an adaptive strategy to phosphorus deficiency. Plant Science 239, 36-43.

Thuynsma R, Valentine A, Kleinert A. 2014. Phosphorus deficiency affects the allocation of below-ground resources to combined cluster roots and nodules in *Lupinus albus*. Journal of Plant Physiology 171, 285-291.

Vardien W, Steenkamp ET, Valentine AJ. 2015. Legume nodules from nutrient-poor soils exhibit high plasticity of cellular phosphorus recycling and conservation during variable phosphorus supply. Journal of Plant Physiology 191, 73-81.